

NAVAL POSTGRADUATE SCHOOL

Monterey, California

AD-A220 423



THEESIS

Co

EFFECTS OF LARGE DOSES OF HIGH
ENERGY ELECTRONS ON A $\text{YBa}_2\text{Cu}_3\text{O}_{6+\delta}$
HIGH TEMPERATURE SUPERCONDUCTOR

by

Gregory John Wolfe

December 1989

Thesis Advisor

X. K. Maruyama

Approved for public release; distribution is unlimited.

REPORT DOCUMENTATION PAGE

1a. REPORT SECURITY CLASSIFICATION Unclassified		1b. RESTRICTIVE MARKINGS	
2a. SECURITY CLASSIFICATION AUTHORITY		3. DISTRIBUTION/AVAILABILITY OF REPORT Approved for public release; distribution is unlimited.	
2b. DECLASSIFICATION/DOWNGRADING SCHEDULE			
4. PERFORMING ORGANIZATION REPORT NUMBER(S)		5 MONITORING ORGANIZATION REPORT NUMBER(S)	
6a. NAME OF PERFORMING ORGANIZATION Naval Postgraduate School	6b OFFICE SYMBOL (if applicable) 33	7a. NAME OF MONITORING ORGANIZATION Naval Postgraduate School	
6c. ADDRESS (City, State, and ZIP Code) Monterey, CA 93943-5000		7b. ADDRESS (City, State, and ZIP Code) Monterey, CA 93943-5000	
8a. NAME OF FUNDING/SPONSORING ORGANIZATION	8b. OFFICE SYMBOL (if applicable)	9. PROCUREMENT INSTRUMENT IDENTIFICATION NUMBER	
8c. ADDRESS (City, State, and ZIP Code)		10. SOURCE OF FUNDING NUMBERS	
		PROGRAM ELEMENT NO.	PROJECT NO.
		TASK NO.	WORK UNIT ACCESSION NO.
11. TITLE (Include Security Classification) EFFECTS OF LARGE DOSES OF HIGH ENERGY ELECTRONS ON A Y-BA-CU-O HIGH TEMPERATURE SUPERCONDUCTOR			
12. PERSONAL AUTHOR(S) Gregory John Wolfe			
13a. TYPE OF REPORT Master's Thesis	13b. TIME COVERED FROM _____ TO _____	14. DATE OF REPORT (Year, Month, Day) 1989, December	15 PAGE COUNT 112
16. SUPPLEMENTARY NOTATION The views expressed in this thesis are those of the author and do not reflect the official policy or position of the Department of Defense or the U. S. Government.			
17. COSATI CODES		18. SUBJECT TERMS (Continue on reverse if necessary and identify by block number) High Temperature Superconductors, Irradiation Effects, Electron Irradiation, Radiation Hardness, Superconductivity	
19. ABSTRACT (Continue on reverse if necessary and identify by block number) Two samples of Y-Ba ₂ -Cu ₃ -O _{6+x} high temperature (93 K) superconductor samples were irradiated with 67 MeV electrons. Both samples were cut from the same parent, manufactured by the University of Houston. Radiation effects were studied by measuring resistance as a function of dose during exposure. The samples were exposed to dose up to 100 Mrads. One sample was irradiated at near room temperature, while the second sample was irradiated at 30 K, below the superconducting transition temperature. Resistance as a function of temperature data was obtained prior to and immediately after exposures for both samples. The samples evidenced little or no shifts due to radiation effects in either the normal state resistance or the transition temperature outside of measurement accuracies. Both samples showed evidence of overall crumbling and flaking of the leads, likely due to the continual thermal expansion and contraction of the different materials throughout the different measurements. These mechanical effects produced measurable changes in the normal state resistances. It is concluded that the Y-Ba ₂ -Cu ₃ -O _{6+x} high temperature superconductor is significantly radiation-hard.			
20. DISTRIBUTION/AVAILABILITY OF ABSTRACT <input checked="" type="checkbox"/> UNCLASSIFIED/UNLIMITED <input type="checkbox"/> SAME AS RPT. <input type="checkbox"/> DTIC USERS		21. ABSTRACT SECURITY CLASSIFICATION Unclassified	
22a. NAME OF RESPONSIBLE INDIVIDUAL Prof. Xavier K. Maruyama		22b. TELEPHONE (Include Area Code) (408) 646-2431	22c. OFFICE SYMBOL 61Mx

Approved for public release; distribution is unlimited

Effects of Large Doses of High Energy Electrons on a
 $\text{YBa}_2\text{Cu}_3\text{O}_{6+\delta}$ High Temperature Superconductor

by

Gregory J. Wolfe
United States Army Tank-Automotive Command
B.S.E., University of Michigan, 1977

Submitted in partial fulfillment of the
requirements for the degree of

MASTER OF SCIENCE IN PHYSICS

from the

NAVAL POSTGRADUATE SCHOOL
December 1989

Author:

Gregory J. Wolfe
Gregory J. Wolfe

Approved by:

Xavier K. Maruyama -
Xavier K. Maruyama, Thesis Advisor

Fred R Buskirk
F.R. Buskirk, Second Reader

KarlHeinz E. Woehler, Chairman,
Department of Physics

L. J. S.

ABSTRACT

Two samples of $\text{YBa}_2\text{Cu}_3\text{O}_{6.9}$ high temperature (93 K) superconductor samples were irradiated with 67 MeV electrons. Both samples were cut from the same parent, manufactured by the University of Houston. Radiation effects were studied by measuring resistance as a function of dose during exposure. The samples were exposed to dose up to 100 Mrads. One sample was irradiated at near room temperature, while the second sample was irradiated at 30 K, below the superconducting transition temperature. Resistance as a function of temperature data was obtained prior to and immediately after exposures for both samples. The samples evidenced little or no shifts due to radiation effects in either the normal state resistance or the transition temperature outside of measurement accuracies. Both samples showed evidence of overall crumbling and flaking of the leads, likely due to the continual thermal expansion and contraction of the different materials throughout the different measurements. These mechanical effects produced measurable changes in the normal state resistances. It is concluded that the $\text{YBa}_2\text{Cu}_3\text{O}_{6.9}$ superconductor is significantly radiation-hard.

Nuclear Al Ceria, Inc., Dept. of Materials Science (F.D.)

J. C. S.

TABLE OF CONTENTS

I.	INTRODUCTION	1
	A. BACKGROUND	1
	1. Purpose of Experiment	1
	2. Previous Work	1
	3. Overview of Experiment	2
II.	EXPERIMENTAL SETUP AND PROCEDURE	4
	A. EQUIPMENT SETUP	4
	1. Target Area	4
	2. Control Room	9
	B. PROCEDURE	12
	1. Hot Sample	12
	2. Cold Sample	13
III.	EXPERIMENTAL RESULTS	1
	A. RESULTS	15
	B. CONCLUSIONS	63
	C. RECOMMENDATIONS	68
APPENDIX A	LINAC CHARACTERISTICS	69
APPENDIX B	COMPUTER PROGRAM LISTINGS	71
APPENDIX C	EQUIPMENT LAYOUT	85
APPENDIX D	DOSIMETRY	87
APPENDIX E	SUPERCONDUCTOR THEORY	96

APPENDIX F ELECTRON INTERACTIONS WITH MATTER	100
LIST OF REFERENCES	102
BIBLIOGRAPHY	103
INITIAL DISTRIBUTION LIST	104



Acknowledgements

I wish to thank Professor Xavier Maruyama for providing the opportunity to explore this topic area as a thesis. His timely guidance, direction, and optimism helped make the experience enjoyable as well as instructive.

Dr. Larry Dries of the Research and Development Division of Lockheed Missiles and Space Co., Inc., deserves special thanks for providing the samples, loan of special purpose equipment, and advice, all delivered in several trips to the NPS campus during the conduct of this investigation. Additionally, Dr. Kuo Fu Chien, Dr. C. Y. Huang, and Dr. W. Anderson are thanked for their desire in working with NPS and their valuable guidance.

In terms of countless hours of operation, maintenance, repair of the linear accelerator, and assistance in the experiment in all aspects, Mr. Don Synder and Mr. Harold Reitdyk should receive special recognition. I am very grateful for all their help in turning ideas into hardware.

Finally, but foremost, I wish to thank my wife Donna for her endless patience and support while caring for me and our son Alan. It wasn't easy taking care of "us guys". I dedicate this work to them.

I. INTRODUCTION

A. BACKGROUND

1. Purpose of Experiment

$\text{YBa}_2\text{Cu}_3\text{O}_{6+\delta}$ (known as Y123 material) comprises a class of ceramics, known as Type II superconductors, which exhibit superconducting properties above the 77K operating point for liquid-nitrogen cooled systems. While the potential of the Y123 material is limited by its low current density of approximately 400 A/cm^2 at 77K (magnetic resonance imaging, power generation-transmission-storage systems require materials with current densities on the order of 10^4 - 10^5 A/cm^2), Type II superconductors could see potential use. For this reason it is useful to study the response of these materials to high radiation environments.

2. Previous Work

Previous research on radiation effects on the Y123 materials has demonstrated slight changes to the normal state resistances exhibited by these materials after irradiation to high (greater than 1 megarad) dose, and small decreases in transition temperatures. Sweigard [Ref.1] observed an increase in the normal state resistance after subsequent dose of 0.3, 3.0, 30, and 150 megarads delivered to small bulk samples of Y123 materials. C.Y. Huang et. al., at Lockheed Missiles and Space Company [Ref. 2] observed a decrease in

the normal state resistance of Y123 samples when exposed up to 10 megarads of 1.17 and 1.33 MeV gamma rays from a Co⁶⁰ source. The transition temperature was likewise shown to decrease slightly with successive exposures. W. G. Maisch et. al. [Ref 3] from the Naval Research Laboratory, exposing 100 mm thick film samples of Y123 as opposed to the bulk samples utilized by NPS and Lockheed, observed increasing normal state resistance with increasing exposure up to 100 megarads. A corresponding drop in the transition temperature was seen, as noticed by the previously referenced experiments. Shinashi, K. et. al., [Ref 4] observed a linear decrease in transition temperature with increasing electron dose up to 3 MeV, and concurrent linear increase in resistivity at normal state. Bohandy et. al. [Ref 5] irradiated 2-3 miligram bulk samples of Y123 up to dose of 1.3 megarads with a Co⁶⁰ gamma source. By using a variation of a microwave absorption method to measure microwave signal versus temperature, the material was observed to be virtually unaffected by the high dose. Subsequent observations taken after 7 days indicated that no delayed effects of irradiation were present.

3. Overview of Experiment

It was the purpose of this experiment to irradiate the Y123 samples to very high electron dose, up to 100 megarads, using a 67 MeV electron beam produced by the linear accelerator (LINAC), located at the Naval Postgraduate School

(NPS), Monterey, California to obtain dynamic measurement of the resistivity of the samples while irradiated as well as to obtain before/after resistance versus temperature measurements. Two Y123 samples, manufactured by C.W. Chu's group at the University of Houston, were cut from the same parent. Samples were exposed to various dose up to 100 megarads. Resistance versus temperature data was taken prior to and after each subsequent irradiation. This data is displayed in the form of resistance versus temperature plots. Observations were made of the change in resistances at normal state, and any shifts in the transition region which may have been indicative of damage caused by the bombardment of 67 MeV electrons. Data was also obtained while the samples were undergoing irradiation. This data is displayed in the form of resistance and temperature versus cumulative dose plots. This procedure was carried out for 2 samples of the Y123 material, with one sample undergoing irradiation at a near-constant temperature of 270 K (well above the transition region), and the second sample undergoing irradiation below the transition region.

II. EXPERIMENTAL SETUP AND PROCEDURE

A. EQUIPMENT SETUP

1. Target Area

This experiment was performed using the electron linear accelerator located at the Naval Postgraduate School, Monterey, California. The characteristics of the LINAC are described in Appendix A. The experimental setup is detailed in terms of two stations, the target area and control room. Diagrams and equipment listings are contained in Appendix B. Figure 1 shows the cryostat through which liquid helium flows at 7-10 psig. The sample holder is located at the tip of the liquid helium transfer tube inside the cryostat, referred to as the "cold finger", shown in figure 2. On the sample are 4 indium contacts, upon which platinum leads are attached, employing the AC four-probe resistance measuring method. The four leads are soldered to bronze phosphorous attachments which serve to control the up-down and sideways location of the leads by use of individual sets of 3 positioning screws. The sample is held in place on the copper holder by thermal insulator and pressure exerted by the leads. Positioning of the leads onto the indium contacts is accomplished under a microscope. The bronze phosphorous positioners and leads are shown in figure 3. An AC excitation current of 30 microamps is applied to the outer two contacts on the superconductor

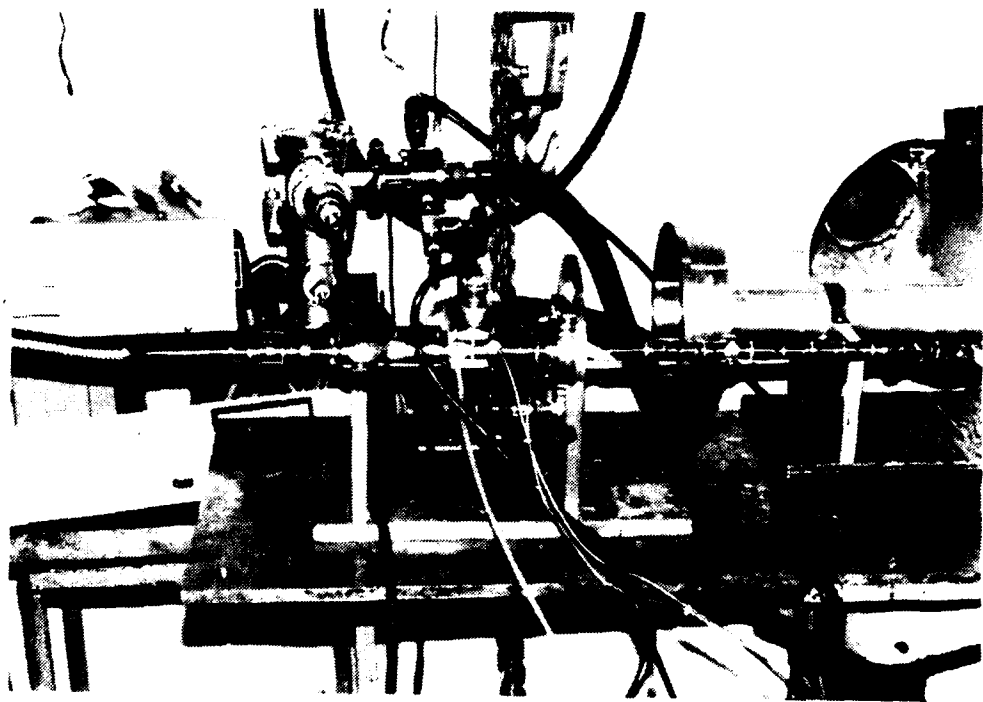


Figure 1: Cryostat with sample and turbopump located in the target area.

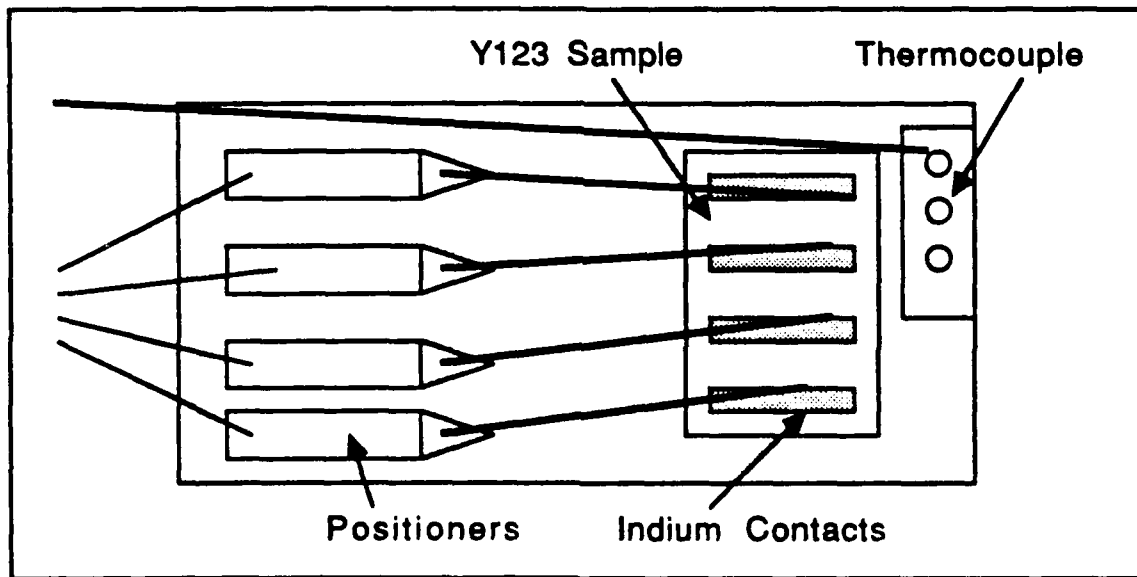


Figure 2: Y123 Sample and thermostat located on the sample holder.

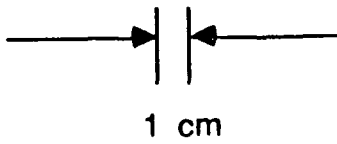
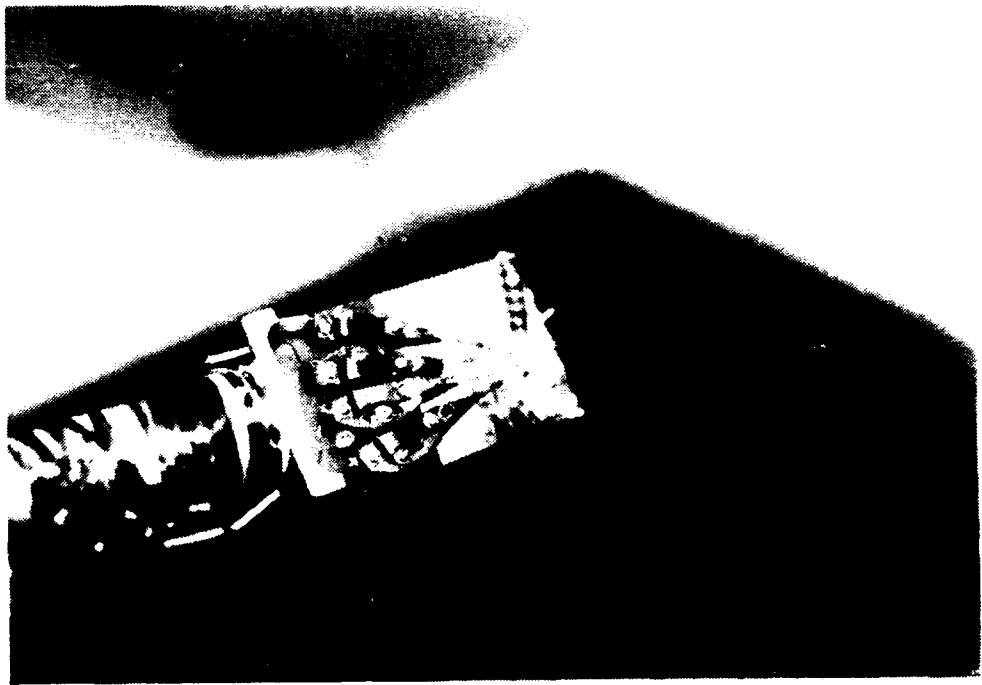


Figure 3: Sample holder positioners and leads.

sample from the four-wire AC resistance bridge, producing an induced voltage across the inner 2 sample leads that is proportional to the electrical resistance of the sample. This proportional voltage is transferred, via braided, shielded coaxial cable, to the control room data collection station. A thermocouple mounted in close proximity to the superconductor sample provides a voltage proportional to the temperature via the selectable temperature controller/indicator. This voltage is also transferred, via braided, shielded coaxial cable, to the control room data collection station. The sample holder and transfer line, through which liquid helium is transferred, is enclosed within a 2 and 1/2 inch outer diameter cylindrical aluminum casing, which is evacuated to approximately 10^{-2} torr. Liquid helium flows through the high-efficiency transfer line to the sample holder interface at a constant rate. A micrometer needle valve in the transfer line permits control of the flow rate. The vacuum within the cyrostat is established with a high vacuum turbopump. The other end of the flexible transfer line tube is inserted into the liquid helium dewar, which is pressurized with gaseous helium to 7-10 psig. Once a vacuum of 10^{-2} torr is achieved, then cooldown commences. Typical cooldown from room temperature to 50 K takes around 45 minutes. Temperature is controlled via setting the temperature controller/indicator. A combination of tip flow control and electrical heating is

used to conserve helium and provide uniform cooling/heating. Figure 4 shows the sample temperature controller/indicator, cryostat temperature controller/indicator, helium flow indicators, and four wire AC resistance bridge. Outputs to the control room collection station are from the tip temperature indicator/controller and resistance bridge. The electron beam target area is marked on the outside of the cyrostat by careful measurement of the sample location. The beam is blown up to encompass the sample holder and to provide more uniform intensity. The cyrostat is positioned after careful monitoring of the beam location. The position is established by a two-axis telescopic level. The beam is positioned on a target mark on the flourescent screen. Cross hairs on the level are then also positioned on the target mark. The screen is removed and the cryostat, with target mark, is aligned by the cross hairs. The cyrostat is not moved until a series of exposures is completed. This procedure is to ensure that no movement of the equipment is necessary after beam-target alignment is performed.

2. Control Room

An output voltage from the voltage integrater was transferred to the data collection station. This voltage is linearly proportional to the dose delivered by the electron beam. Figure 5 shows the data collection station, consisting of a plotter, computer, and hard disk. The 3 channel plotter utilized analog-to-digital converters and retains up to 1000

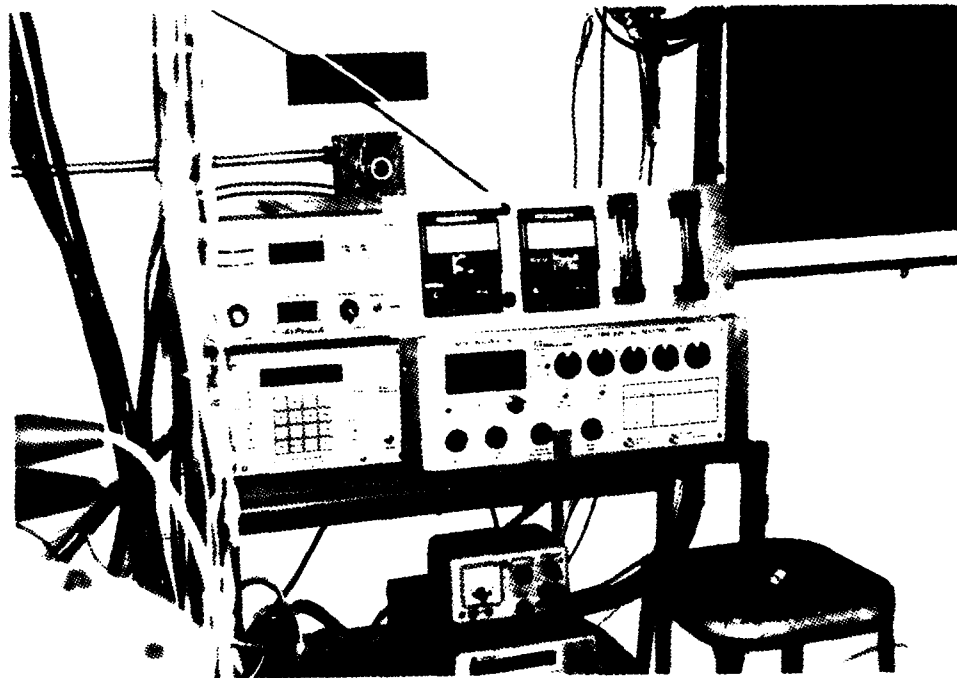


Figure 4: Temperature and helium flow controllers, and 4 probe AC resistance bridge.

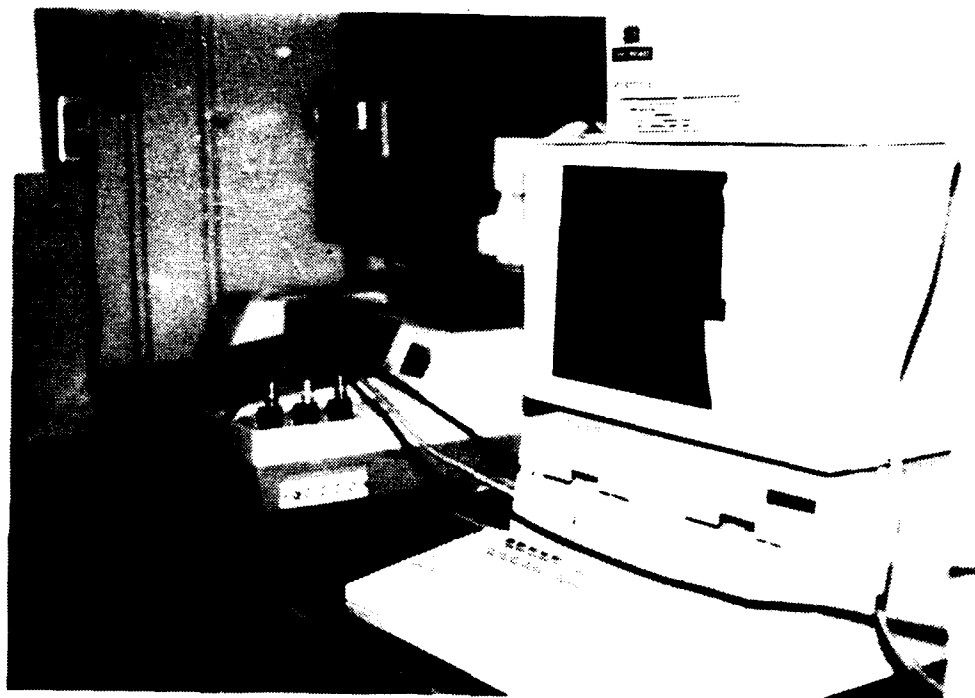


Figure 5: Data Collection station located in the LINAC control room.

data values per channel. The data was stored in buffers and transferred to the computer for analysis and manipulation. In this experiment the 3 inputs were voltages proportional to the electrical resistance (channel 1), the temperature (channel 2), and the total charge , hence dose (channel 3). The stored values were transferred to the computer after data collection, where they were converted to values for superconductor sample resistance, temperature, and exposure level by use of programs written specifically for the experiments. This data was then plotted, while the raw data was saved to hard disk for further analysis. Appendix B contains listings of the controller programs and file listings. The equipment layout is shown in Appendix C.

B. PROCEDURE

1. Hot Sample

One sample of the Y123 superconductor which was irradiated at 270 K, was designated as the "hot" sample. Resistance (as a function of temperature) data was collected prior to irradiation. Cooldown was accomplished at a slow rate to insure uniform cooling of the sample, taking about 45 minutes to cool from room temperature to 50 K. After dosimetry was performed (as described in Appendix D), the sample was cooled to 270 K by use of the temperature controller/indicator and liquid helium flow indicators. This

value was chosen so that some cooling was provided to the sample to hold the temperature constant during the period of irradiation, some of which would require exposure times on the order of four hours. During the period of exposure the parameters of the temperature controllers and flow controller could not be changed since the instruments were located within the target area. While the sample was irradiated, continuous output voltages were received at the three channel plotter located in the control area. An analog to digital converter on the plotter allowed sampling of the signals. 1000 samples were taken of each signal throughout the irradiation periods. The hot sample was exposed to doses of 6, 40, and 54 megarads resulting in cumulative doses of 6, 46, and 100 megarads. Data taken during the three irradiation periods was converted to dose, resistance, and temperature, stored on hard disk, and plotted. Immediately after each of the three exposures, the sample was cooled, and resistance versus temperature data taken. The sample was allowed to slowly reheat to room temperature, and left overnight under vacuum in the cryostat prior to the next set of dosimetry and subsequent irradiation.

2. Cold Sample

A different sample of Y123 from the same parent material was subsequently emplaced in the cryostat and

irradiated at 30 K. This sample was designated the "cold" sample. Pre-irradiation resistance versus temperature data was taken. Three sets of data were obtained to determine the spread of the curves in order to determine the accuracy of the resistance versus temperature curve, found to be \pm 2 K. In a manner similar to the hot sample, dosimetry was performed prior to irradiation. The cold sample was exposed to dose increments of 1k, 10k, 100k, 1M, 10M, and 48M rads (cumulative doses of 1k, 11k, 111k, 1.1M, 11.1, and 59.1 rads) while the sample was maintained below the transition temperature. The data were taken in small dose increments to be sensitive to a low temperature threshold for damage. Again during the irradiations, resistance and temperature versus dose data was taken and plotted. Immediately after each irradiation the samples were allowed to warm up to room temperature, and cooled back down while resistance versus temperature data was obtained. This permitted two resistance curves to be obtained after each irradiation.

III. EXPERIMENTAL RESULTS

A. RESULTS

Resistance versus temperature data was obtained from the hot sample prior to irradiation. Figure 6 shows the curve resulting from the plotting of this data. Figure 7 is the same plot expanded to show details near the transition region. Resistance (milliohms) is shown on the y-axis as a function of the temperature (Kelvins). Figure 6 displays a range from 0-300 K while figure 7 displays a range from 80-120 K, focusing on the transition region. In figure 7, onset, considered here to be the highest temperature at which the transition region commences, is around 92 K. Midpoint appears at 91 K, and offset, where resistance drops to zero, occurs at about 88 K. The curve in figure 7 displays discrete steps due to the sampling limitation of the HP 7090 plotter, 1000 data samples per channel being the maximum obtainable during a collection period.

Figures 8 and 9 display resistance versus temperature curves taken after the hot sample was exposed to 6 megarads. From figure 9 it is observed that onset occurs at 90 K, midpoint at 89 K, and offset at about 86 K. These values appear to be shifted from the pre-exposure values by 2 K, however, as found in subsequent plots, the measurement accuracy is \pm 2 K. Figures 10 and 11 show resistance versus temperature curves after exposure to an additional 40

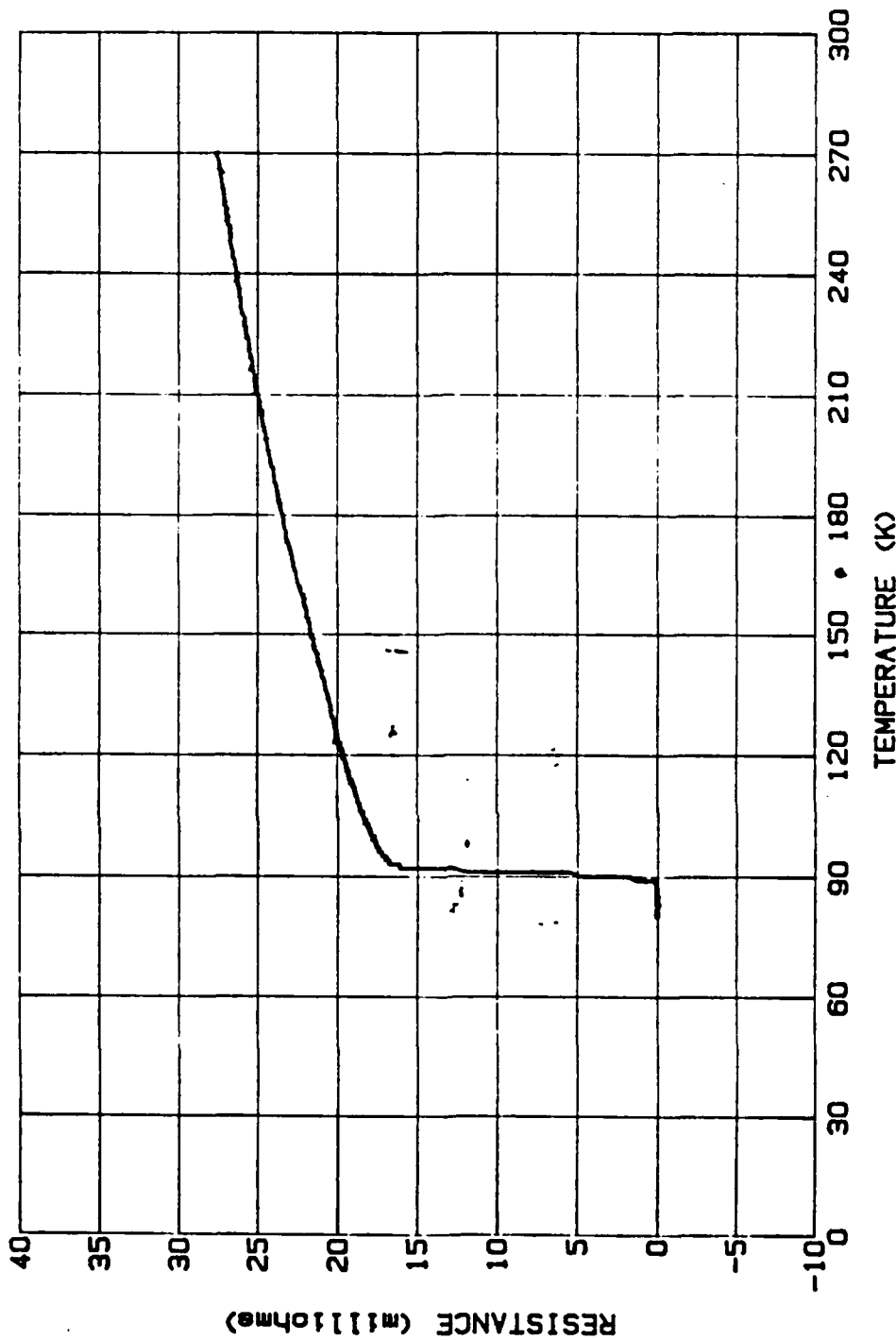


Figure 6: Resistance versus temperature curve for the hot sample prior to exposure.

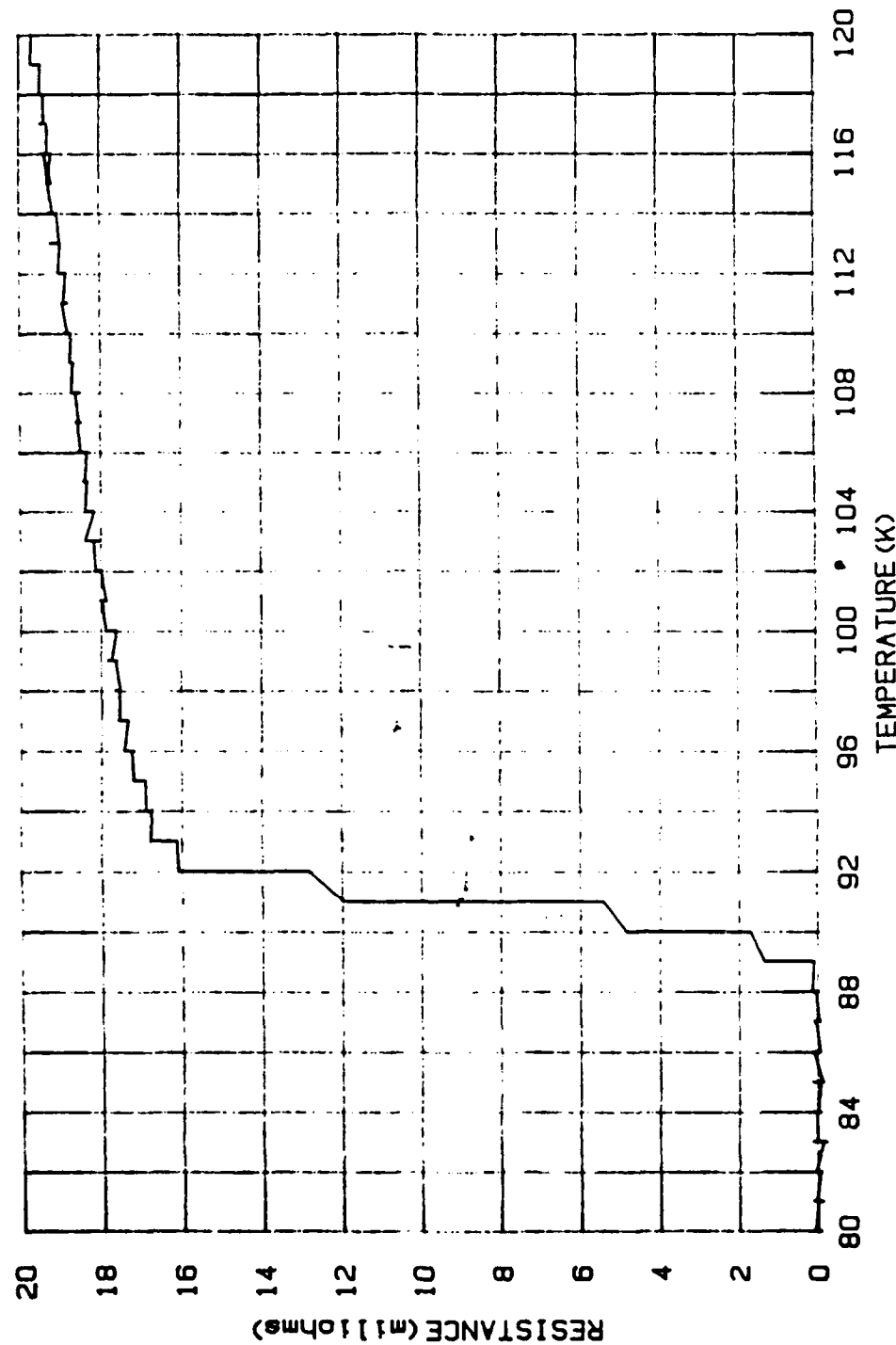


Figure 7: Resistance versus temperature curve for the hot sample prior to exposure. The temperature range is from 80-120 K.

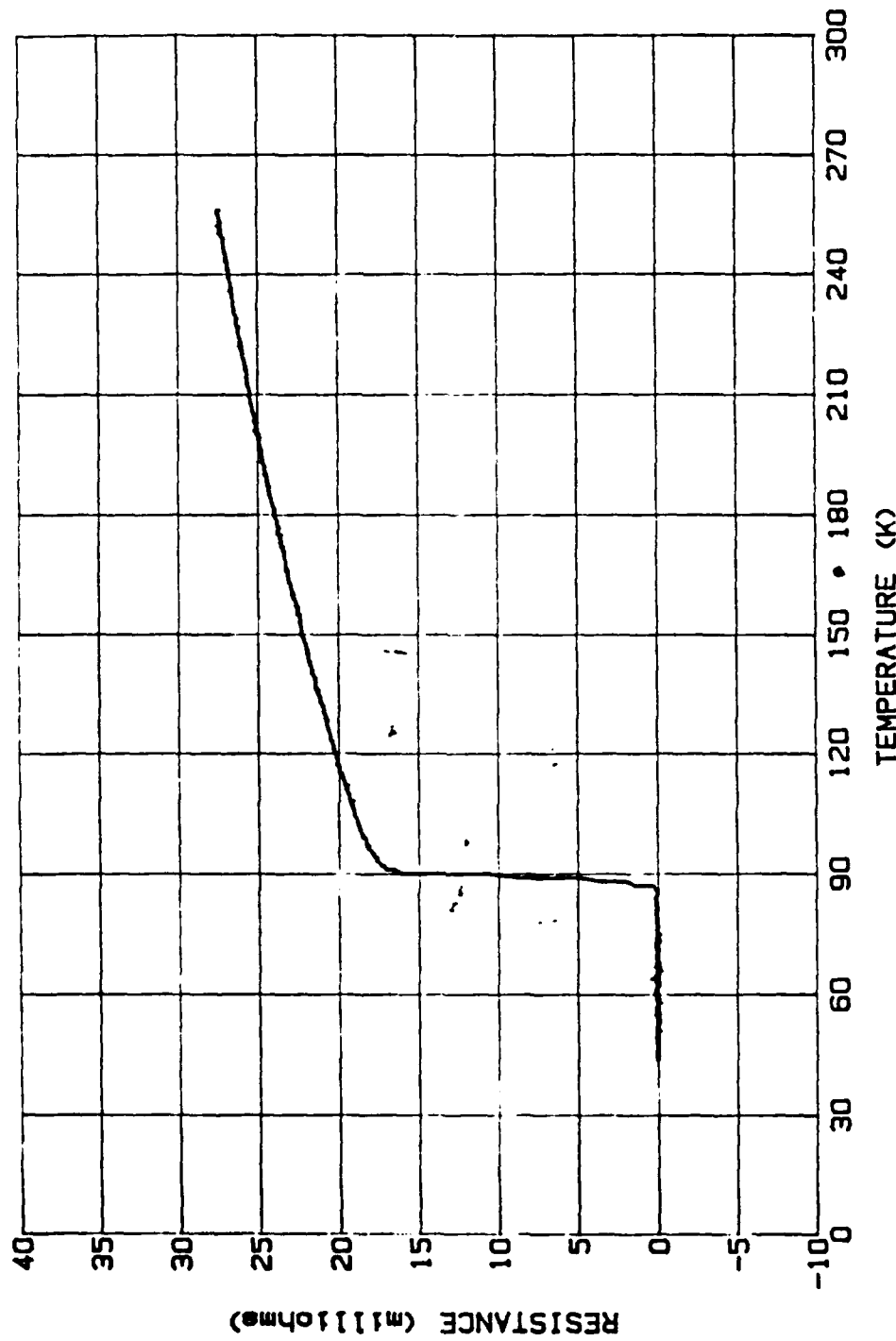


Figure 8: Resistance versus temperature curve for the hot sample after exposure to 6 megarads.

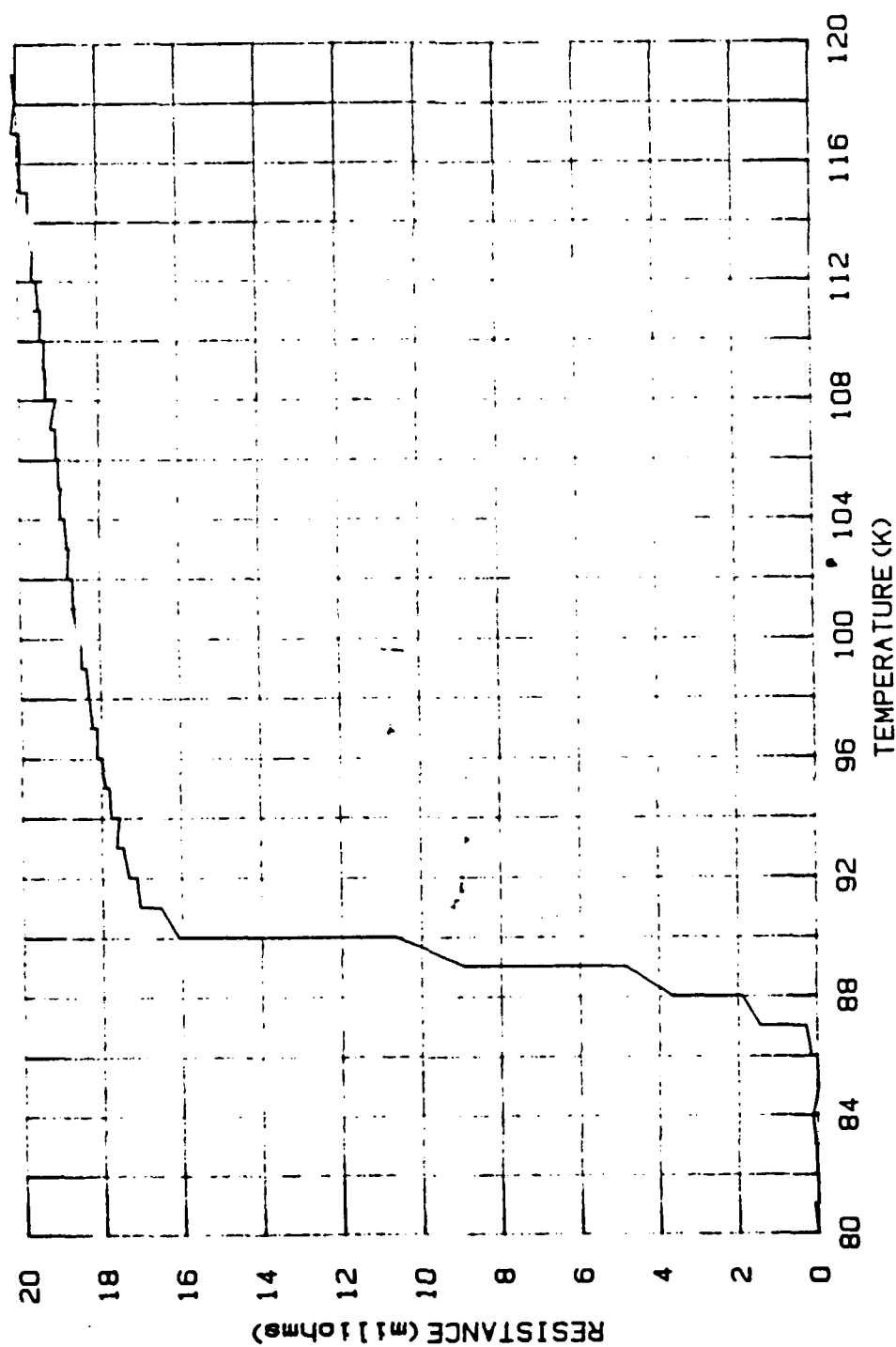


Figure 9: Resistance versus temperature curve for the hot sample after exposure to 6 megarads. The temperature range is 80-120 K.

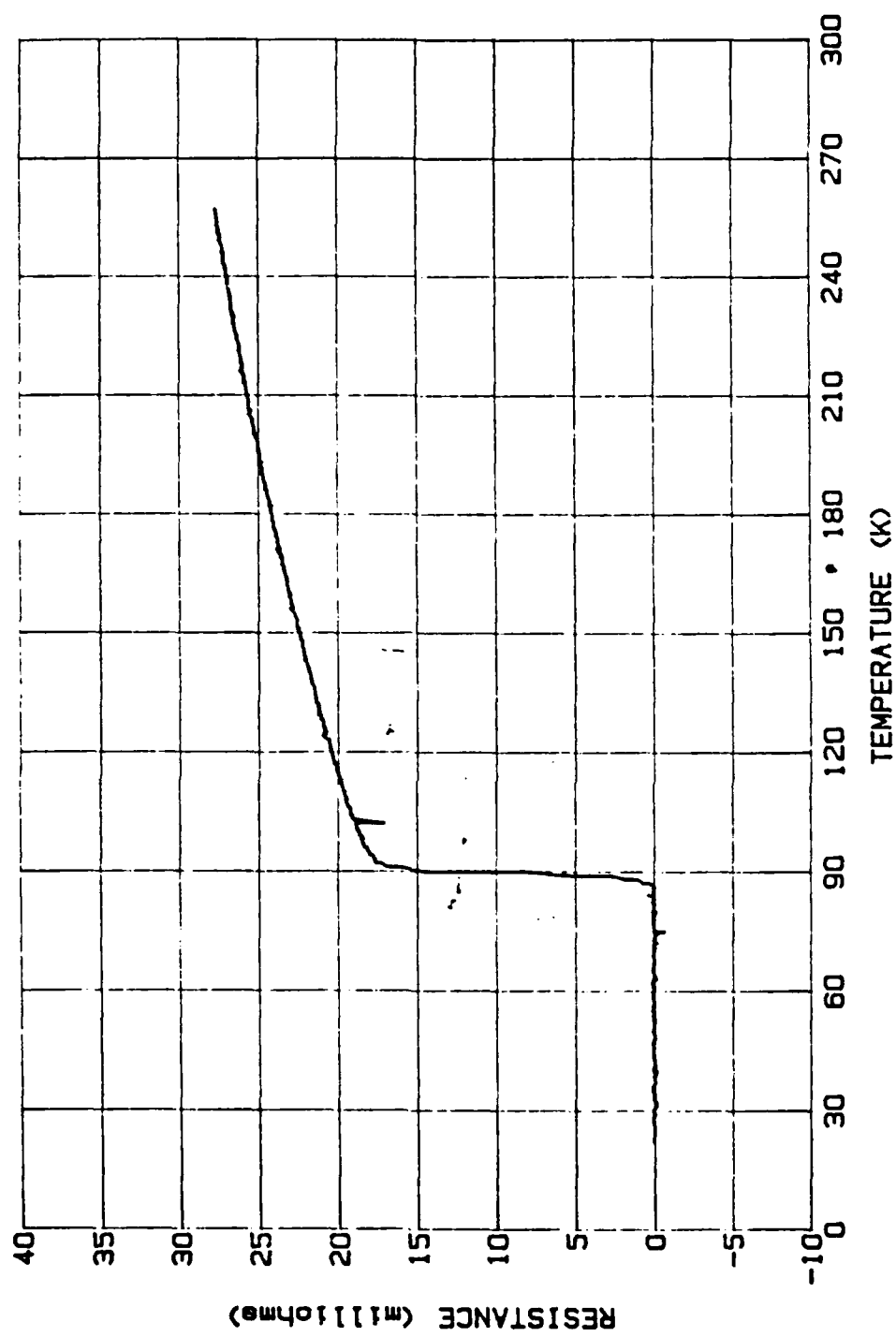


Figure 10: Resistance versus temperature curve for the hot sample after exposure to 40 megarads (46 megarads cumulative).

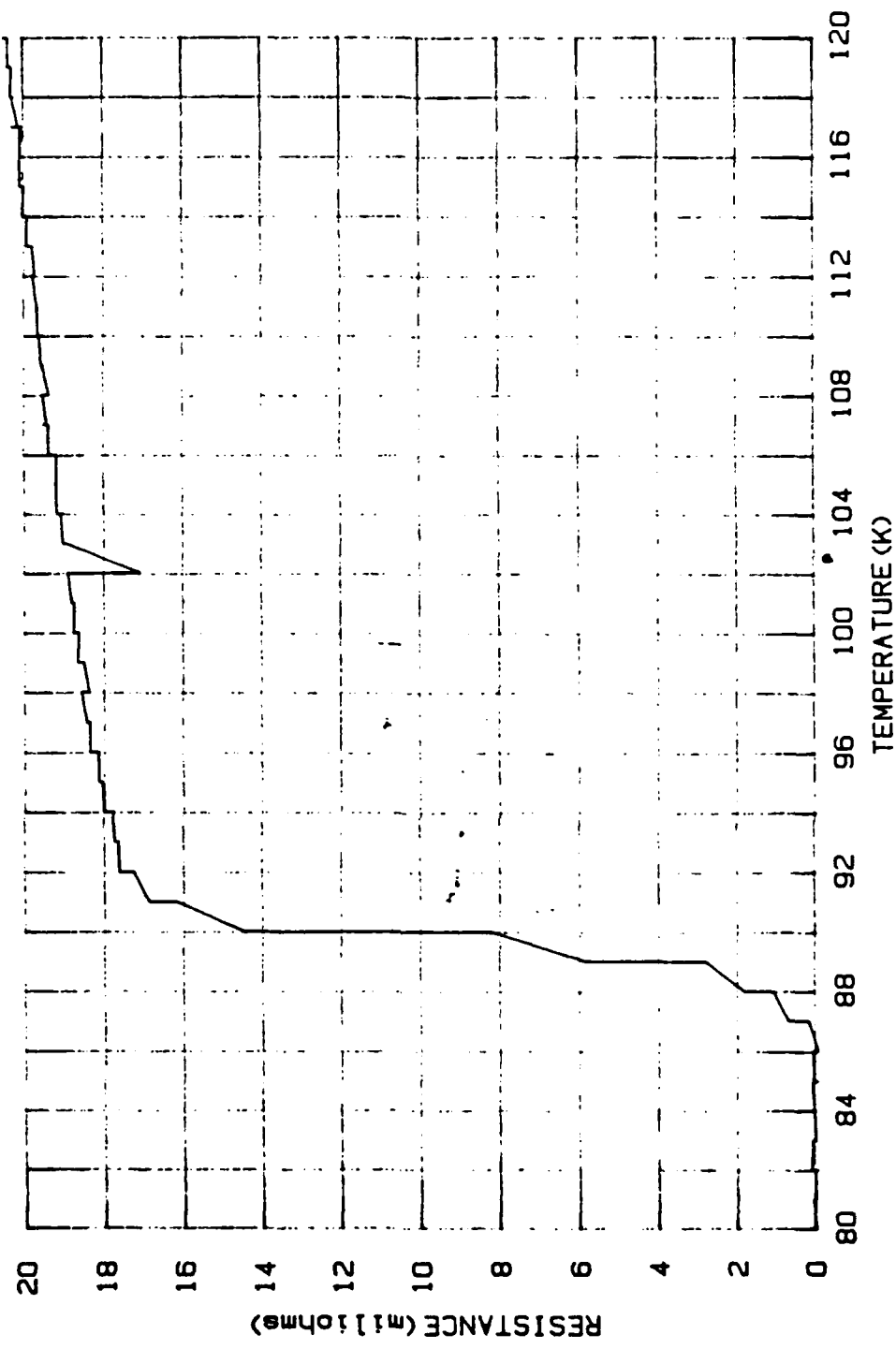


Figure 11: Resistance versus temperature curve for the hot sample after exposure to 40 megarads (46 megarads cumulative). The temperature range is 80-120 K.

megarads incremental dose. From figure 11 it is observed that onset occurs at about 91 K, midpoint at 90 K, and offset at 87 K. These values are 1-2 K lower than the corresponding pre-exposure values, and are similar to those seen after exposure to 6 megarads. Figures 12 and 13 display resistance versus temperature data after exposure to 54 megarads (100 megarads cumulative dose). From figure 13 it is seen that values for onset, midpoint, and offset are 91 K, 90 K, and 87 K respectively. These are likewise similar to the corresponding values found after exposures to 6 and 40 megarads. Figure 14 is an overlay of the 4 curves of resistance versus temperature from the pre-exposure and post-exposure to 6, 40, and 54 megarad measurements. This plot showed a definite shift in the normal state resistances of the hot sample after exposure to doses of 6, 40, and 54 megarads. However, after the initial shift after exposure to 6 megarads, subsequent exposures did not result in further changes in resistance. No firm conclusion was drawn from the apparent shift the resistance because this apparent shift could be induced by a temperature measurement shift of \pm 2 K. Furthermore, measurements of the smaller dose increments in the cold sample did not confirm this type of behavior.

Figures 15 and 16 are dual-axis plots of resistance and temperature versus dose delivered to the hot sample during exposure. During the period of exposure the resistance curve displayed definite positive slope, shown by the solid line in

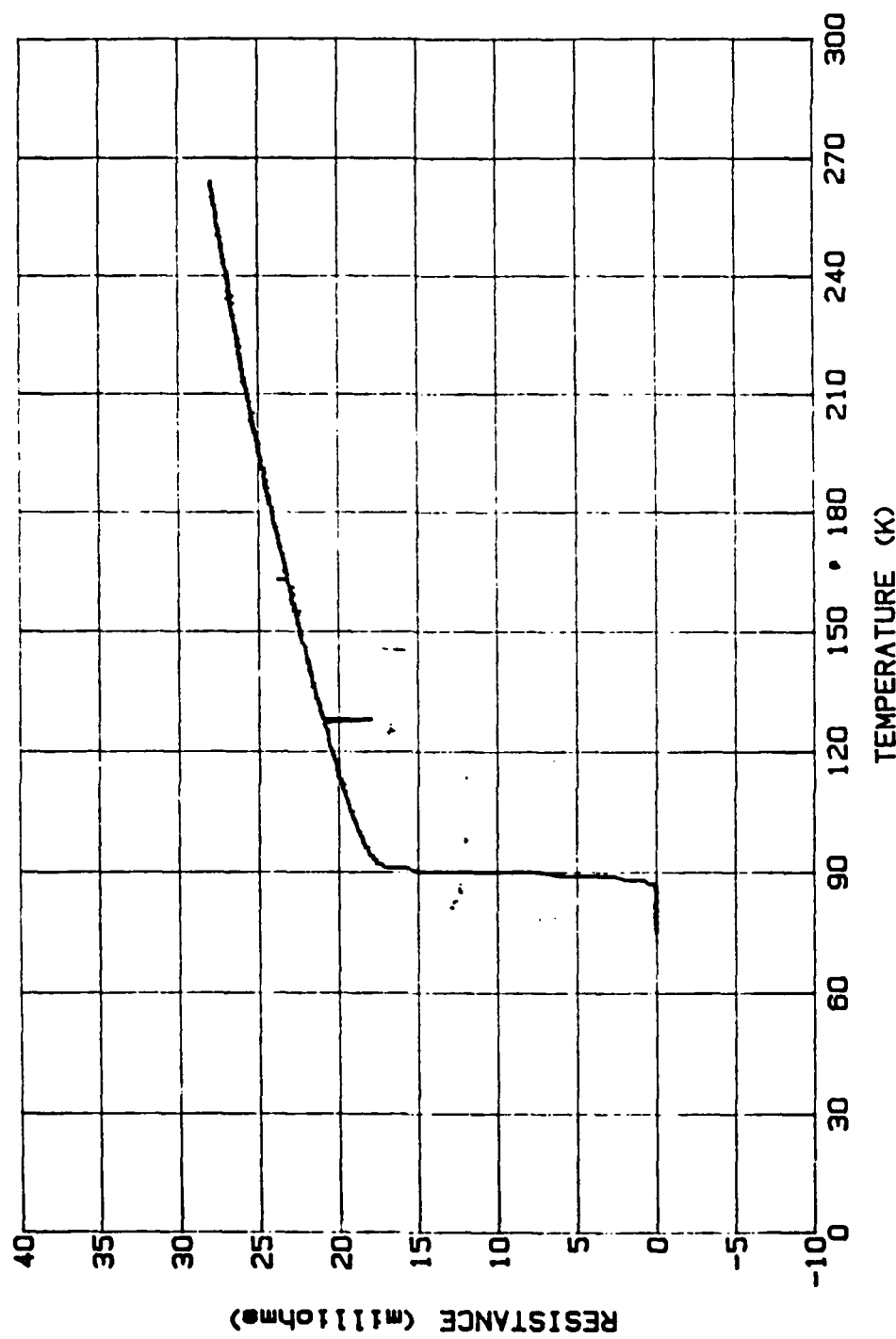


Figure 12: Resistance versus temperature curve for the hot sample after exposure to 54 megarads (100 megarads cumulative).

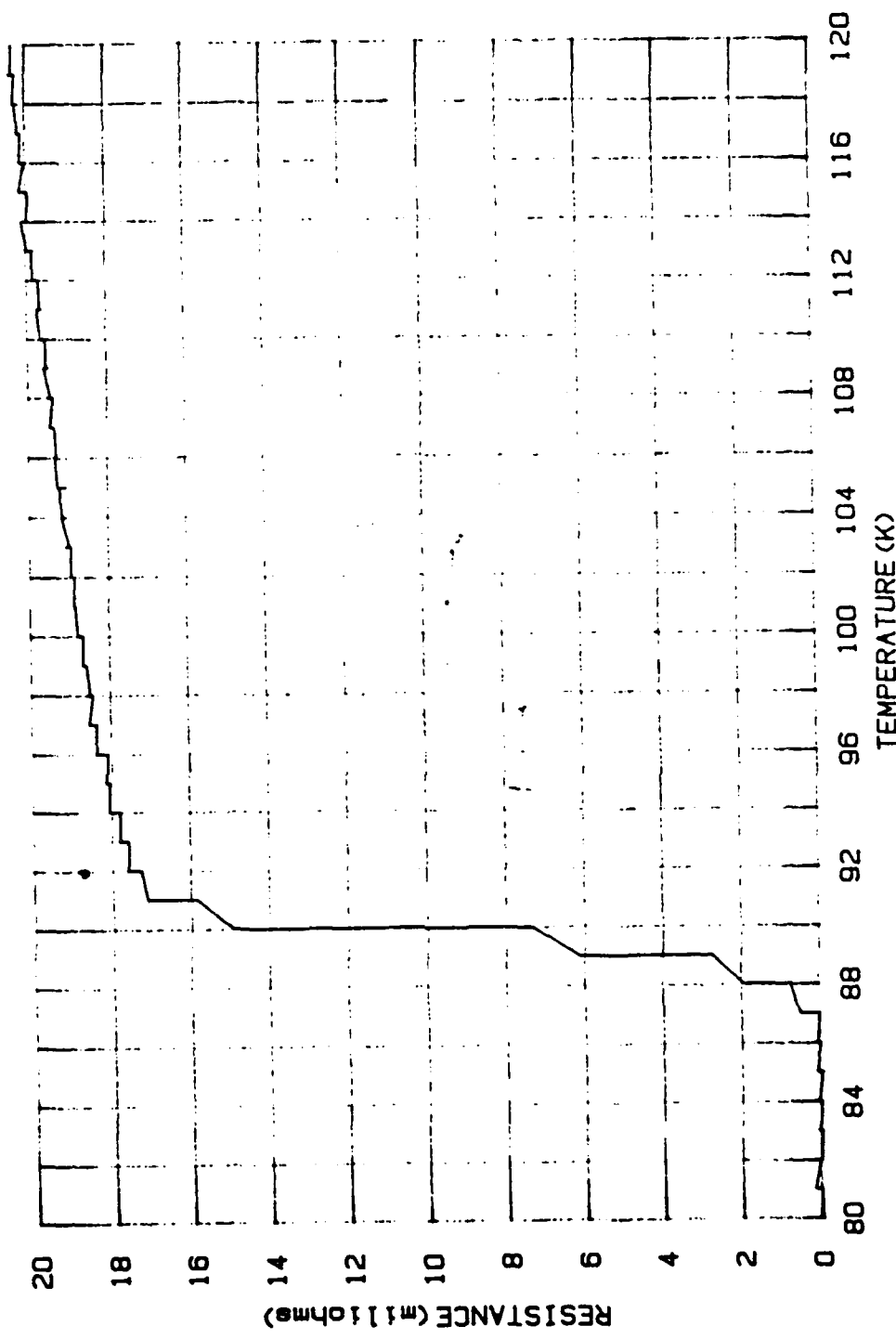


Figure 13: Resistance versus temperature curve for the hot sample after exposure to 54 megarads (100 megarads cumulative). The temperature range is 80-120 K.

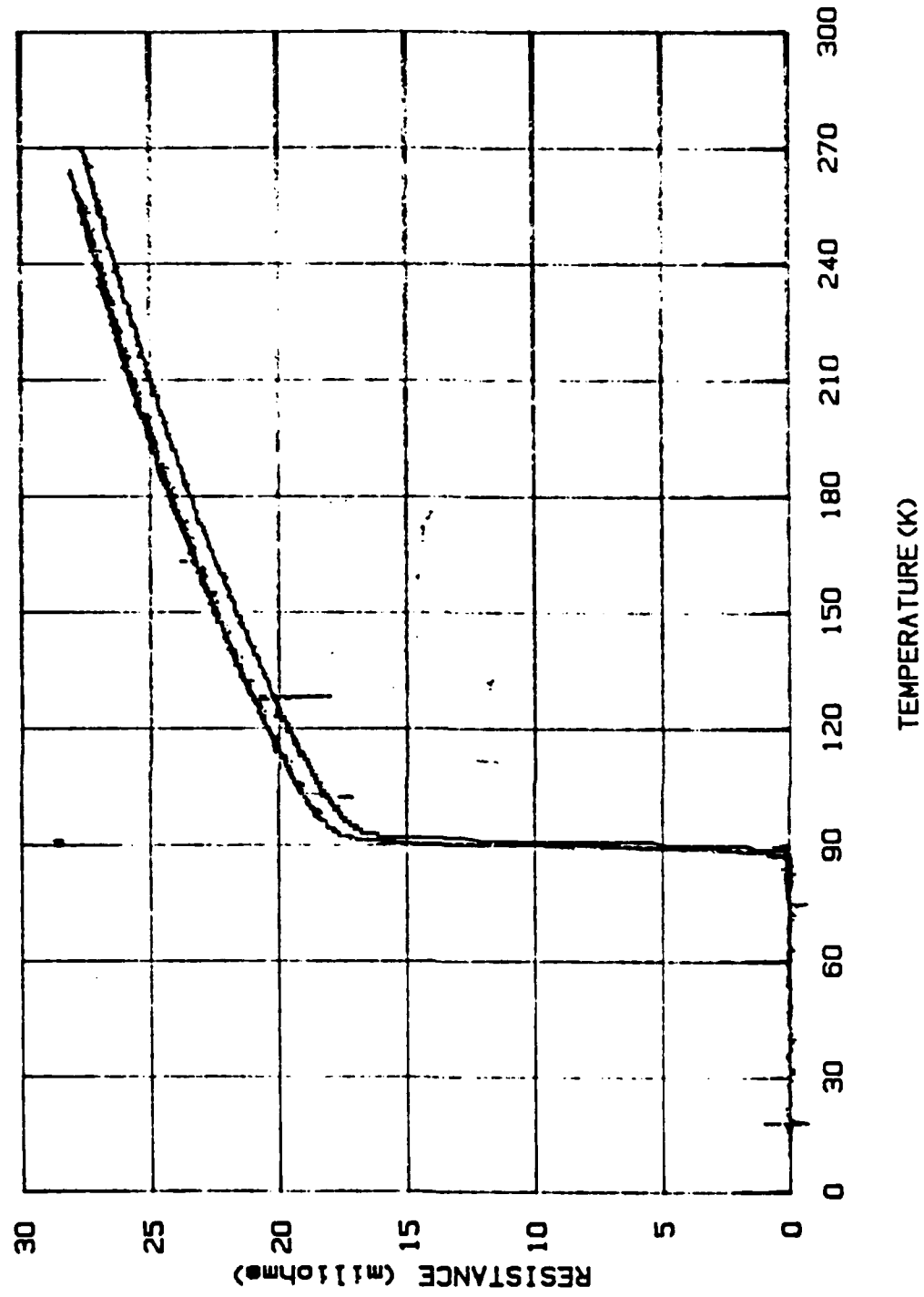


Figure 14: Overlay of the hot sample pre and post-exposure resistance versus temperature curves.

Sample 2 6 MRads 8 Aug 89

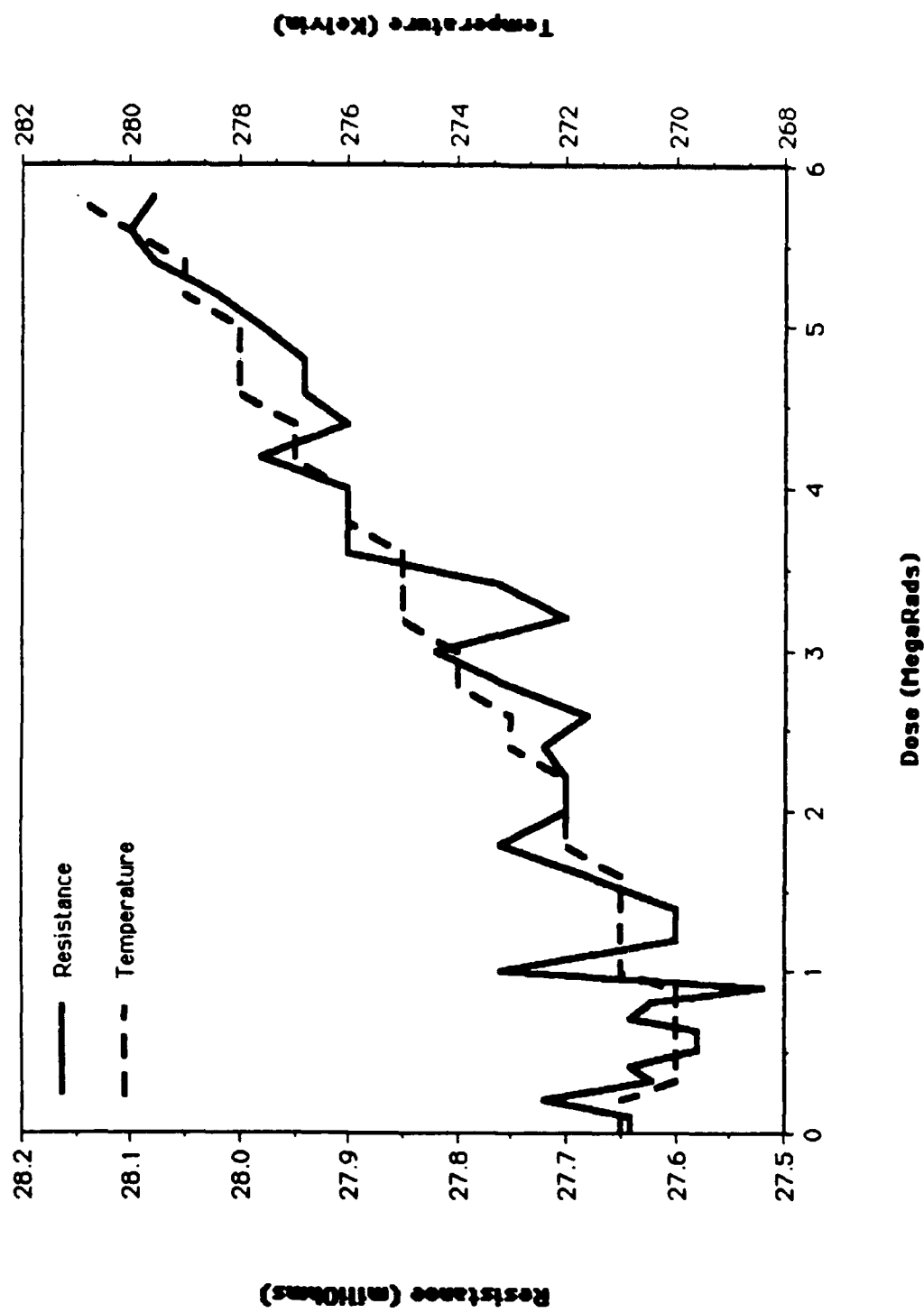


Figure 15: Dual-axis plot of resistance and temperature versus dose during exposure of hot sample to 6 megarads.

Sample 2 53 MRads 10 Aug 89
(100 MRads Cumulative 8-10 Aug)

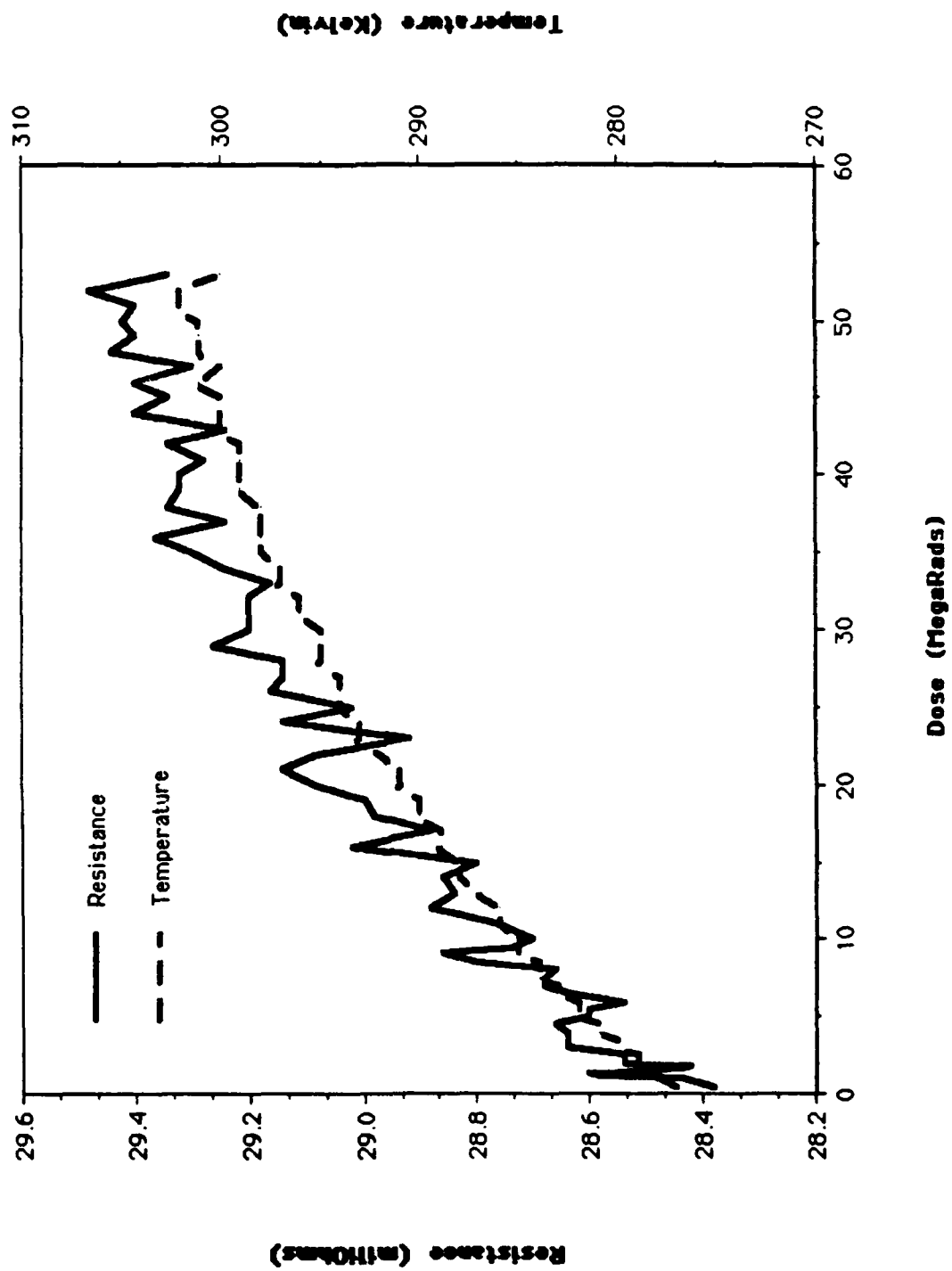


Figure 16: Dual-axis plot of resistance and temperature versus dose during exposure of hot sample to 54 megarads.

the figures. However, when the temperature of the sample during exposure was plotted, the slopes of resistance and temperature nearly coincided, indicating that the increase in resistance was due to the rise in temperature of the sample rather than to the dose received by it. The temperature increased due to the inability to properly adjust the liquid helium flow and electrical heater while the sample was being irradiated, resulting in a drift from the set value of 270 K to 281 K. Figure 16 shows a similar plot for an exposure of 54 megarads. Once again the resistance increased in concert with the temperature drift from 280 to 300 K. These plots indicated that any change in resistance of the hot sample was a result of temperature increase rather than exposure to high energy electrons.

To further analyze the apparent shift in the resistance plots after exposure to 6, 40, and 54 megarads, figures 17, 18, and 19 were constructed by taking the ratios of the resistances (as a function of temperature) after irradiation to the pre-irradiation resistance values. Figure 17 is this ratio after an exposure of 6 megarads, figure 18 after 46 megarads (cumulative dose), and figure 19 after 100 megarads (cumulative dose). In all three figures the post-exposure resistances increase from 3-5% above the transition region. Near the transition temperature, the resistance gradient with respect to temperature is too steep to allow a meaningful determination of resistance values. These plots indicated

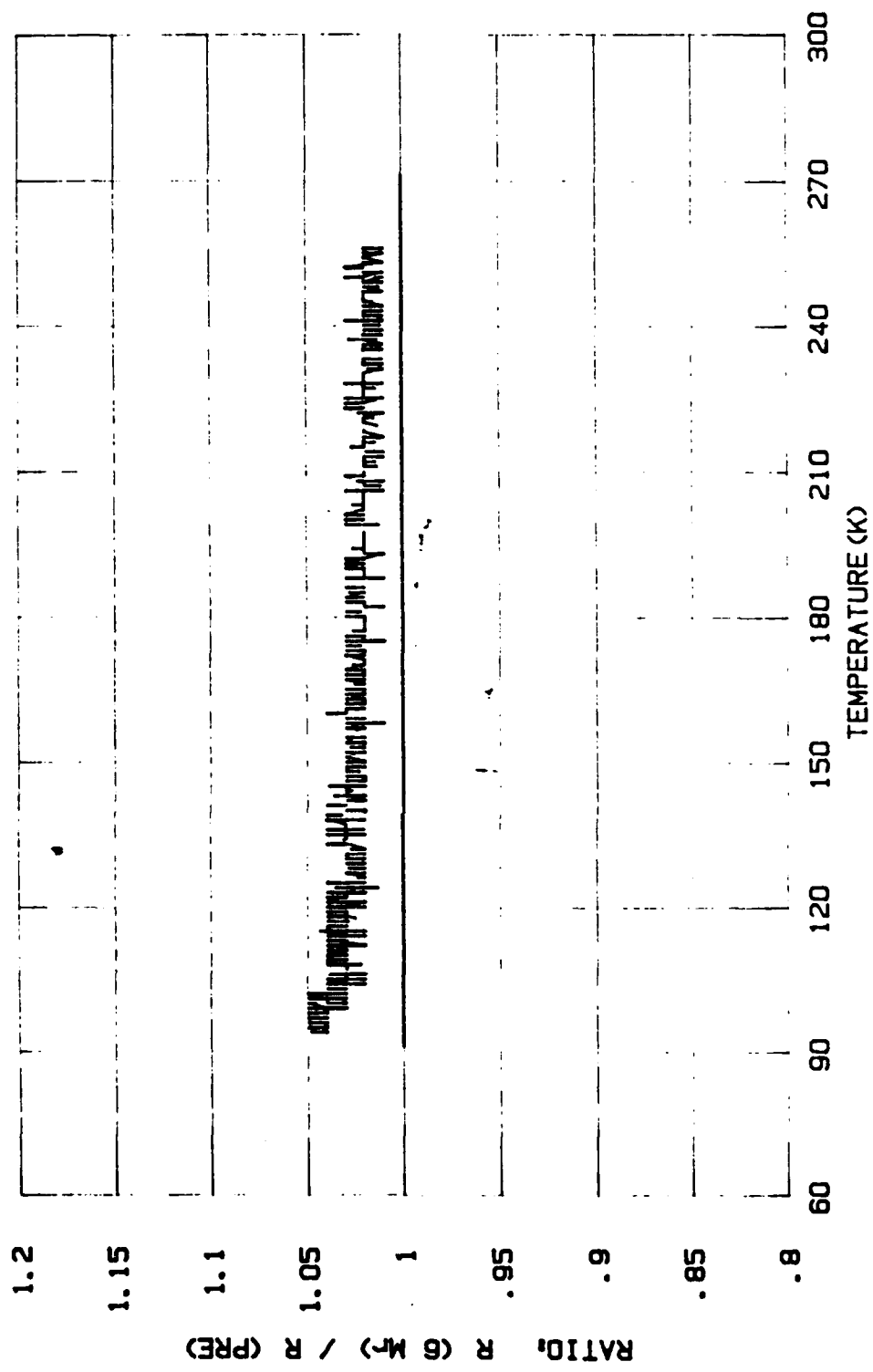


Figure 17: Plot of the ratio of post-6 megarad exposure resistance to pre-exposure resistance values.

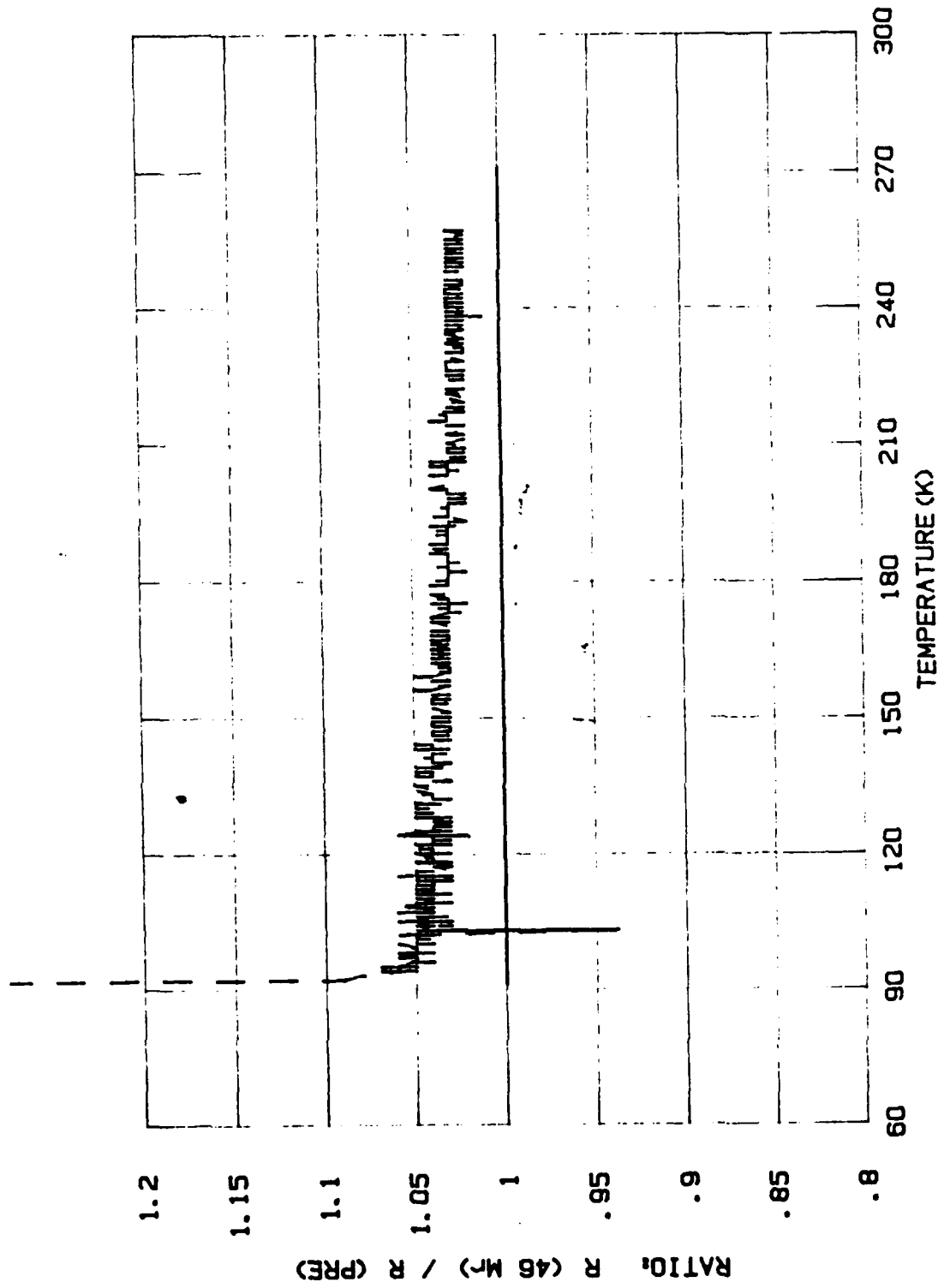


Figure 18: Plot of the ratio of post-40 megarad (46 megarad cumulative) exposure resistance to pre-exposure resistance values.

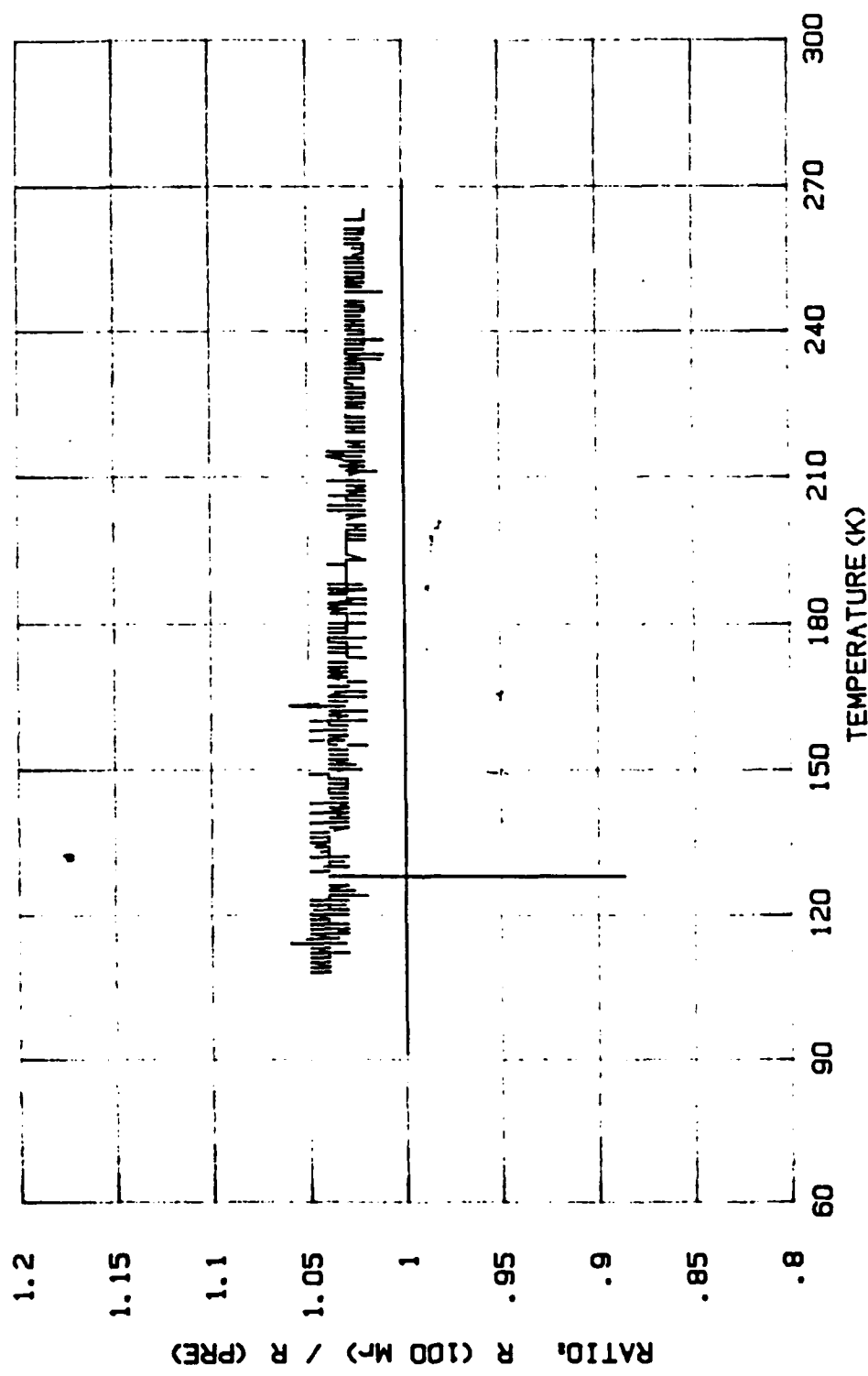


Figure 19: Plot of the ratio of post-54 megarad (100 megarad cumulative) exposure resistance to pre-exposure resistance values.

that some effect had occurred to the hot sample resulting in a shift in the normal state resistances. The accuracy of measurement is no better than the ± 2 K above the transition region.

Figures 20, 21, and 22 are overlays of resistance versus temperature prior to and after exposure to 6 megarads. In figure 20 the upper of the two curves is the post-6 megarad exposure curve. In figure 21, the pre-exposure curve has been shifted to the left by subtracting 2 K from all temperature-dependent resistance values. This causes the curves to overlay in the transition region, indicating a 2% lower shift in the transition region values. In figure 22, the pre-exposure curve has been shifted to the left by subtracting 6 K from the temperature-dependent resistance values, causing the curves to overlay in the region above the transition region. This results in 3-5% higher resistance values above the transition region.

Figures 23, 24, and 25 display resistance versus temperature curves for the pre-exposure condition of a new sample of Y123, referred to here as the "cold" sample. Figure 26 is an overlay of figures 23, 24, and 25, indicating excellent agreement above the transition region. However, it can be seen that the accuracy of measurement in the transition region was ± 2 K. Measurements were taken consecutively, with the sample cooled, warmed, and again cooled. This discrepancy in measurement accuracy in the

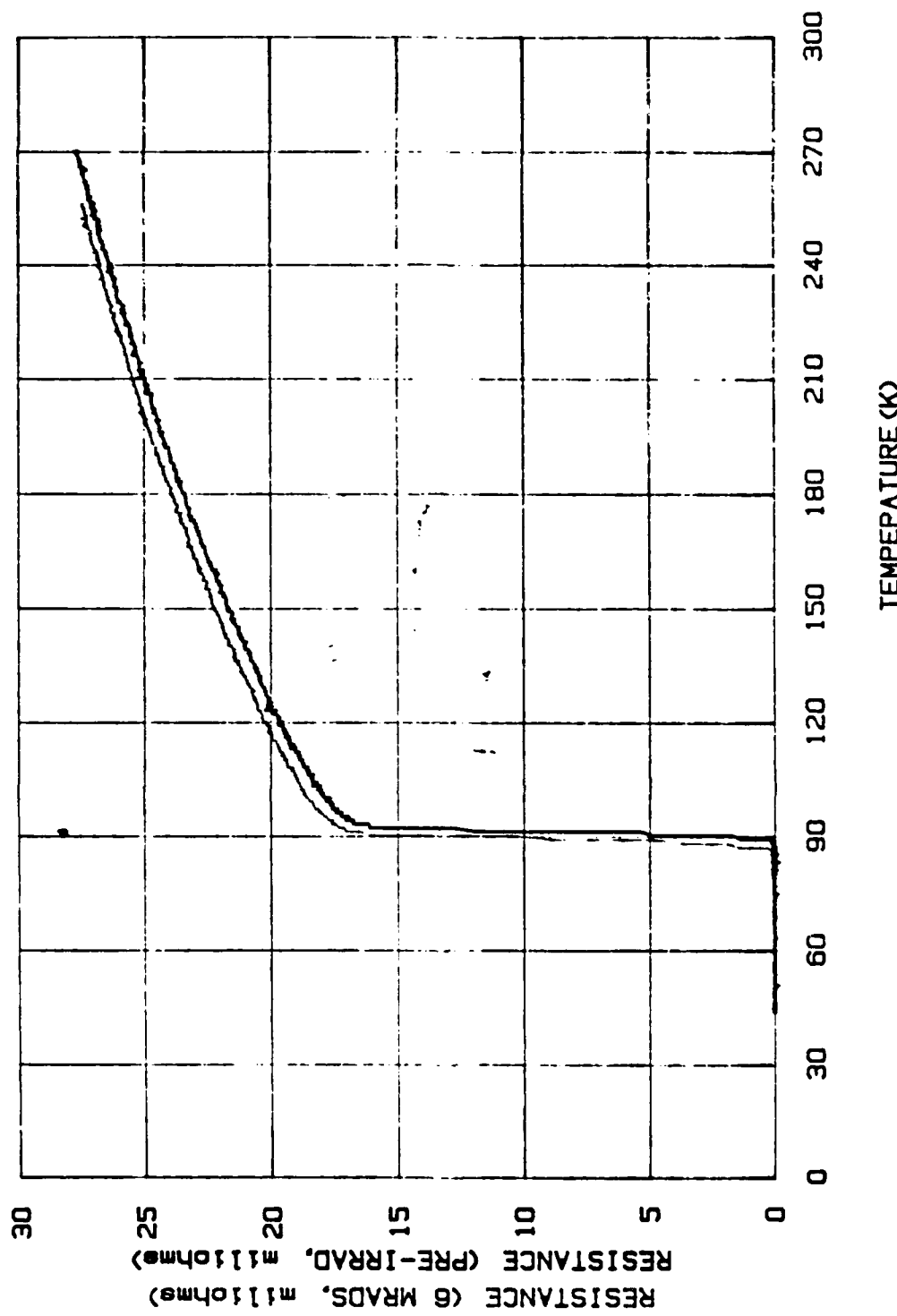


Figure 20: Resistance versus temperature overlay of pre-exposure and post-6 megarad exposure.

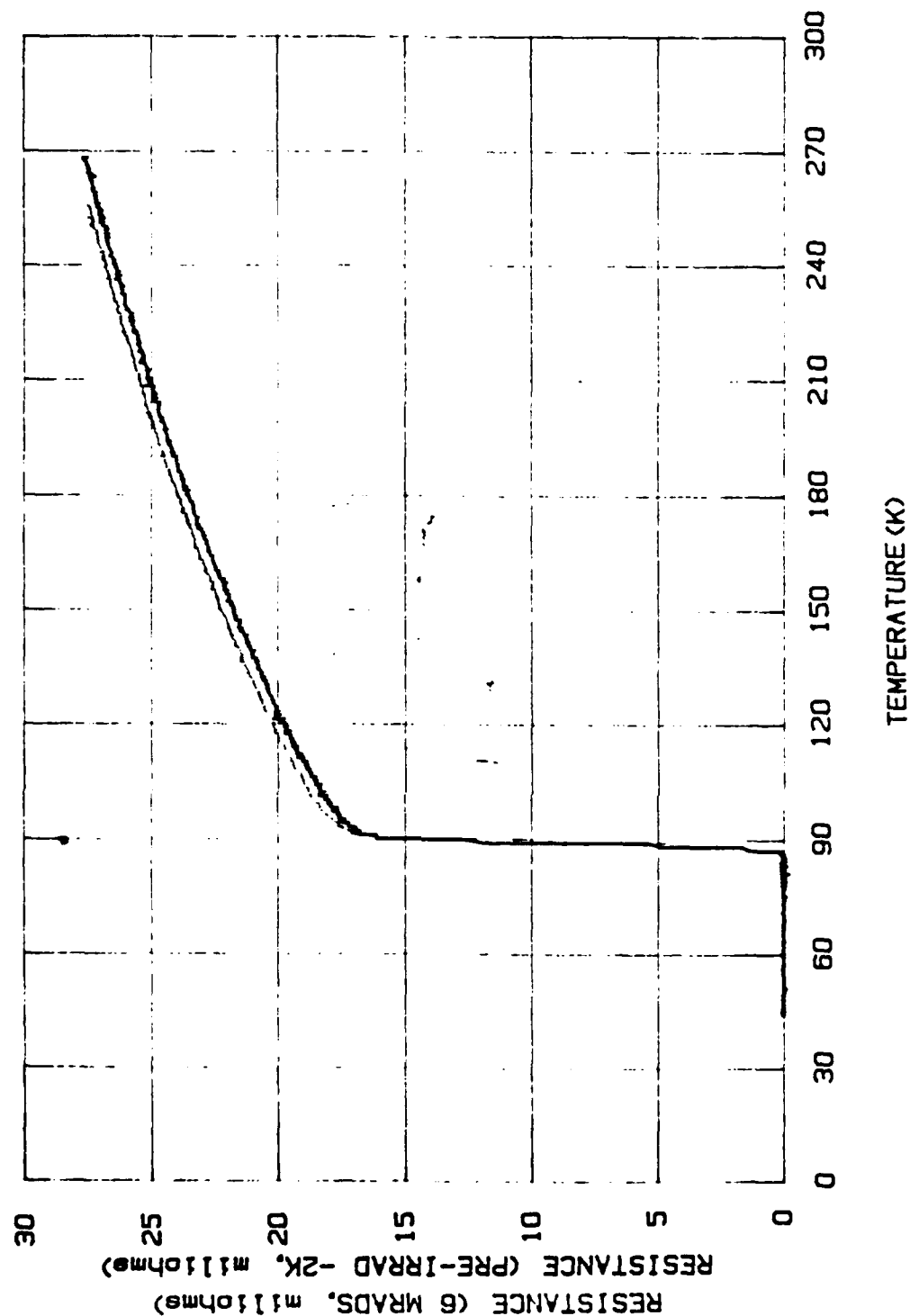


Figure 21: Resistance versus temperature overlay of pre-exposure and post-6 megarad exposure. Pre-exposure values are shifted by subtracting 2 K from the resistance values.

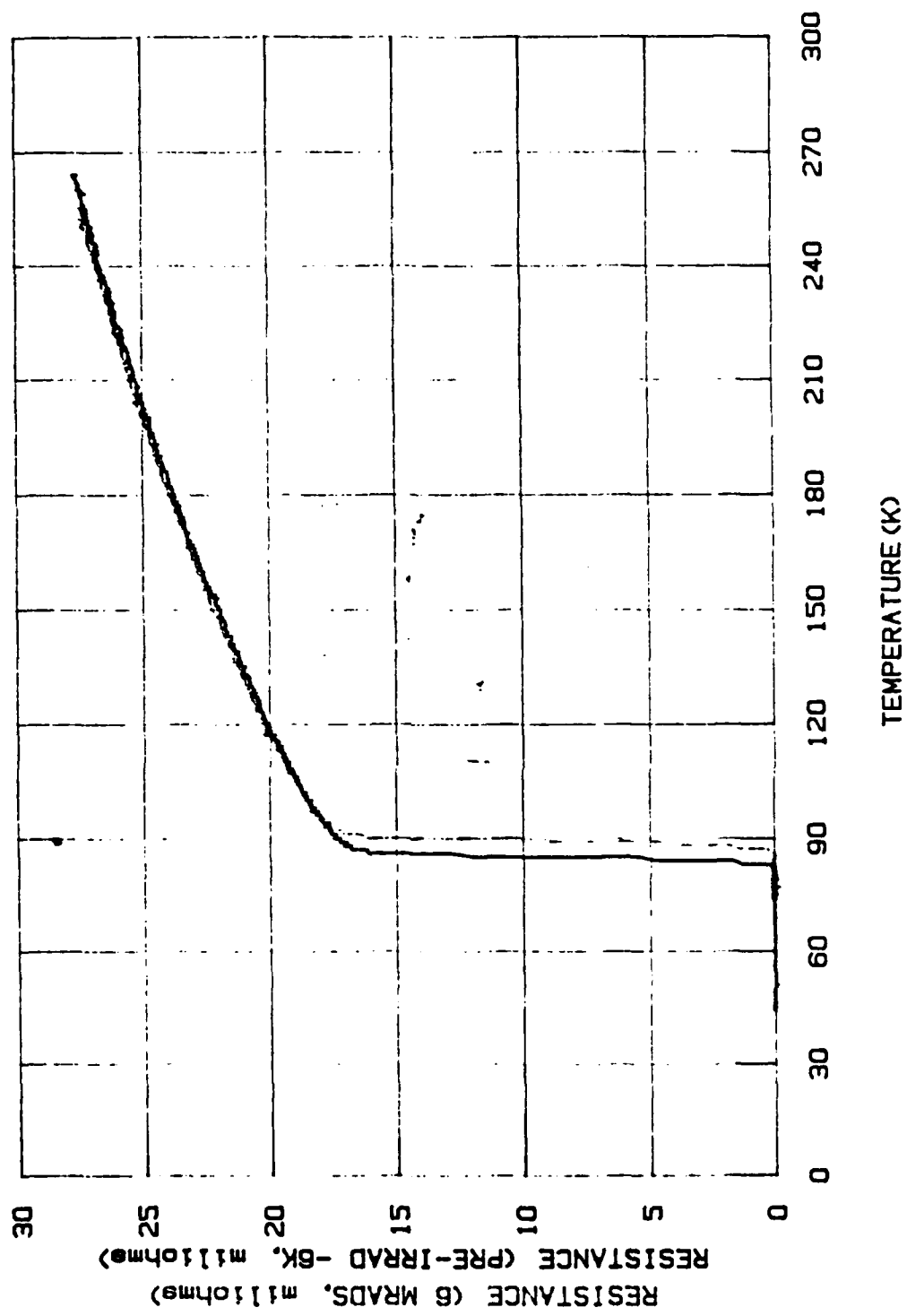


Figure 22: Resistance versus temperature overlay of pre-exposure and post-6 megarad exposure. Pre-exposure values are shifted by subtracting 6 K from the resistance values.

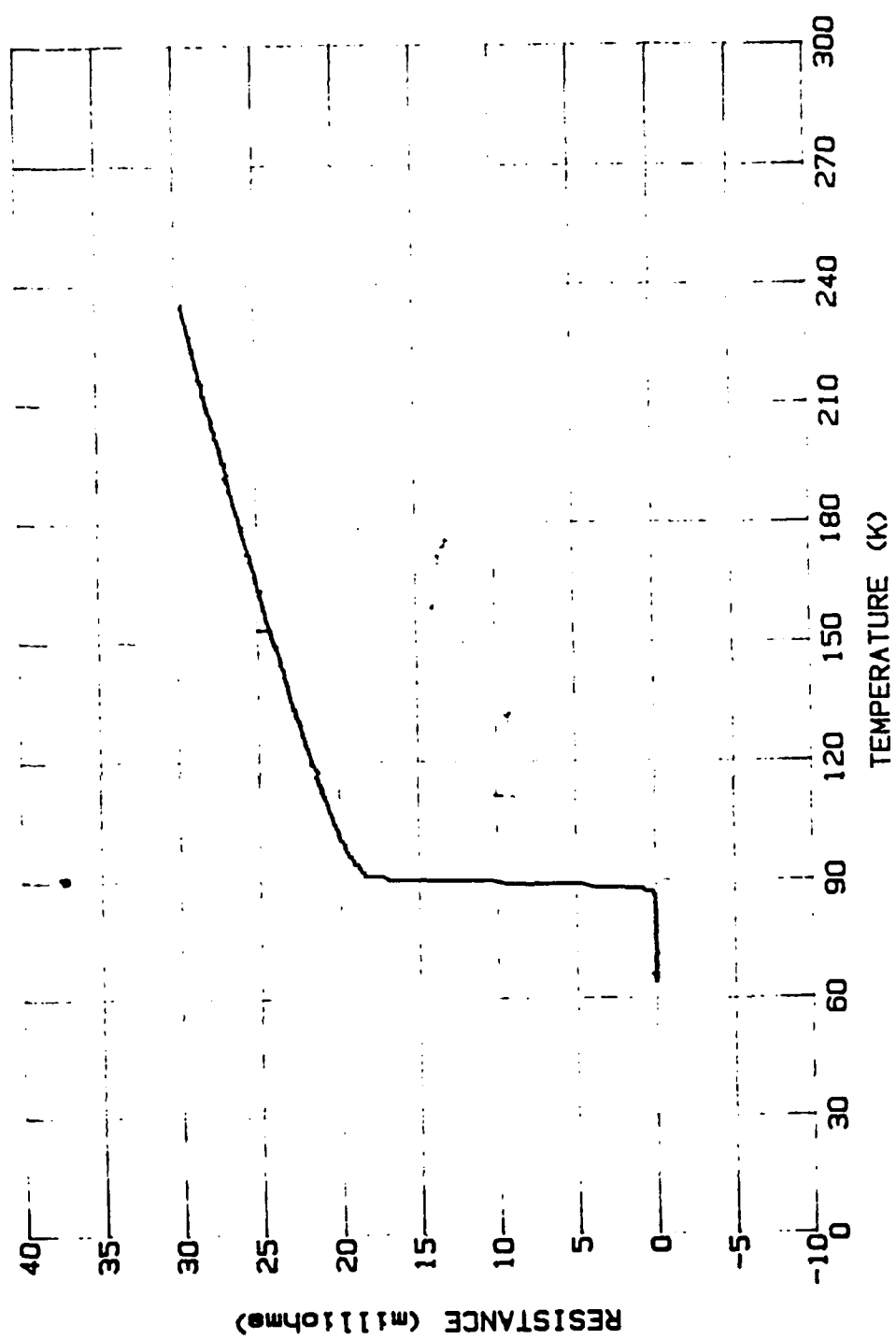


Figure 23: Resistance versus temperature curve for the cold sample, pre-exposure, during cooldown.

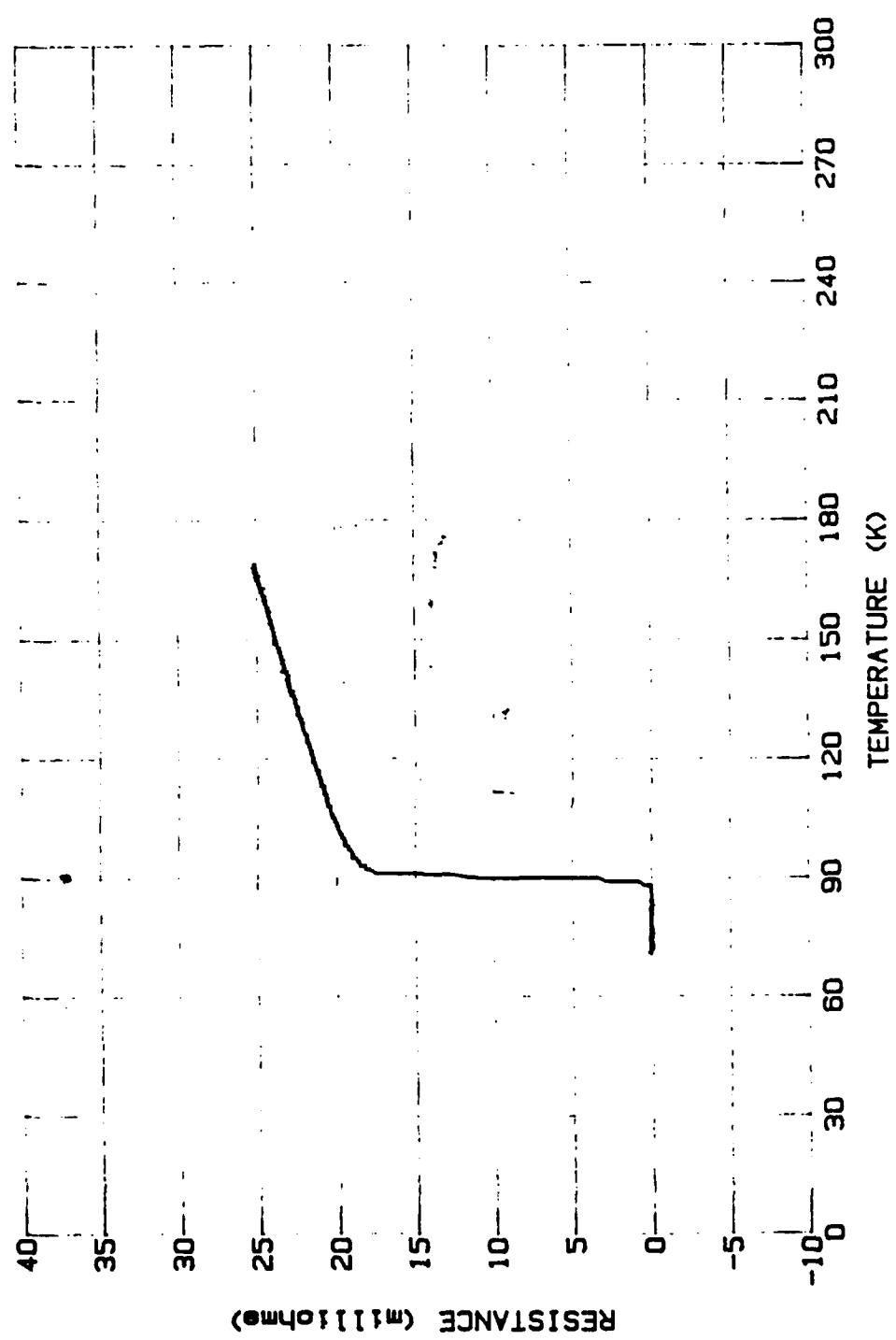


Figure 24: Resistance versus temperature curve for the cold sample, pre-exposure, during warmup.

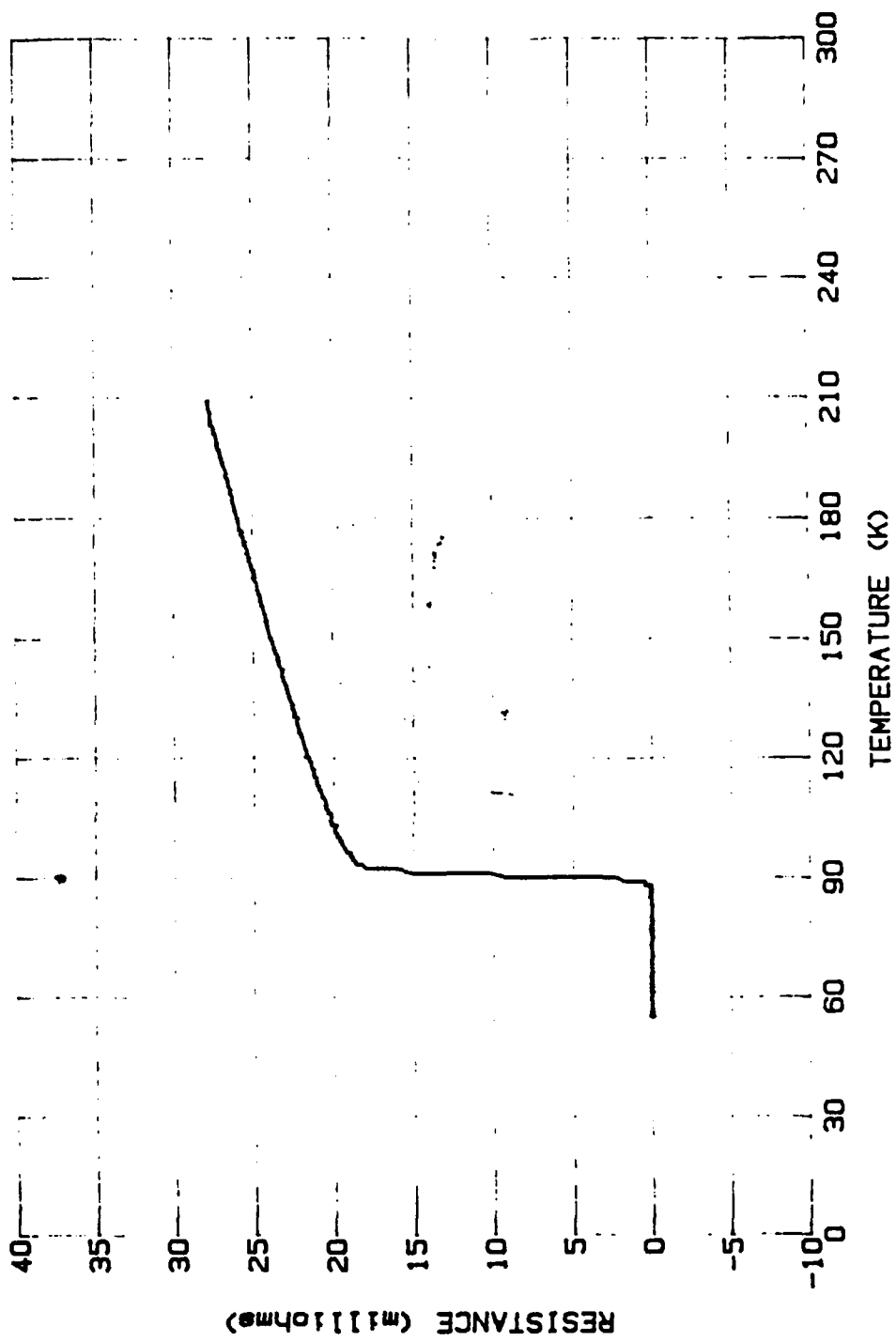


Figure 25: Resistance versus temperature curve for the cold sample, pre-exposure, during cooldown.

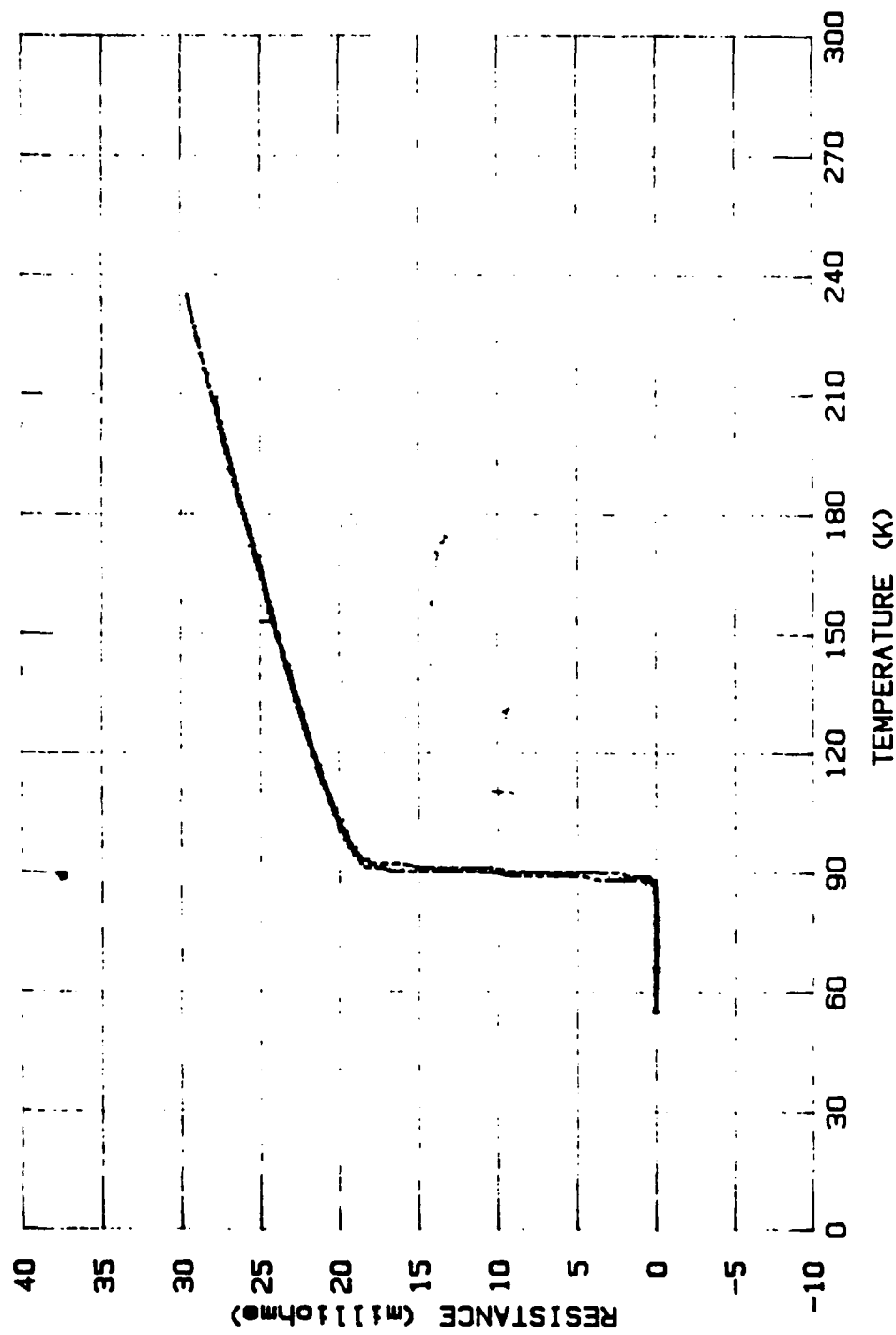


Figure 26: Overlay of resistance versus temperature for the cold sample, pre-exposure.

transition region was most likely due to the sharp change in resistance values in a small temperature region, the data sampling response rate of the temperature controller/indicator, and limited number of data sets available to be stored in the plotter channels. Figures 27 and 28 display resistance versus temperature curves during warmup and cooldown, respectively, after exposure to 1 kilorad. Figure 29 is an overlay of figures 23, 24, 25, 27, and 28. It displays the pre-exposure and post-1 kilorad exposure resistance versus temperature data. The curves fall within the expected measurement accuracy and tend to indicate that no radiation-induced effects occurred.

Figures 30, 31, and 32 display resistance versus temperature during warmup, cooldown, and cooldown after 15 hours, respectively, for the cold sample after exposure to an incremental 10 kilorads (11 kilorads cumulative dose). Figure 33 displays a resistance versus temperature after exposure to an additional 100 kilorads (111 kilorads cumulative dose). Figures 34 and 35 show resistance versus temperature curves during warmup and cooldown, respectively, after exposure to an additional 1.04 megarads (1.15 megarads cumulative dose). The slight broadening of the curves indicated that some noise entered into the data collection, either as a function of the measuring equipment, or a slight degradation of the cold sample. Figure 36 displays a resistance versus temperature curve after an additional

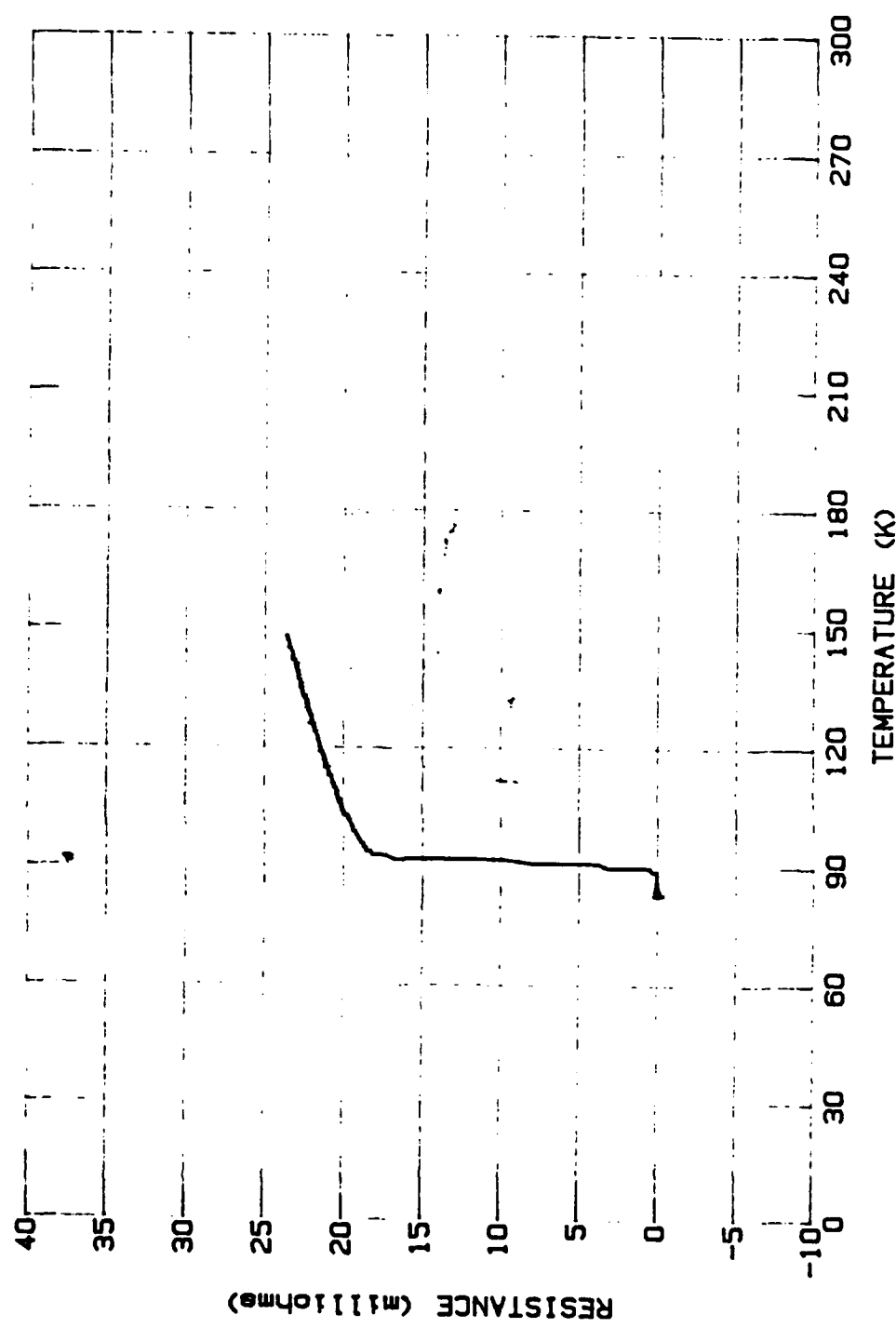


Figure 27: Resistance versus temperature curve for the cold sample after exposure to 1 kilorad, during warmup.

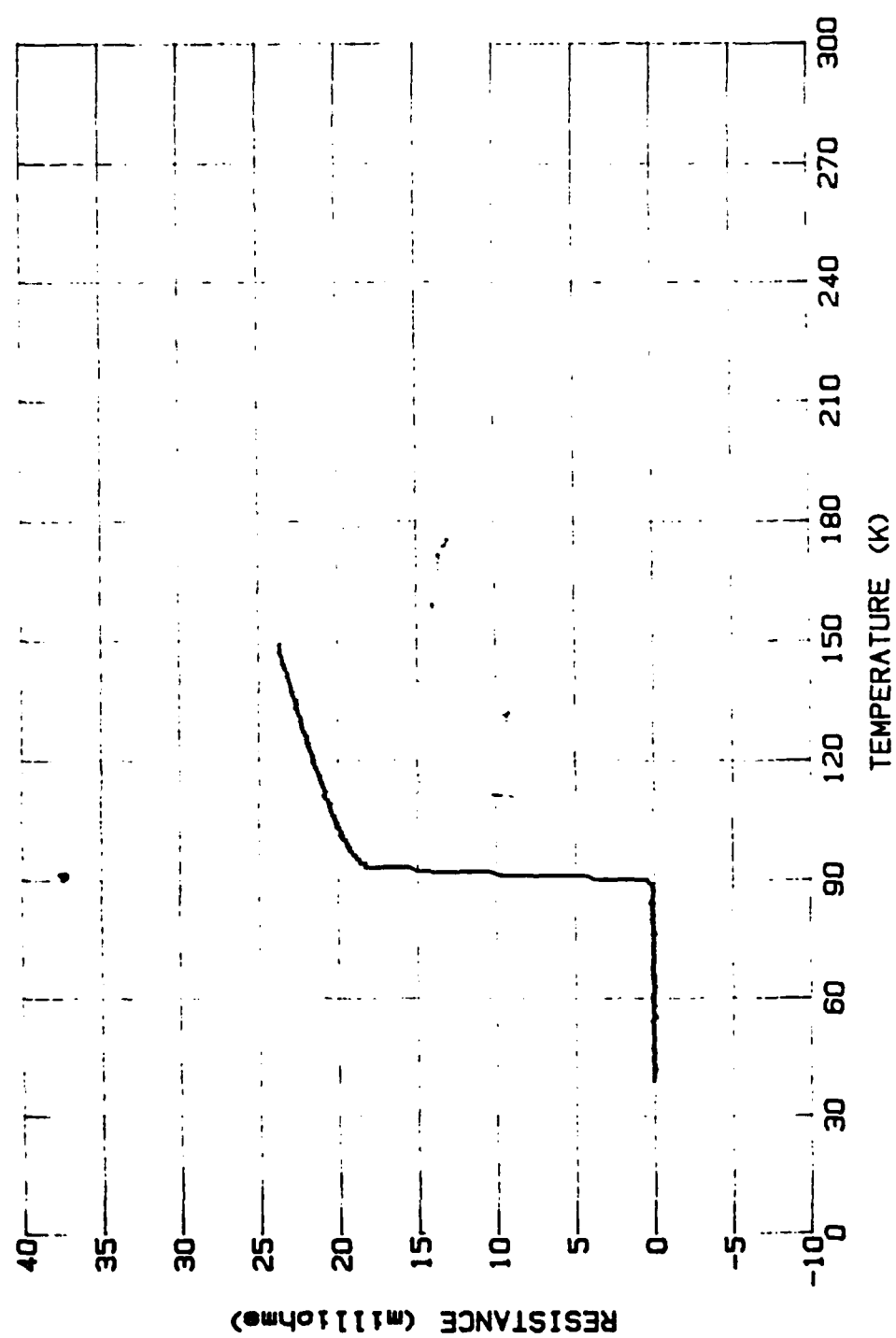


Figure 28: Resistance versus temperature curve for the cold sample after exposure to 1 kilorad, during cooldown.

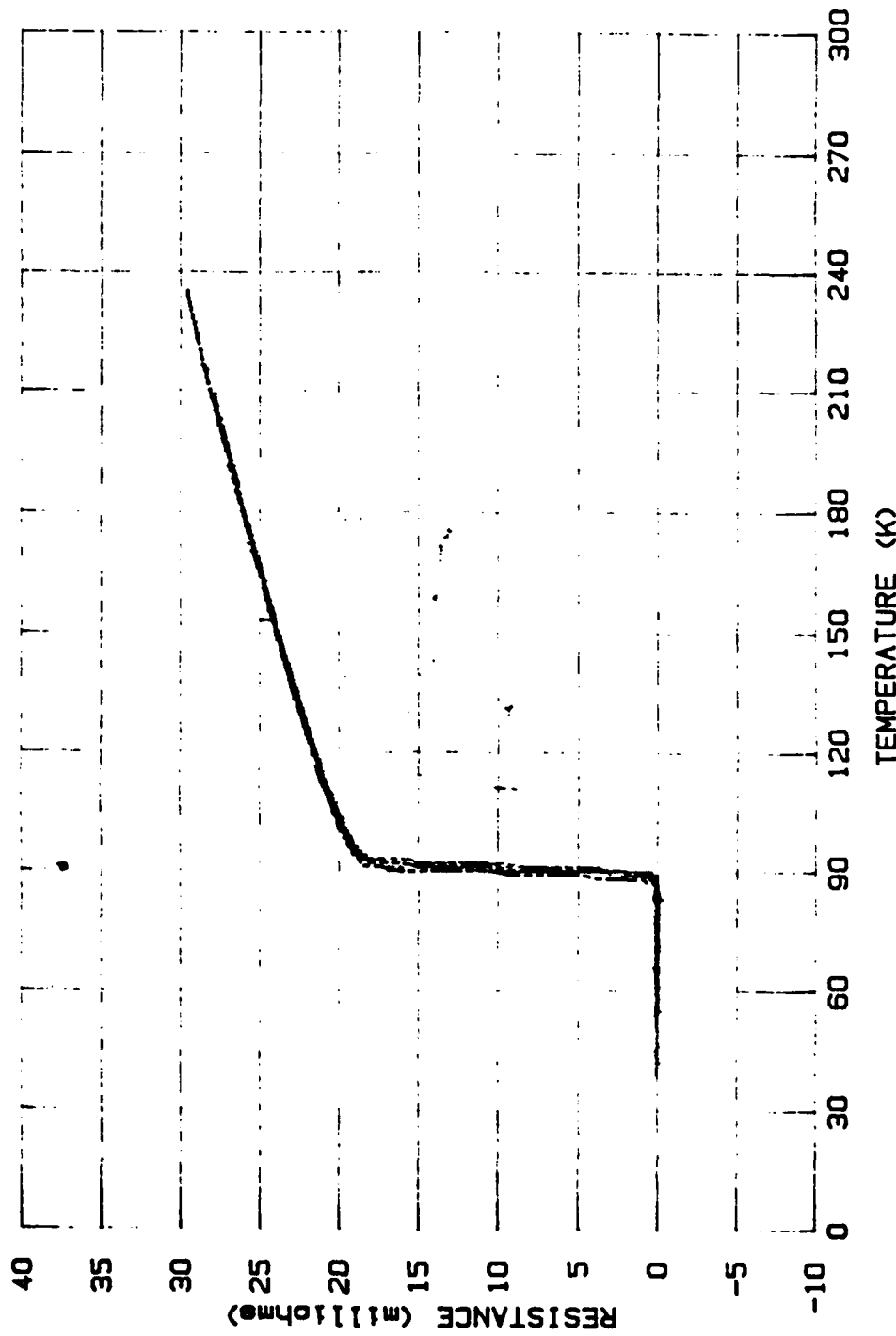


Figure 29: Overlay of resistance versus temperature curves for the cold sample, pre and post-1 kilorad exposure.

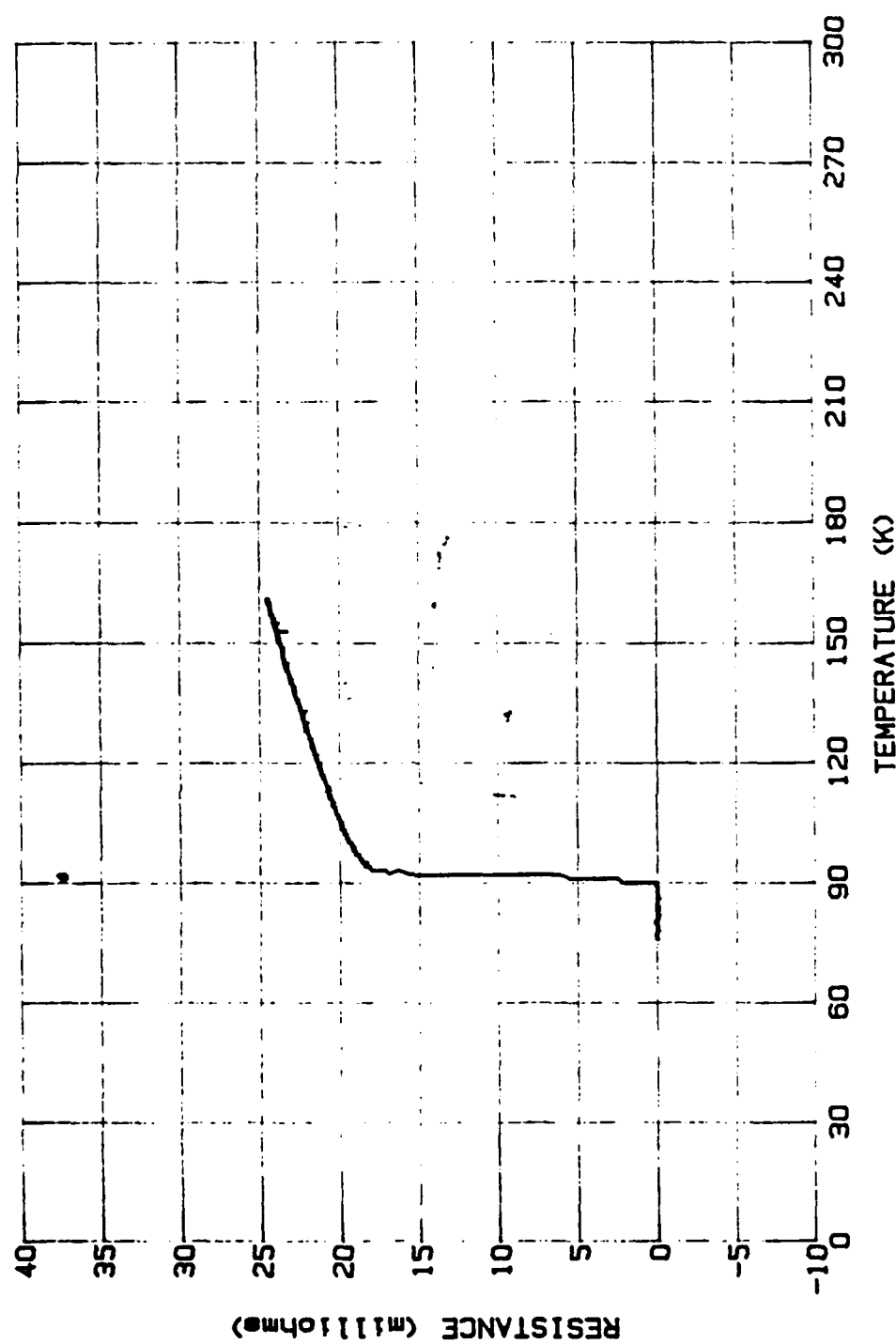


Figure 30: Resistance versus temperature curve for the cold sample after exposure to 10 kilorads (11 kilorads cumulative), during warmup.

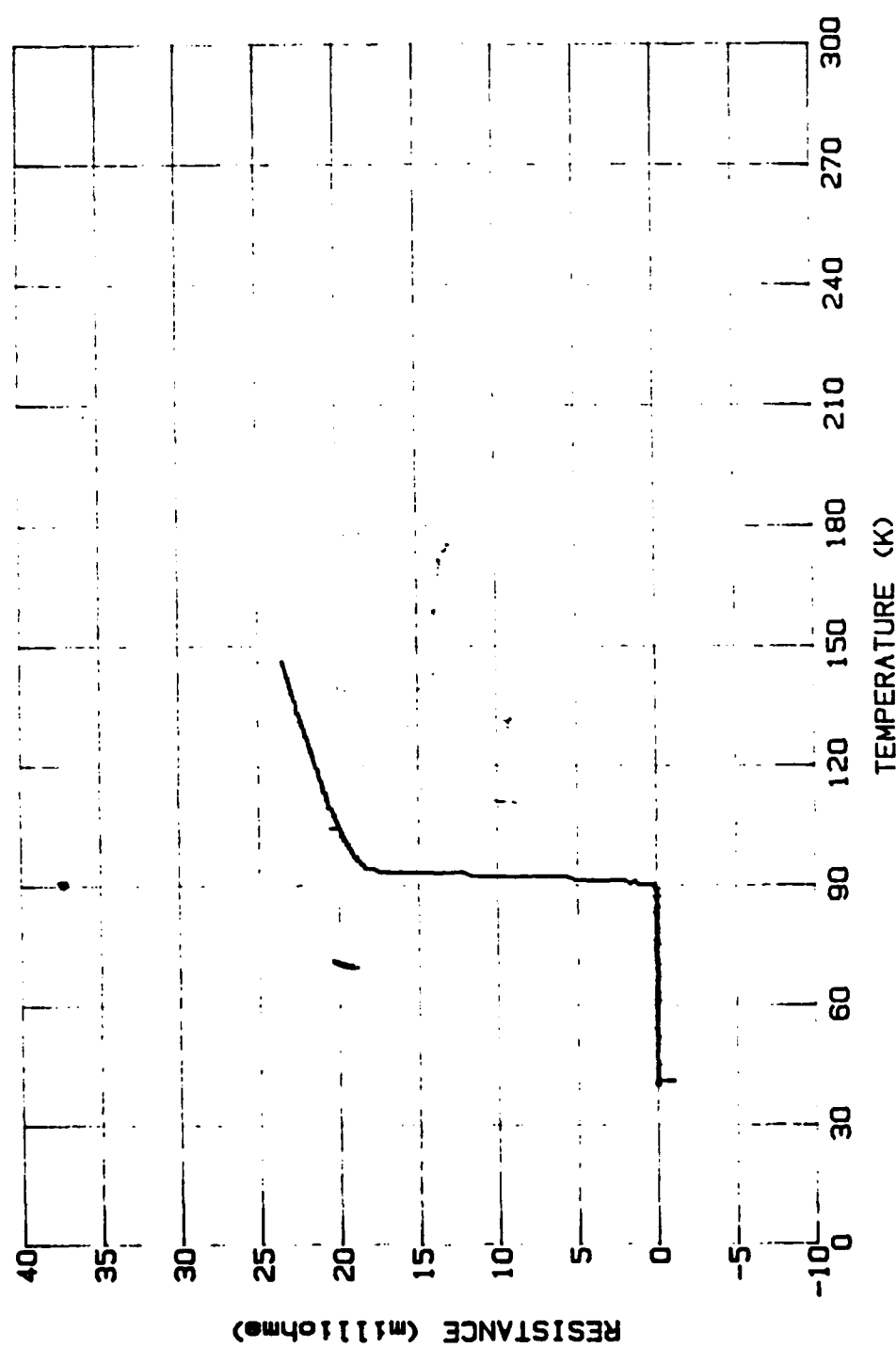


Figure 31: Resistance versus temperature curve for the cold sample after exposure to 10 kilorads (11 kilorads cumulative), during cooldown.

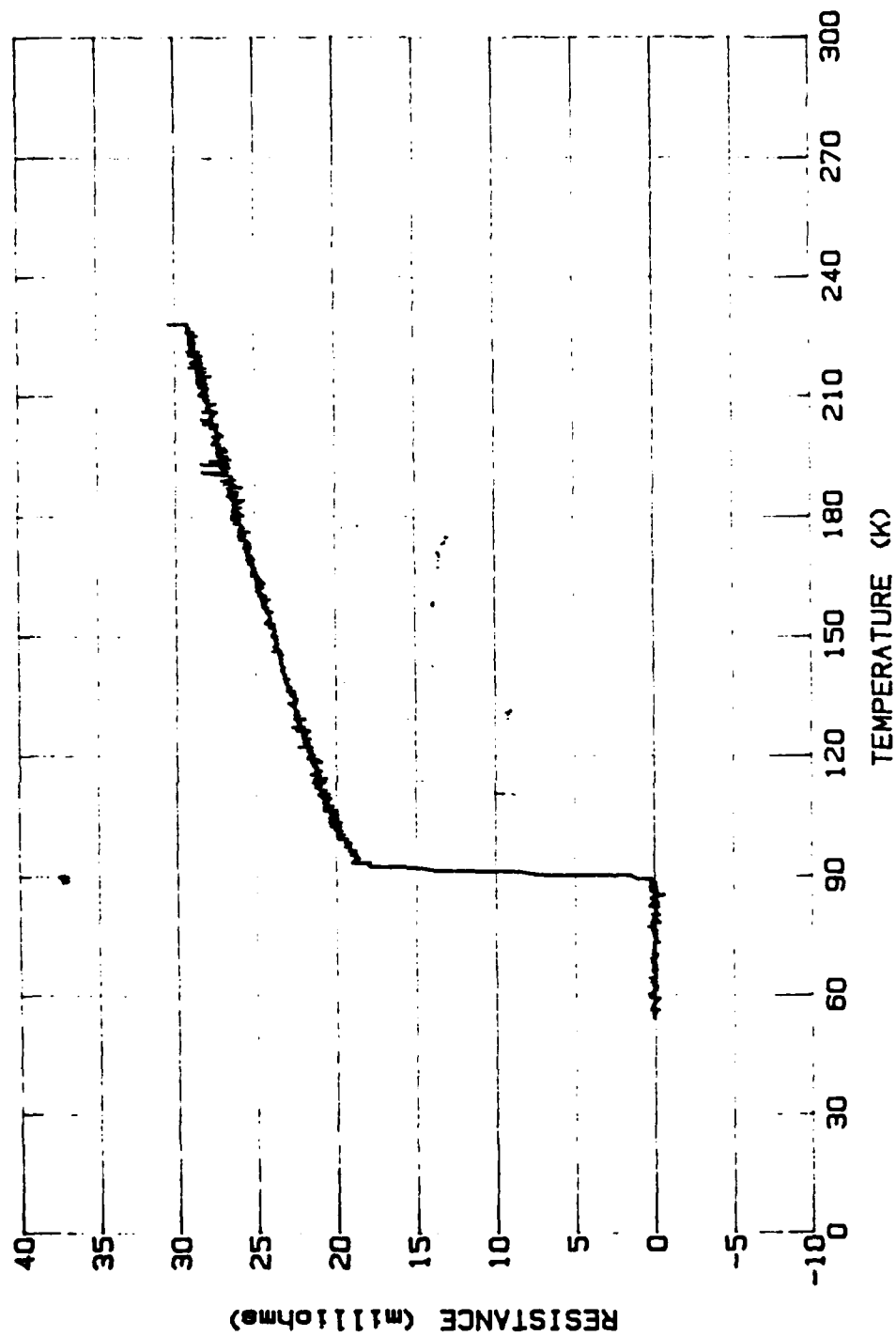


Figure 32: Resistance versus temperature curve for the cold sample after exposure to 10 kilorads (11 kilorads cumulative), during cooldown, after 15 hours.

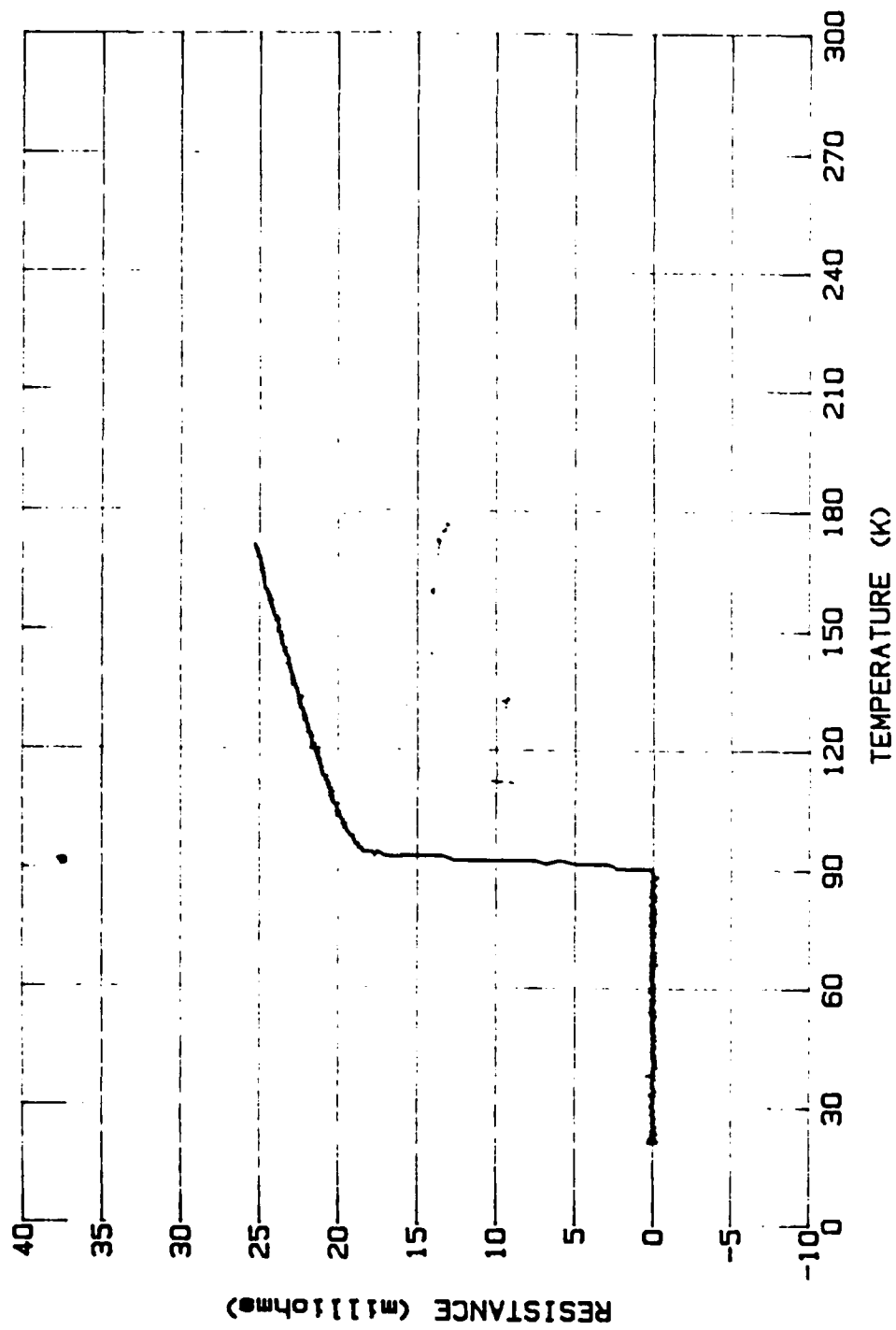


Figure 33: Resistance versus temperature curve for the cold sample after exposure to 100 kilorads (111 kilorads cumulative), during cooldown.

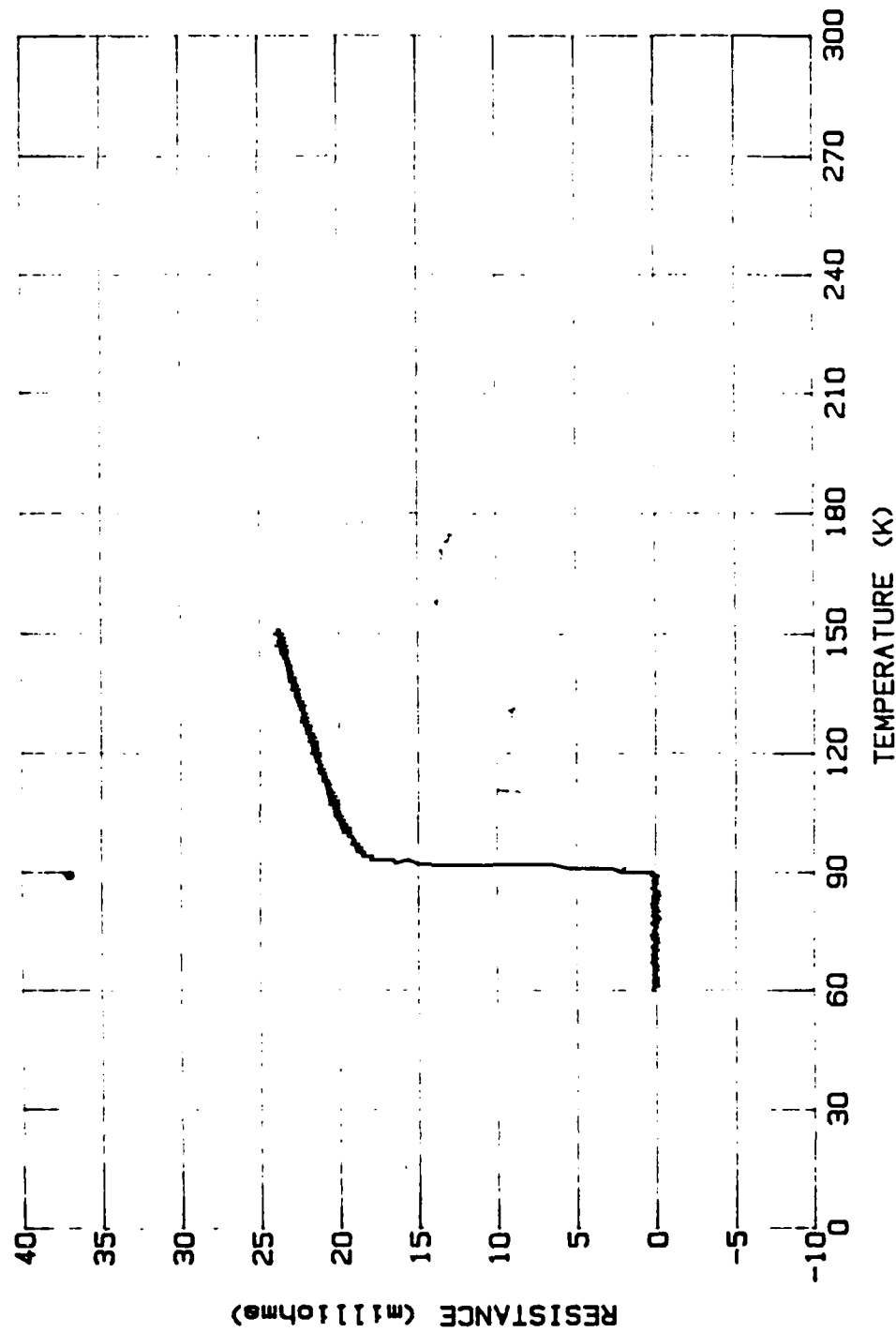


Figure 34: Resistance versus temperature curve for the cold sample after exposure to 1.04 megarads (1.15 megarads cumulative), during warmup.

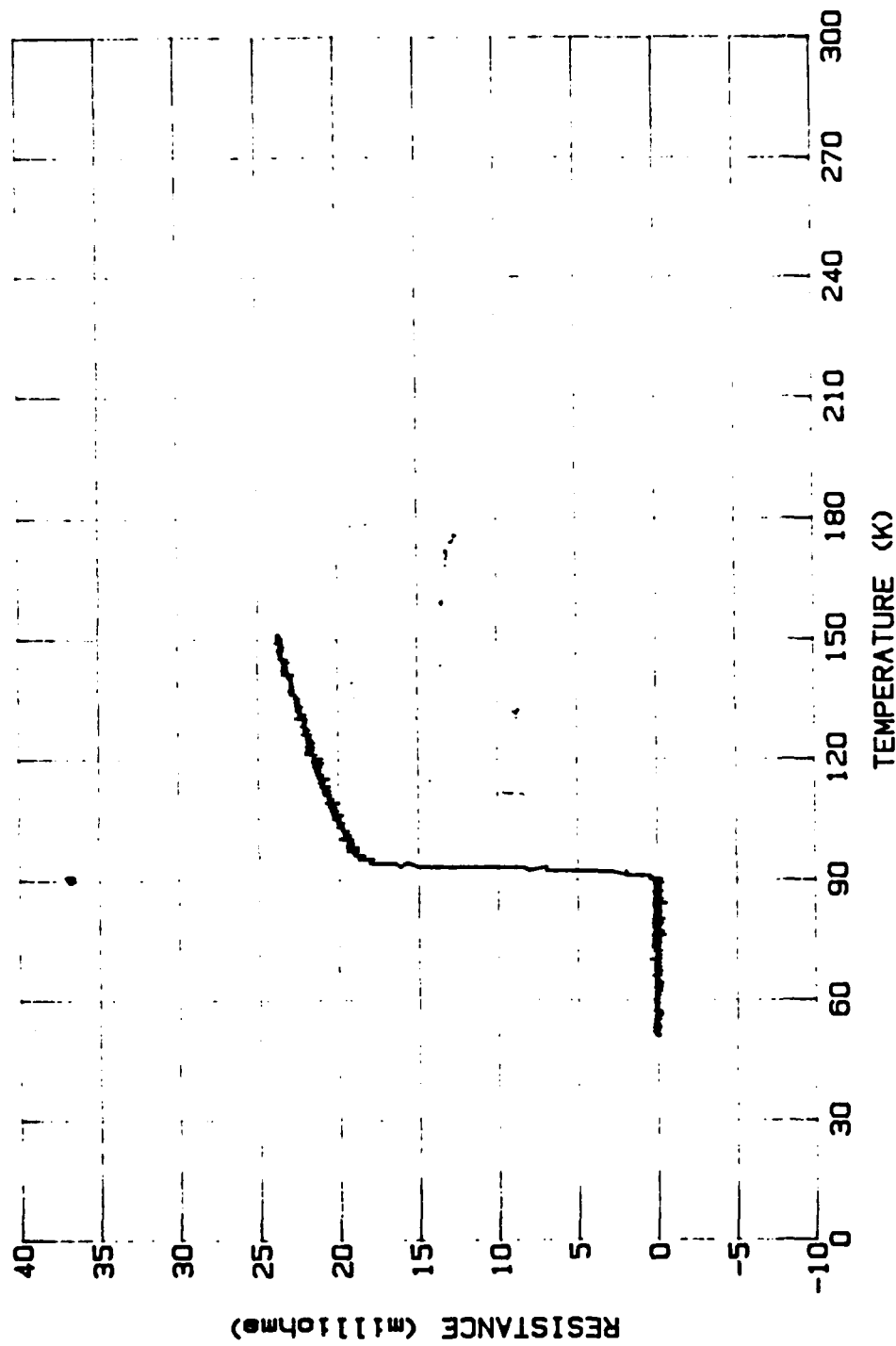


Figure 35: Resistance versus temperature curve for the cold sample after exposure to 1.04 megarads (1.15 megarads cumulative), during cooldown.

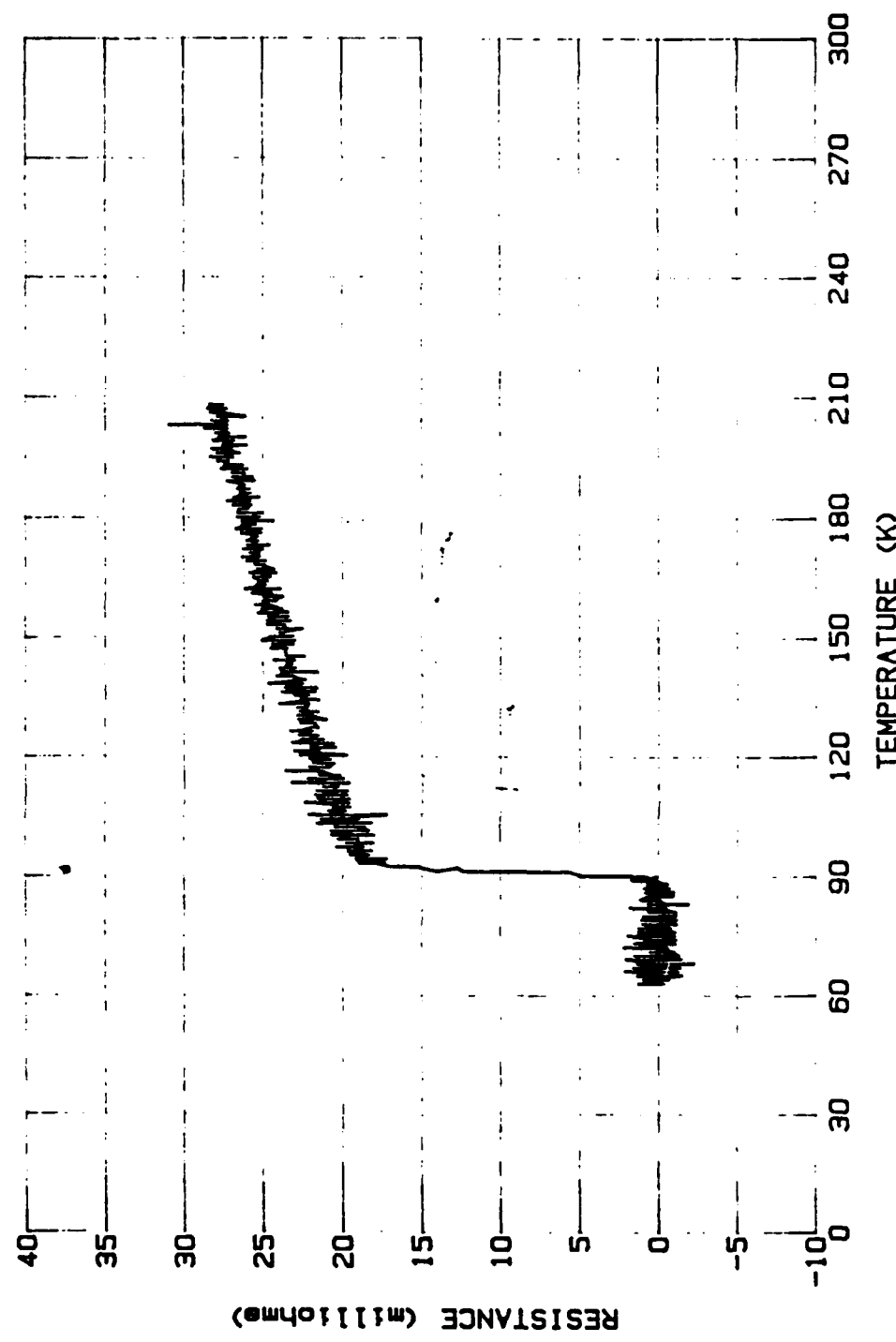


Figure 36: Resistance versus temperature curve for the cold sample after exposure to 10 megarads (11.15 megarads cumulative), during cooldown.

exposure increment to 10 megarads (11.15 megarads cumulative dose). It shows a great deal more noise in the resistance values, however the basic shape of the curve and region of location were retained. It appeared that some degradation or breakdown in the sample structure may have been occurring at this point. Figure 37 finally shows a resistance versus temperature curve after exposure to an additional 48 megarads (59.15 megarads cumulative dose). The curve was produced from data taken approximately 18 hours after exposure due to change of liquid helium dewars and a subsequent problem in keeping the dewar pressurized above 1 psig. In these measurements, sharp excursions of the resistance are observed. It is believed to be instrumental effects due to deterioration of the indium contacts and the Y123 superconducting material. Tables I and II summarize the transition region measurements, taken from the raw data, for both the hot and cold samples.

Figures 38-44 are dual-axis plots that display resistance and temperature as functions of dose. Temperatures were held constant around 30 K in figures 38-42. No significant nor consistent changes in the resistance of the sample at any levels of exposure were observed. The large negative values for resistance seen in figure 39 are not repeated, and are considered to be instrumental and of no consequence. Figures 43 and 44 are plotted using the 48 megarad exposure measurement. In this series, the temperature was allowed to rise at a

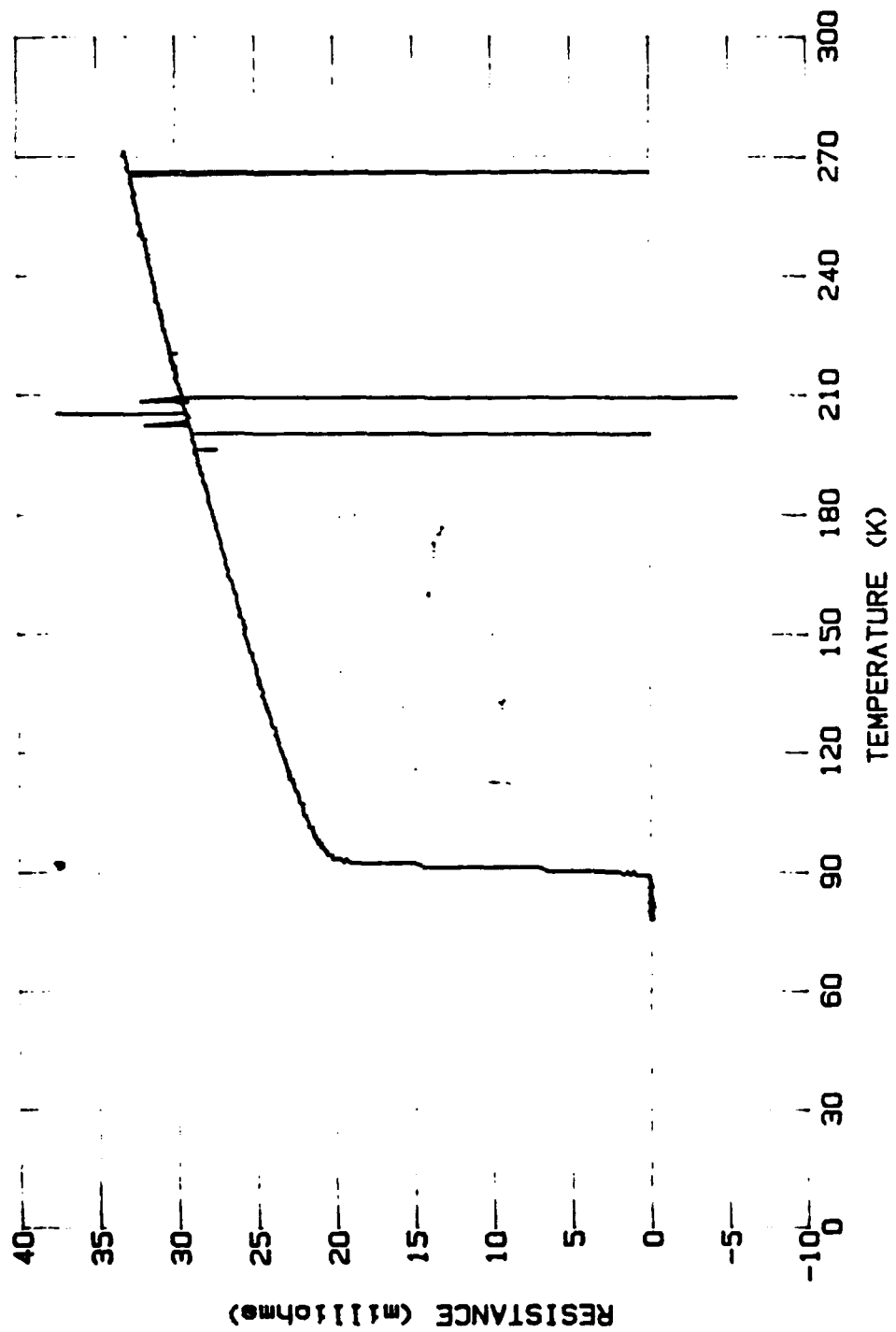


Figure 37: Resistance versus temperature curve for the cold sample after exposure to 48 megarads (59.15 megarads cumulative), during cooldown.

Sample 4 1 Krad 26 September

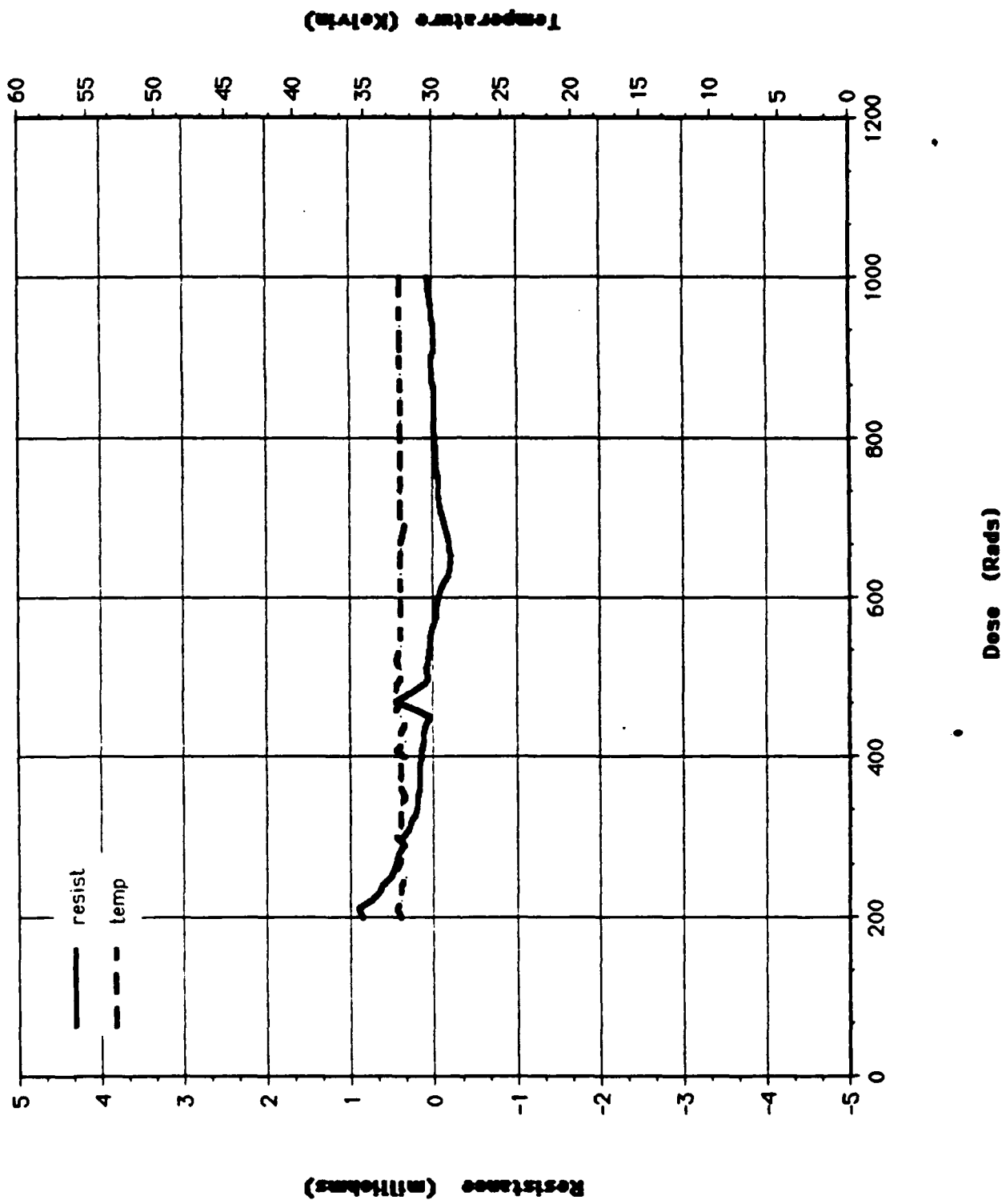


Figure 38: Dual-axis plot of resistance and temperature versus dose during exposure of the cold sample to 1 kilorad.

Sample 4 11 krads 26 September

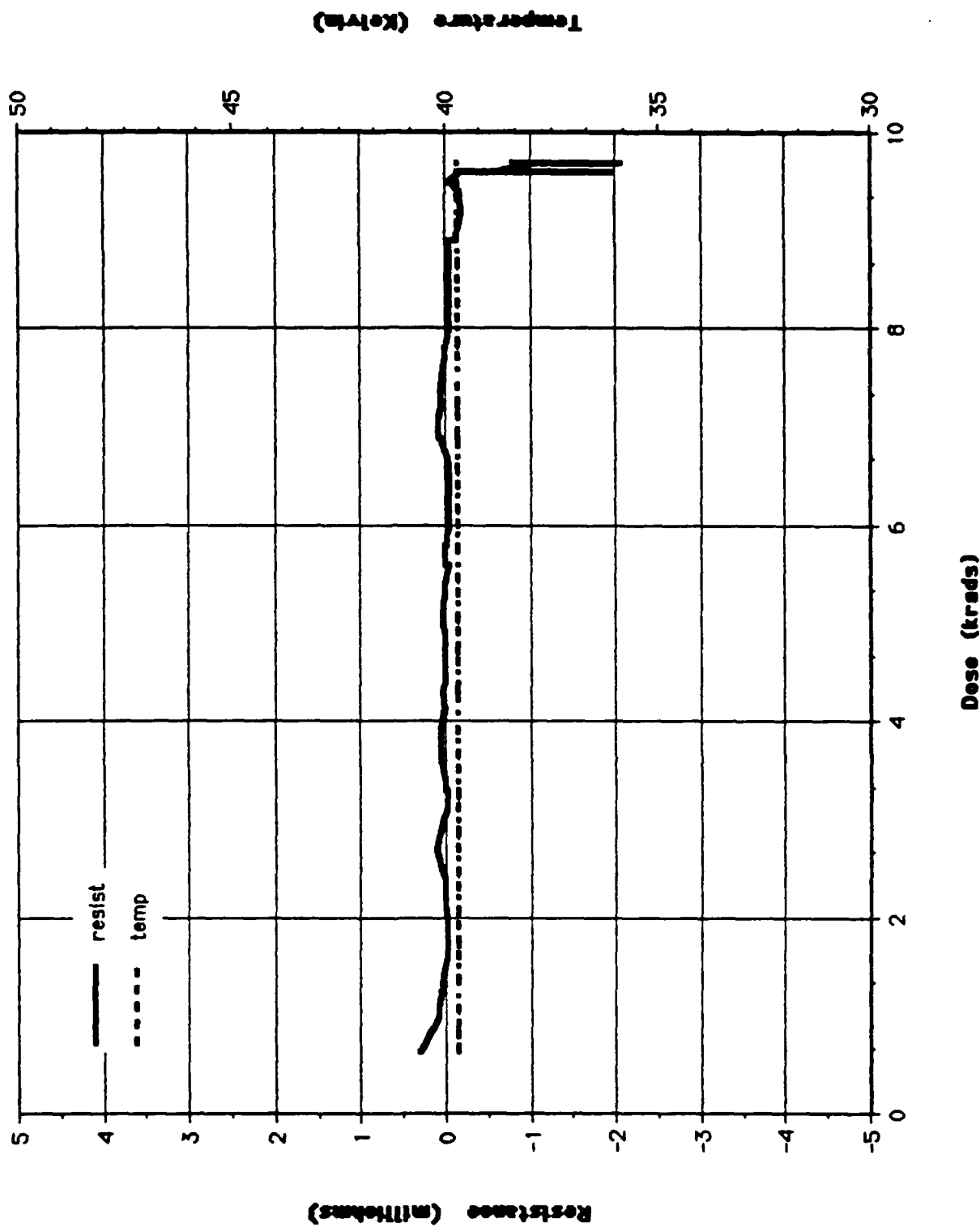


Figure 39: Dual-axis plot of resistance and temperature versus dose during exposure of the cold sample to 10 kilorads (11 kilorads cumulative).

Sample 4 111 Krad 27 September

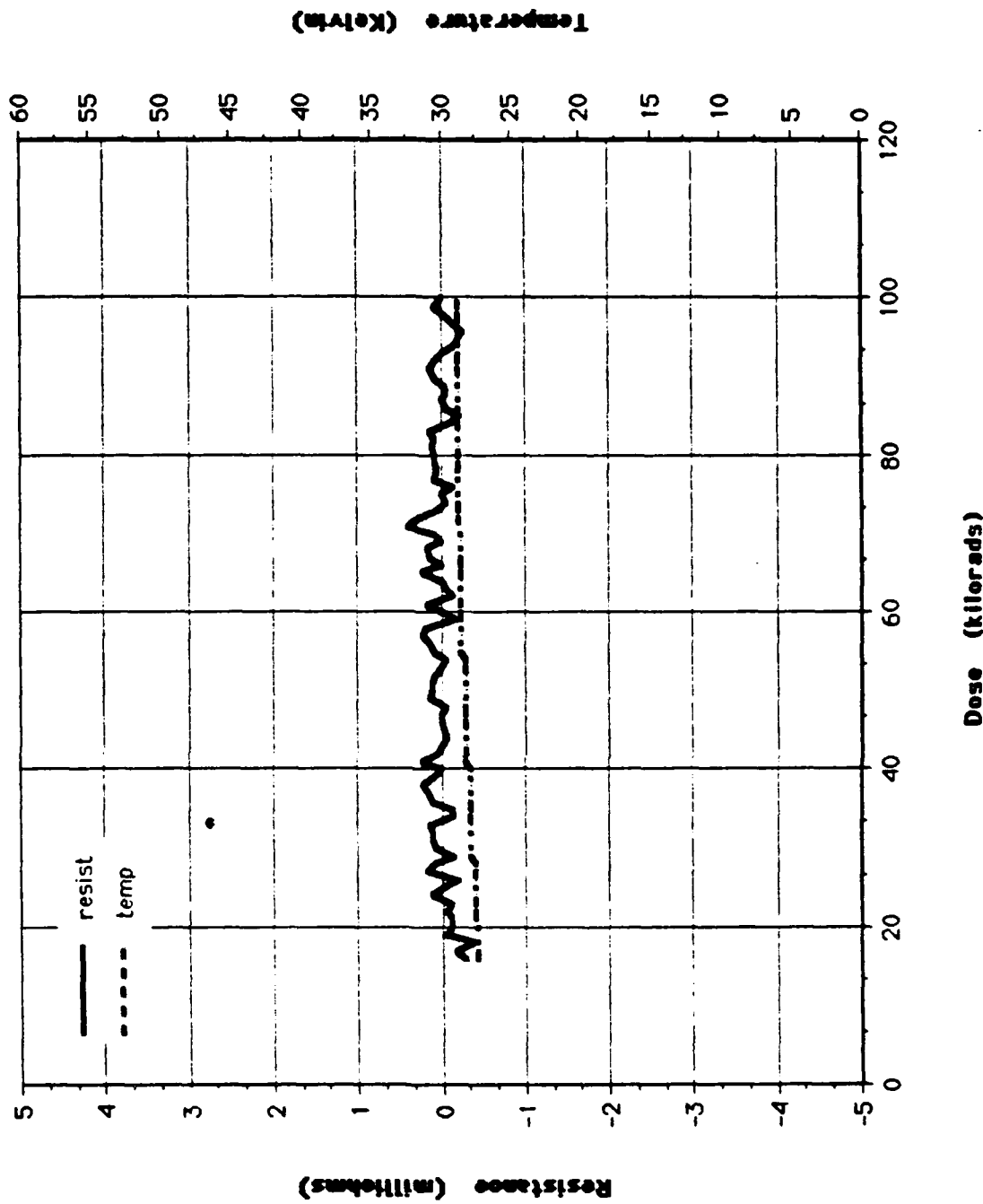


Figure 40: Dual-axis plot of resistance and temperature versus dose during exposure of the cold sample to 100 kilorads (111 kilorads cumulative).

Sample 4 1.15Mrads 27 September

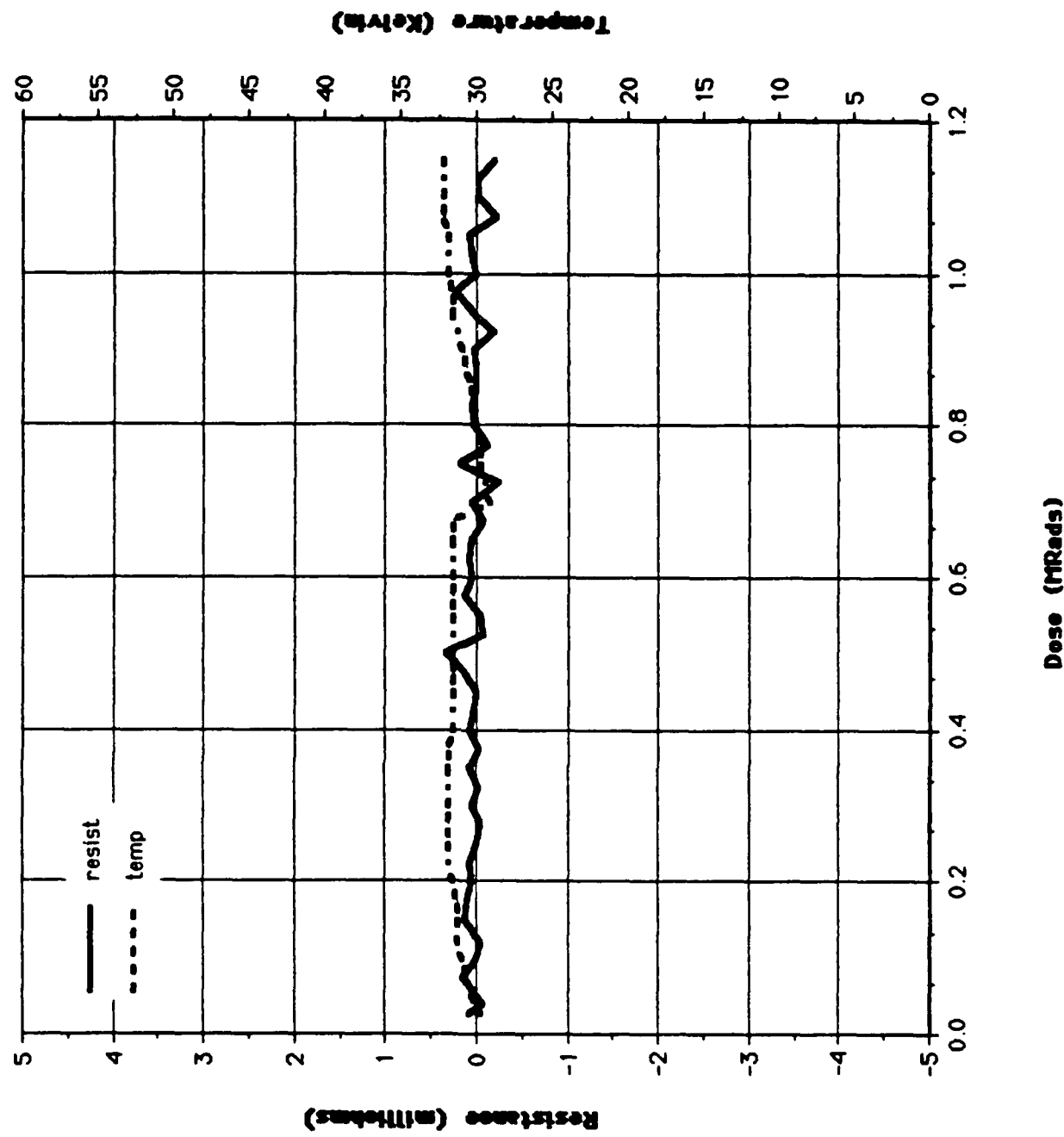


Figure 41: Dual-axis plot of resistance and temperature versus dose during exposure of the cold sample to 1.04 megarads (1.15 megarads cumulative).

Sample 4 11.15 Mrad 27 September

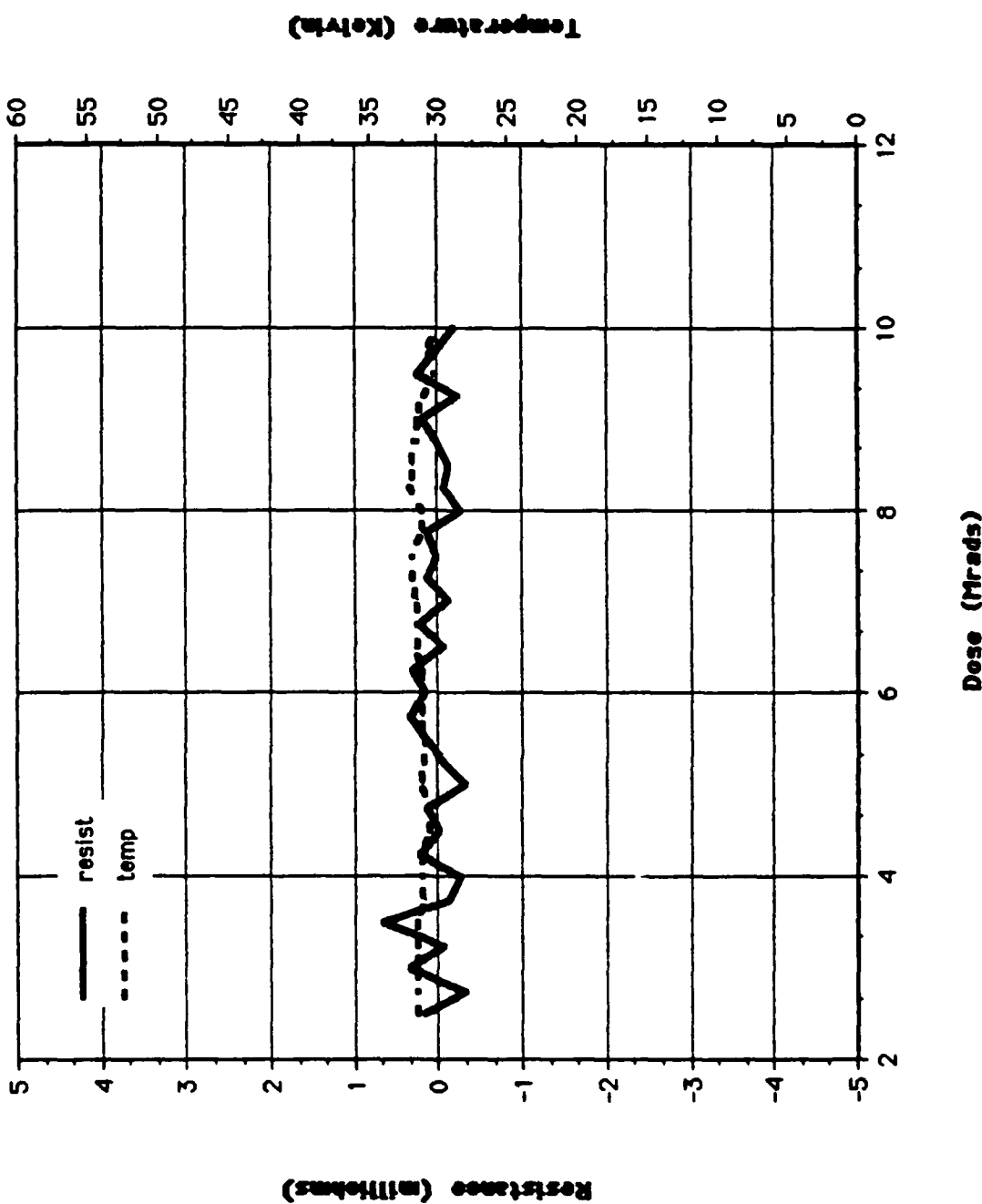


Figure 42: Dual-axis plot of resistance and temperature versus dose during exposure of the cold sample to 10 megarads (11.15 megarads cumulative).

Sample 4 48 Mrads 28 September

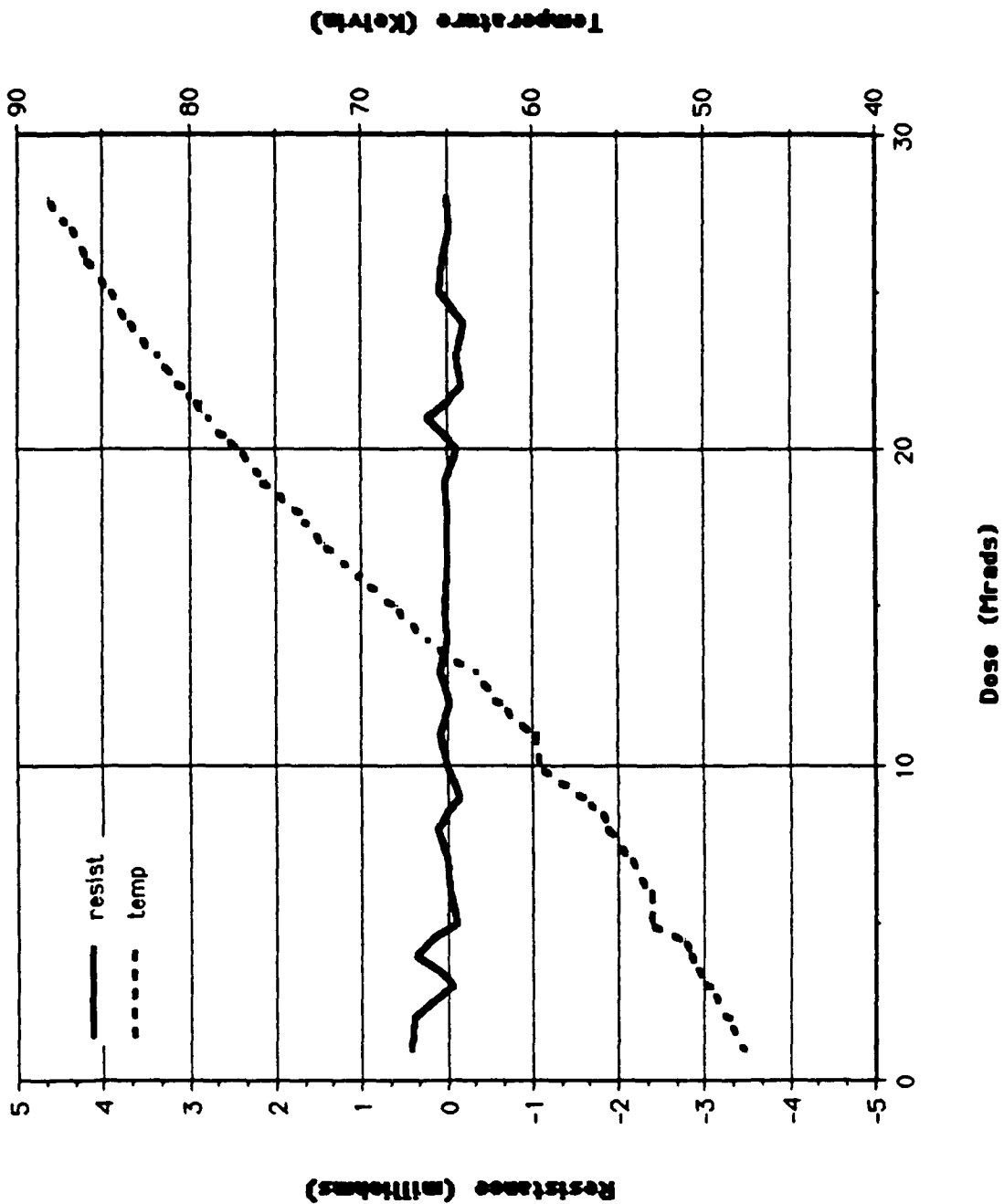


Figure 43: Dual-axis plot of resistance and temperature versus dose during exposure of the cold sample to 48 megarads (59.15 megarads cumulative) below the transition region.

Sample 4 48 Mrads 28 September

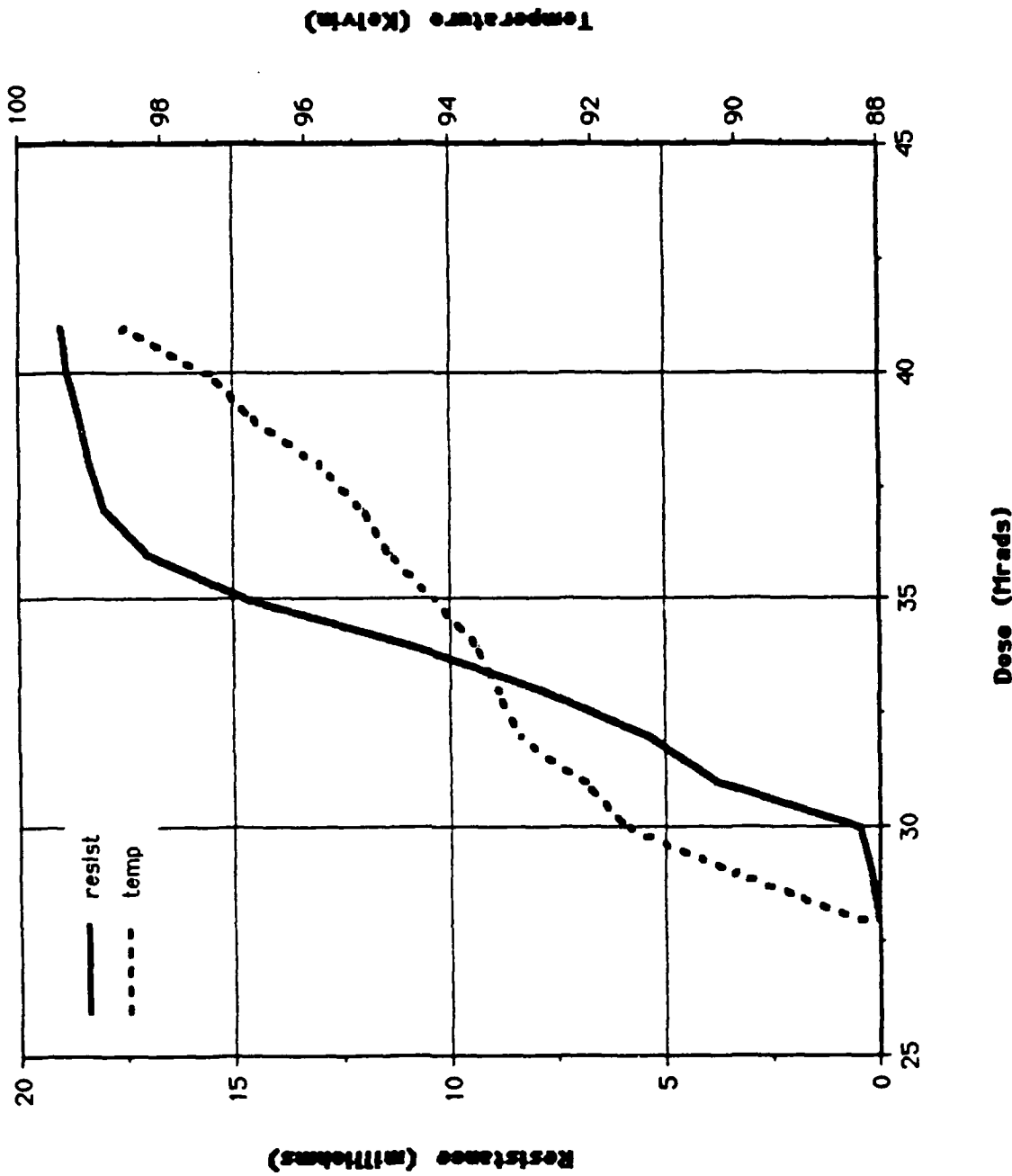


Figure 44: Dual-axis plot of resistance and temperature versus dose during exposure of the cold sample to 48 megarads (59.15 megarads cumulative) in the transition region.

TABLE I: SUMMARY OF TRANSITION REGION MEASUREMENTS FOR HOT SAMPLE PRIOR TO AND AFTER EXPOSURES TO 6, 40, AND 54 MEGARADS .

Sample Condition	Date	Dose (Rads)	Dose Cumulative (Rads)	Onset (K)	Mid Temperatures (K)	Offset (K)
Hot Cooldown	3 Aug	Pre	0	92	91	88
Hot Cooldown	4 Aug	6 M	6 M	90	89	86
Hot Cooldown	9 Aug	40 M	46 M	91	90	87
Hot Cooldown	10 Aug	54 M	100 M	91	90	87

TABLE II: SUMMARY OF TRANSITION REGION MEASUREMENTS FOR COLD SAMPLE PRIOR TO AND AFTER EXPOSURES TO 1K, 10K, 100K, 1M, 10M, AND 48 M RADARS.

Sample Condition	Date	Dose (Rads)	Dose Cumulative (Rads)	Onset (K)	Mid Temperatures		Offset (K)
					(K)	(K)	
COLD COOLDOWN	26 SEP	PRE	0	92		90	86
COLD WARMUP	26 SEP	PRE	0	92		91	86
COLD COOLDOWN	26 SEP	PRE	0	93		91	88
COLD WARMUP	26 SEP	1 K	1 K	93		92	88
COLD COOLDOWN	26 SEP	1 K	1 K	93		92	89
COLD WARMUP	26 SEP	10 K	11 K	93		92	89
COLD COOLDOWN	26 SEP	10 K	11 K	94		92	89
COLD COOLDOWN	27 SEP	10 K	11 K	93		91	89
COLD COOLDOWN	27 SEP	100 K	111 K	94		92	90
COLD WARMUP	27 SEP	1.05 M	1.15 M	93		92	89
COLD COOLDOWN	27 SEP	1.05 M	1.15 M	94		93	90
COLD COOLDOWN	28 SEP	10 M	11.15 M	93		91	89
COLD COOLDOWN	28 SEP	48 M	59.15 M	92		91	88

constant rate from 45 K through the transition region, to 99 K. In figure 44, the resistance curve is seen to rise characteristically with an increase in temperature.

B. Conclusions

The overall results of these experiments indicate that the $\text{YBa}_2\text{Cu}_3\text{O}_{6+\delta}$ superconductor in bulk form is "radiation hard". The sample referred to as the "hot" sample was exposed to incremental dose of 6, 40, and 54 megarads (6, 46, and 100 megarads cumulative). Figure 45 shows the resistance versus temperature curves for the six data sets taken for the hot sample. The lower of the resistance versus temperature curves is the pre-irradiation. The middle curve consists of three measurements, virtually plotted on top of one another, after exposure to 6, 46, and 100 megarads. It was initially thought that the normal state resistances had shifted to a higher level, after incremental exposure to 6, 40 and 54 megarads. However, it was not felt that a radiation-damaging mechanism occurred since no subsequent rise in the normal state resistance values was seen with increasing dose. It is possible that some chemical change to the sample occurred, changing the amount of oxygen atoms present. A change in the fraction between 6 and 7 is a factor in determining the transition temperature. However, before and after chemical analysis of this sample would be required to establish this. Upon removal of the sample from the cryostat it was noticed that one of the two outer indium leads evaporated onto the sample had flaked and broken off. A small excitation current is pumped through the two outer leads. A change in the

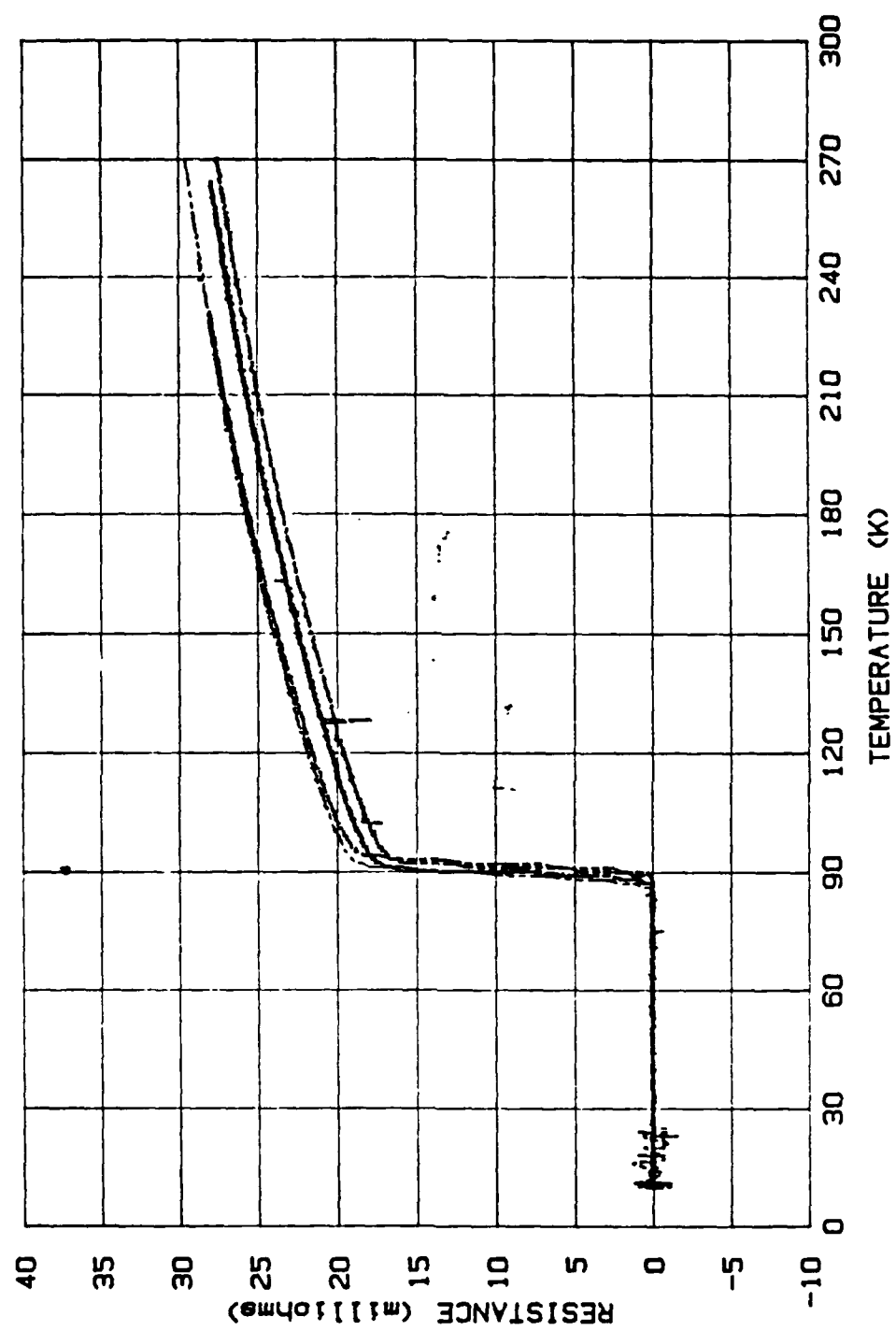


Figure 45: Overlay of all resistance versus temperature for the hot sample, including resistance versus temperature curves taken two months after exposure.

physical size of the area through which the voltage potential is measured could have accounted for the consistently higher resistances after the exposures seen in figure 45. The two uppermost curves were from data taken approximately two months after the exposures. The two curves show even higher values for normal state resistance, while no further deterioration of the indium contact was observed. The material may have exhibited a "shelf life" even though it was maintained in a humidity-free environment. The cold sample was exposed to dose increments of 1k, 10k, 100k, 1M, 10M, and 48M rads up to a cumulative total dose of 59 megarads. Figure 46 overlays all the pre and post-irradiation resistance versus temperature curves. The curves produced from data taken after exposures of 1k, 10k, 100k overlay in the region above the transition temperature, and show a \pm 2K spread in the transition region. The 1 megarad and 10 megarad curves introduce a comparatively greater amount of noise, however they are centered on the previous curves. The 48 megarad curve was less noisy, however exhibited some off-scale values and evidenced 3-5% higher value of normal state resistance. This change may be explained by contact degradation. Prior to the 48 megarad resistance versus temperature data being acquired, the cryostat was brought to atmospheric pressure and room temperature, and the liquid helium dewars changed as the one in use had become empty. The cryostat was evacuated, and the sample allowed to cool

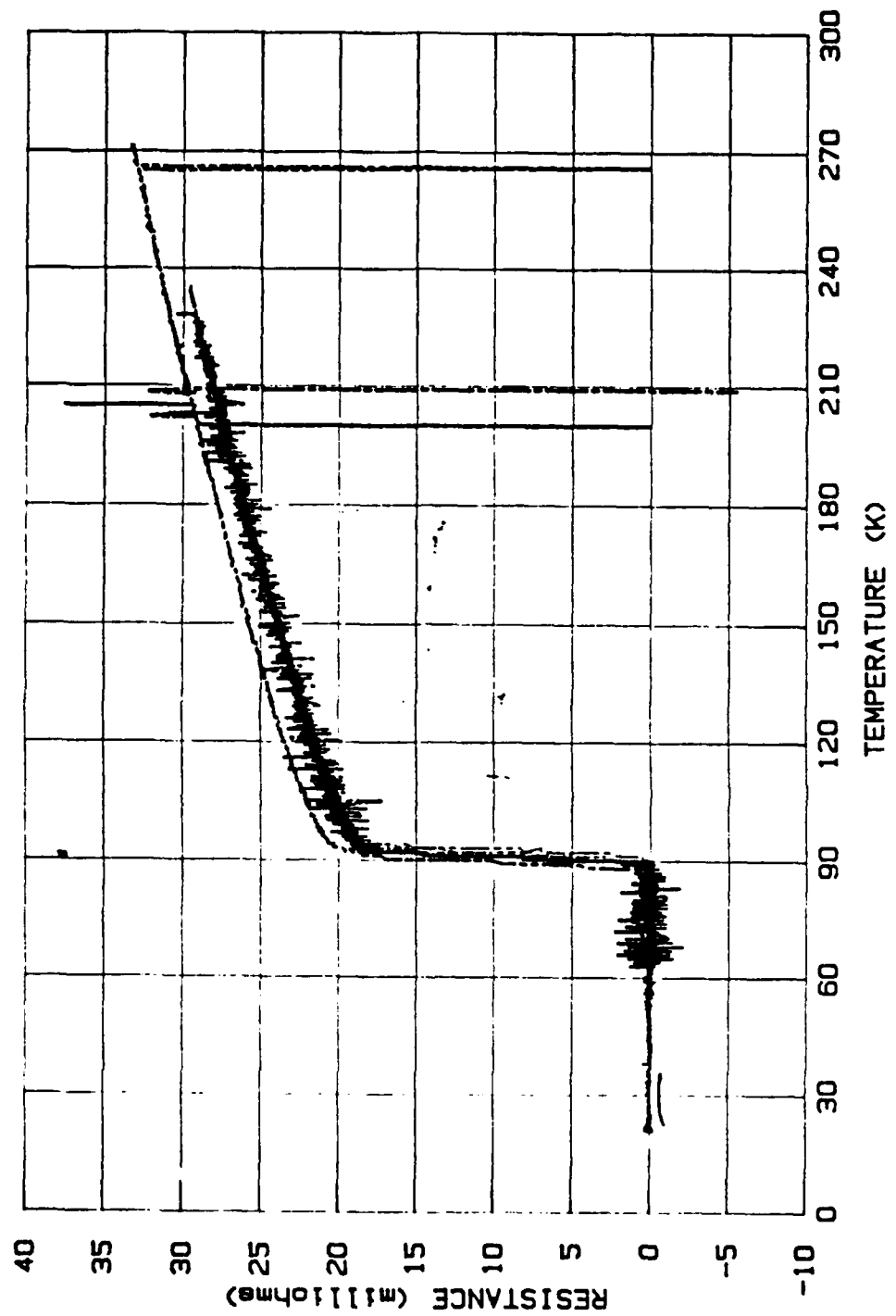


Figure 46: Overlay of all resistance versus temperature curves for the cold samples.

over a 75 minute period. Upon removal of the cold sample, it was noted that the indium contacts showed some evidence of minute flaking and granular breakup. It is concluded therefore, that the sample showed some sign of deterioration, although it was still superconducting. It is possible that damage could have occurred to individual portion(s) of the material, without the overall properties being catastrophically affected. It is more likely that the noise and shifts in resistance values are due to differing rates of thermal expansion and compressions in the materials comprising the Y123. Warmup and cooldown was repeated numerous times for each sample. This phenomena was observed by Sweigard [Ref. 1]. While evaporation of contact leads onto the material has produced a most consistent method to measure resistance data, the leads are still fragile and subject to damage through the cooldown/warmup cycles.

In summary, the Y123 material appears to be very "hard" to high energy electrons, however the material exhibits some shift in normal state resistance, probably due to the stresses involved in the cooldown/warmup cycle. The transition temperature remains unchanged within the measurement accuracy of ± 2 K. In all cases where change in resistance was observed while the sample was being exposed, the change can be attributed solely to changes in the sample temperature.

C. Recommendations

Recommendations arising from this series of experiments for future work include: (1) determination of any chemical property changes in the material after irradiations to various levels, and (2) changes to superconducting properties (normal state resistances, transition shifts) due to repeated cooldown/warmup cycling.

APPENDIX A. LINAC CHARACTERISTICS

This accelerator is a traveling wave type similar to that originally built at Stanford University. It consists of thirteen foot sub-accelerators, each powered by a klystron amplifier which delivers up to 22 megawatts peak power. The RF pulse length is 3.5 microseconds, repeated 120 times per second. The electrons are injected at 80 kilovolts and exit the accelerator at up to a maximum of 120 MeV. An average electron current of less than 1 microamp is obtained. For this experiment, the last klystron was left inactive for optimal performance of the accelerator. The beam energy was 67 MeV. Figure A1 depicts the LINAC at the Naval Postgraduate School.

NAVAL POSTGRADUATE SCHOOL
100 MEV LINEAR ACCELERATOR
BLDG 234 ROOM 001

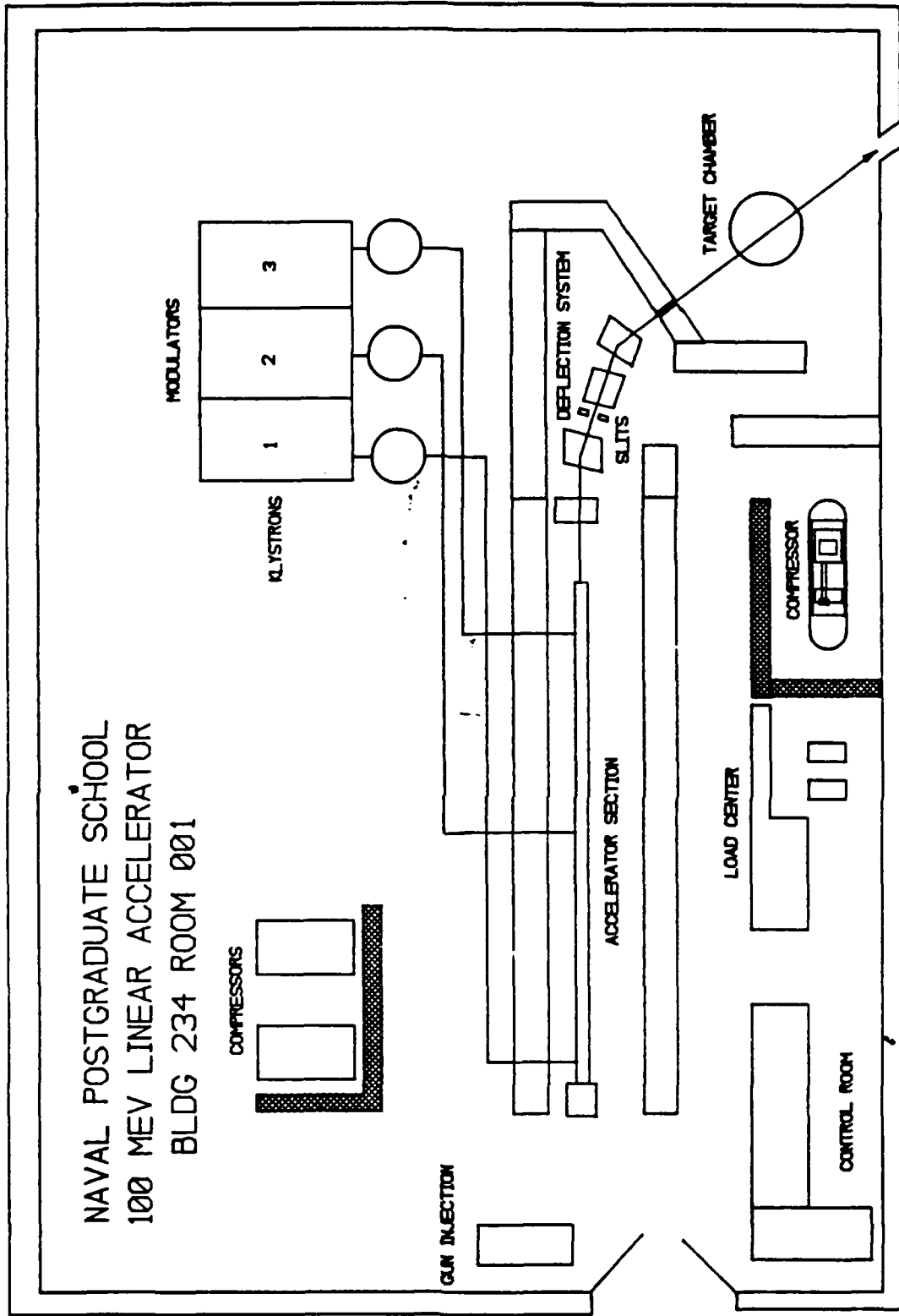


Figure A1: LINAC equipment layout.

APPENDIX B. COMPUTER PROGRAM LISTINGS

```
10 !RAD-COLLECT
20 !This program will take raw data from 4-probe resistance
30 !measurement via channel 1, thermocouple measurement
40 !via channel 2, and E-Beam charge delivered via Channel 3.
50 !Conversion is made to sample resistance, absolute
60 !temperature, and exposure. Plotting is provided by
70 !the HP7090A.
80!
90 !Main Program
100!
110 ASSIGN @Hp7090 TO 705
120 OPTION BASE 1
130!
140 !DEFINE VARIABLES
150 REAL Chan1(1:1000),Chan2(1:1000),Chan3(1:1000),Resist(1:1000)
160 REAL Temp(1:1000),Dose(1:1000)
170 INTEGER I,N
180!
190 !SET INITIAL CONDITIONS FOR THE PLOTTER
200 OUTPUT @Hp7090;"RE12;"           !SELECT CHANNEL 1 and 2 Vs 3
210 OUTPUT @Hp7090;"IR2,10,1001;"    !12 V SCALE CH1, 10/100V CHAN 2&3
220 OUTPUT @Hp7090;"TB75,1"          !SETS TOTAL TIME TO 75 MIN
230 OUTPUT @Hp7090;"MS1;"           !SETS BUFFER TO RECORDING MODE
240!
250 !TAKES DATA INTO BUFFERS THROUGH 3 CHANNELS
260 DISP "PRESS FILL BUFFER. IF FILLED, THEN PRESS CONTINUE."
270 PAUSE
280 WAIT .5
290!
300!
310 GOSUB Data_trans
320 GOSUB Convert_data
330 GOSUB Save_data
340 GOSUB Print_data
350 GOSUB Plot_area
360 GOSUB Plot_data
370 STOP
380!
390!
400 !SUBROUTINES
410 Data_trans: !THIS SUBROUTINE TAKES DATA FROM 3 BUFFERS
420           !AND STORES IN ARRAY VARIABLES CHAN 1,2,3.
430           !
440           !TRANSFER CHANNEL 1 DATA TO CHAN1 ARRAY.
450           DISP "TRANSFERRING CHANNEL 1 DATA"
460           OUTPUT @Hp7090;"D01,1000,0,0;"
470           OUTPUT @Hp7090;"QI;"
480           FOR N=1 TO 1000
490           ENTER @Hp7090 USING "$,K";Chan1(N)
500           DISP N,Chan1(N)
510           NEXT N
520           !TRANSFER CHANNEL 2 DATA TO CHAN2 ARRAY.
530           DISP "TRANSFFERING CHANNEL 2"
540           OUTPUT @Hp7090;"D02,1000,0,0;"
```

```

560      FOR N=1 TO 1000
570      ENTER @Hp7090 USING "*,K";Chan2(N)
580      DISP N,Chan2(N)
590      NEXT N
600      !
610      !TRANSFER CHANNEL 3 DATA TO CHAN3 ARRAY.
620      DISP "TRANSFERRING CHANNEL 3"
630      OUTPUT @Hp7090;"D03,1000,0,01"
640      OUTPUT @Hp7090;"Q1"
650      FOR N=1 TO 1000
660      ENTER @Hp7090 USING "*,K";Chan3(N)
670      NEXT N
680      RETURN
690      !
700 Convert_data: !THIS SUBROUTINE CONVERTS CHAN1 DATA TO
710      !RESISTANCE, CHAN2 DATA TO TEMPERATURE
720      !AND CHAN3 DATA TO DOSE.
730      !
740      !CHAN1 VOLTS TO RESISTANCE (MILLIOHMS)
750      DISP "CONVERTING CHANNEL 1"
760      FOR I=1 TO 1000
770      Resist(I)=Chan1(I)*20 !VOLTS TO MILLIOHMS
780      DISP I,Resist(I)
790      NEXT I
800      !
810      !CHAN2 mVOLTS TO TEMPERATURE (K)
820      DISP "CONVERTING CHANNEL 2"
830      FOR I=1 TO 1000
840      Temp(I)=Chan2(I)/.033 !33 mV PER KELVIN
850      NEXT I
860      !
870      !CHAN3 mVOLTS TO DOSE (MEGARADS)
880      DISP "CONVERTING CHANNEL 3"
890      FOR I=1 TO 1000
900      Dose(I)=(-145.79+53.29*(Chan3(I)*1000))/20
910      !50 MEGA RADS BY 47 VOLTS @1 uFARAD
920      DISP I,Dose(I)
930      NEXT I
940      RETURN
950      !
960 Plot_area: !THIS SUBROUTINE DRAWS THE PLOTTING AREA AND GRIDS.
970      !
980      !DEFINE THE PLOTTING AREA.
990      DISP "PLOT AREA IS DRAWING."
1000      OUTPUT @Hp7090;"IP 1700,1300,9800,6400;"
1010      OUTPUT @Hp7090;"IZ 1700,1300,9800,6400;"
1020      !
1030      !SETTING GRID 10 FOR X-AXIS AND 10 FOR Y-AXIS
1040      OUTPUT @Hp7090;"GL10,10;"
1050      !- 0 TO 50 mOHM for y axis, steps of 5 mohms
1060      !0-50 MRads for x axis, steps of 5 MR
1070      !SELECT PEN1 AND DRAW GRID
1080      OUTPUT @Hp7090;"SP1;DG0;"
1090      RETURN
1100      !
1110 Plot_data: !THIS SUBROUTINE PLOTS THE CONVERTED DATA
1120      DISP "DATA IS BEING PLOTTED."
1130      !
1140      OUTPUT @Hp7090;"SC0,5000,0,5000;"
1150      !
1160      !SELECTS PEN 2 AND LINE TYPE
1170      OUTPUT @Hp7090;"SP2;LT;"
1180      !
1190      !TRANSFERS CONVERTED DATA TO PLOTTER
1200      END N=1 TO 1000

```

```

1220      OUTPUT @Hp7090;"PDPA";Dose(N)/10000,Resist(N)*100
1230      NEXT N
1240      OUTPUT @Hp7090;"PU;SC;IW;"
1250      DISP "PLOT IS COMPLETED"
1260      DISP "PROGRAM IS DONE"
1270      RETURN
1280 !
1290 Save_data: !THIS SUBROUTINE SAVES THE DATA INTO FILES
1300 !WHICH YOU NAME.
1310 !
1320 !SAVING DATA
1330 LINPUT "DO YOU WANT TO SAVE DATA?",Answer$
1340 IF Answer$="N" THEN GOTO Here
1350 LINPUT "ENTER FILENAME TO STORE DATA IN: ",Name$
1360 MASS STORAGE IS ":",700,0"      !HARD DISK AS MSI
1370 CREATE BDAT Name$,3000,8      !3000 REAL NUMBERS
1380 ASSIGN @Path TO Name$        !ASSIGN I/O PATH
1390 OUTPUT @Path:Chan1(*)       !SEND CHAN1 DATA
1400 OUTPUT @Path:Chan2(*)       !SEND CHAN2 DATA
1410 OUTPUT @Path:Chan3(*)       !SEND CHAN3 DATA
1420 DISP Chan1(789)
1430 Here:   MASS STORAGE IS ":",700,0"      !CONTINUE HARD DISK
1440 DISP "STORAGE IS COMPLETE"
1450 RETURN
1460 !
1470 Print_data: !THIS ROUTINE WILL PRINT THE DATA
1480 !
1490 PRINTER IS 701
1500 PRINT "REST","TEMP","DOSE"
1510 FOR I=1 TO 1000
1520 Resist(I)=DROUND(Resist(I),4)
1530 Temp(I)=DROUND(Temp(I),3)
1540 Dose(I)=DROUND(Dose(I),2)
1550 PRINT Resist(I);Temp(I);Dose(I),
1560 NEXT I
1570 RETURN
1580 !
1590 END

```

```

10 Tedata
20 !THIS PROGRAM WILL COLLECT PRE AND POST RESISTANCE VS
30 !TEMPERATURE DATA FOR SUPERCONDUCTOR SAMPLES, CONVERTING THE
40 !RAW INPUTS INTO CONVERTED VALUES, SAVING TO BOAT FILES AND
50 !PRINTING THE RESISTANCE AND TEMPERATURE VALUES.
60 !
70 ASSIGN @Hp7090 TO 705
80 OPTION BASE 1
90 REAL Chan1(1:1000),Chan3(1:1000),Temp(1:1000),Resist(1:1000)
100 INTEGER I
110 !
120 OUTPUT @Hp7090;"REB1"
130 OUTPUT @Hp7090;"IR2,10,121"
140 OUTPUT @Hp7090;"TB60,1;"           !SETS RECORD TIME TO 60 MIN
150 OUTPUT @Hp7090;"MS1"
160 !
170 DISP "BUFFER IS FILLING. PRESS CONTINUE WHEN LIGHT IS STEADY"
180 PAUSE
190 WAIT .5
200 !
210 GOSUB Data_trans
220 GOSUB Convert_data
230 GOSUB Print_data
240 GOSUB Save_data
250 STOP
260 !
270 !
280 Data_trans:   !TRANSFERS DATA FROM PLOTTER TO HP
290 DISP "TRANSFERRING CH1"
300 OUTPUT @Hp7090;"001,1000,0,0;"
310 OUTPUT @Hp7090;"QI;"
320 FOR I=1 TO 1000
330 ENTER @Hp7090 USING "$,K";Chan1(I)
340 DISP I,Chan1(I)
350 NEXT I
360 !
370 DISP "TRANSFERRING CH3"
380 OUTPUT @Hp7090;"003,1000,0,0;"
390 OUTPUT @Hp7090;"QI;" ;
400 FOR I=1 TO 1000
410 ENTER @Hp7090 USING "$,K";Chan3(I)
420 DISP I,Chan3(I)
430 NEXT I
440 RETURN
450 !
460 Convert_data: !THIS ROUTINE CONVERTS TO mOHMS AND KELVIN
470 FOR I=1 TO 1000
480 Resist(I)=Chan1(I)*20      !VOLTS TO mOHMS
490 DISP I,Resist(I)
500 NEXT I
510 !
520 FOR I=1 TO 1000
530 Temp(I)=Chan3(I)/.033    1.033 VOLT/KELVIN
540 DISP I,Temp(I)
550 NEXT I
560 RETURN
570 !
580 Print_data:   !THIS ROUTINE WILL PROVIDE HARD COPY PRINTOUT
590 !
600 PRINTER IS 701
610 FOR I=1 TO 1000
620 Resist(I)=DROUND(Resist(I),4)
630 Temp(I)=DROUND(Temp(I),5)
640 PRINT Resist(I),Temp(I),
650 NEXT I

```

```
670
680 Save_data:
690
700
710      !THIS ROUTINE WILL SAVE TO A BOAT FILE WHICH
720      !YOU PROVIDE THE NAME FOR.
730
740      LINPUT "DO YOU WANT TO SAVE DATA?",Answer$  :
750      IF Answer$="N" THEN GOTO Here
760
770      LINPUT "ENTER FILENAME TO STORE DATA IN: ",Name$  :
780      MASS STORAGE IS ":",700,0"
790      CREATE BOAT Name$,2000,8
800      ASSIGN @Path TO Name$
810      OUTPUT @Path;Chan1(*)
820      OUTPUT @Path;Chan3(*)
830      MASS STORAGE IS ":",700,0"
840      DISP "STORAGE COMPLETE, PROGRAM END"
850      RETURN
860
870      END
```

```

420   10 !DRAWTR
20   ! THIS PROGRAM RETRIEVES SAVED BDAT FILES AND PLOTS
30   !RESISTANCE VS TEMPERATURE
40   ASSIGN @Hp7090 TO 705
50   OPTION BASE 1
60   REAL Chan1(1:1000),Chan2(1:1000),Chan3(1:1000)
70   REAL Resist(1:1000),Temp(1:1000),Dose(1:1000)
80   INTEGER I
90   !
100  GOSUB Plot_area
110  GOSUB Label
120  GOSUB Load_data
130  GOSUB Convert_data
140  GOSUB Plot_data
150  STOP
160  !
170  !
180  !SUBROUTINES
190  !
200 Load_data: !THIS LOADS RAW DATA FROM BDAT FILE
210   !MASS STORAGE IS ":,700,0"
220   LINPUT "ENTER A BDAT FILENAME:",File$           !CONNECTS TO FILE
230   ASSIGN @Path TO File$    !CONNECTS TO FILE
240   ENTER @Path;Chan1(*)    !LOAD CH1
250   ENTER @Path;Chan3(*)    !LOAD CH3
260   ASSIGN @Path TO +-      !CLOSE PATH
270   RETURN
280   !
290 Convert_data: !THIS CONVERTS THE RAW DATA TO DESIRED PLOT
300   !
310   FOR I=1 TO 1000
320   Resist(I)=Chan1(I)*20    !VOLTS TO mOHMS
330   DISP I,Resist(I)
340   NEXT I
350   !
360   FOR I=1 TO 1000
370   Temp(I)=Chan3(I)/.033
380   DISP I,Temp(I)
390   NEXT I
400   !
410   RETURN
420   !
430 Plot_area: !THIS ROUTINE PROVIDES DESIRED PLOT AREA
440   !FOR LARGE AREA PLOT OF R VS T
450   !
460   OUTPUT @Hp7090;"IP1700,1700,9800,7000;"        !PLOT AREA
470   OUTPUT @Hp7090;"IZ1700,1700,9800,7000;"        !PLOT AREA
480   OUTPUT @Hp7090;"GL10,10;"                      !PLOT AREA
490   OUTPUT @Hp7090;"SP1,DG0;"                      !PLOT AREA
500   !
510   !ABOVE PROVIDES 10 BY 10 GRIDS.
520   RETURN
530   !
540   !
550 Plot_data: !THIS ROUTINE RELOTS CONVERTED DATA
560   !
570   !
580   OUTPUT @Hp7090;"SC0,300,-1000,4000;"          !PLOT AREA
590   !X-AXIS IS 0 TO 300 KELVIN
600   !Y-AXIS IS -10 TO 40 mOHMS
610   OUTPUT @Hp7090;"SP2,LT;"                      !PLOT AREA

```

```

630      FOR I=1 TO 1000
640      IF I=1 THEN OUTPUT @Hp7090;"PUPA";Temp(I);Resist(I)=100
650      OUTPUT @Hp7090;"PDPA";Temp(I);Resist(I)=100
660      NEXT I
670      OUTPUT @Hp7090;"SC;PU;"  

680      RETURN
690      !
700 Label:    !LABEL THE PLOT
710      OUTPUT @Hp7090;"IP1700,1700,9800,7000;"  

720      OUTPUT @Hp7090;"IZ1700,1700,9800,7000;"  

730      OUTPUT @Hp7090;"GL10,10;"  

740      OUTPUT @Hp7090;"SC0,300,-10,40;"  

750      OUTPUT @Hp7090;"SP2,PUPA0,0;"  

760      OUTPUT @Hp7090;"L04,SI.2.,3;"  

770      FOR X=0 TO 300 STEP 30
780      OUTPUT @Hp7090 USING "K","PA";X;"-12;LB";X;CHR$(3)
790      NEXT X
800      !
810      OUTPUT @Hp7090;"PA150,-15;LBTEMPERATURE (K)";CHR$(3)
820      OUTPUT @Hp7090;"PA0,0;L018;"  

830      !
840      FOR Y=-10 TO 40 STEP 5
850      OUTPUT @Hp7090 USING "K","PA-.5,";Y;"LB";Y;CHR$(3)
860      NEXT Y
870      !
880      OUTPUT @Hp7090;"L04;PA-30,15;DI0,1,LBRESISTANCE (milliohms)";CH
R$(3)
890      OUTPUT @Hp7090;"DI1,0,SC;L0;"  

900      RETURN
910      !
920      !
930      END

```

```

10    !REPLOT
20    ! THIS PROGRAM RETRIEVES SAVED BDAT FILES TO PLOT
30    !RESISTANCE VS DOSE AND PRINT RESULTS R,T,DOSE.
40    ASSIGN @Hp7090 TO 705
50    OPTION BASE 1
60    REAL Chan1(1:1000),Chan2(1:1000),Chan3(1:1000)
70    REAL Resist(1:1000),Temp(1:1000),Dose(1:1000)
80    INTEGER I
90    !
100   GOSUB Load_data
110   GOSUB Convert_data
120   GOSUB Plot_area
130   GOSUB Plot_data
140   GOSUB Print_data
150   STOP
160   !
170   !
180   !SUBROUTINES
190   !
200 Load_data: !THIS LOADS RAW DATA FROM BDAT FILE
210   !MASS STORAGE IS ":,700,0"
220   LINPUT "ENTER A BDAT FILENAME:",File$           !CONNECTS TO FILE
230   ASSIGN @Path;Chan1(*)           !LOAD CH1
240   ENTER @Path;Chan1(*)           !LOAD CH2
250   ENTER @Path;Chan2(*)           !LOAD CH3
260   ENTER @Path;Chan3(*)           !CLOSE PATH
270   ASSIGN @Path TO *
280   RETURN
290   !
300 Convert_data: !THIS CONVERTS THE RAW DATA TO DESIRED PLOT
310   !
320   FOR I=1 TO 1000
330   Resist(I)=Chan1(I)*20          !VOLTS TO mOHMS
340   DISP I,Resist(I)
350   NEXT I
360   !
370   FOR I=1 TO 1000
380   Temp(I)=Chan2(I)/.033         !33 MV PER K
390   DISP I,Temp(I)
400   NEXT I
410   !
420   FOR I=1 TO 1000
430   Dose(I)=(-10.158+24.753*(Chan3(I)*1000))*20
440   NEXT I
450   RETURN
460   !
470 Plot_area: !THIS ROUTINE PROVIDES DESIRED PLOT AREA
480   !
490   OUTPUT @Hp7090;"IP1700,1300,9800,6400;"
500   OUTPUT @Hp7090;"IZ1700,1300,9800,6400;"
510   OUTPUT @Hp7090;"GL7,10;"
520   OUTPUT @Hp7090;"SP1,D60;"
530   !
540   !ABOVE PROVIDES 7 BY 10 GRIDS,
550   !0 TO 50 mOHMS ON Y-AXIS
560   !0-7 MRADS ON X-AXIS
570   RETURN
580   !
590   !
600 Plot_data: !THIS ROUTINE RELOTS CONVERTED DATA
610   !
620   !
630   OUTPUT @Hp7090;"SC0,7,0,50;"

```

```
660      FOR I=1 TO 1000
670      IF I=1 THEN OUTPUT @Hp7090;"PUPA";Dose(I)/1000000;Resist(I)
680      OUTPUT @Hp7090;"PDPA";Dose(I)/1000000;Resist(I)
690      NEXT I
700      OUTPUT @Hp7090;"PU;SC;IW;"
710      RETURN
720      !
730      !
740 Print_data: !THIS ROUTINE DUMPS CONVERTED DATA TO PRINTER
750      !
760      PRINTER IS 701
770      PRINT "REST";"TEMP";"DOSE"
780      FOR I=1 TO 1000
790      Resist(I)=DROUND(Resist(I),4)
800      Temp(I)=DROUND(Temp(I),3)
810      Dose(I)=DROUND(Dose(I),2)
820      PRINT Resist(I);Temp(I);Dose(I),
830      NEXT I
840      RETURN
850      !
860      !
870      END
```

```

10 !RTOVER
20 ! THIS PROGRAM RETRIEVES SAVED BOAT FILES
30 !AND PLOTS AN OVERLAY OF R VS T (FULL SCALE)
40 !FROM -10 TO 40 MILIOHMS RESISTANCE"
50 ASSIGN @Hp7090 TO 705
60 OPTION BASE 1
70 REAL Chan1(1:1000),Chan2(1:1000),Chan3(1:1000)
80 REAL Resist(1:1000),Temp(1:1000),Dose(1:1000)
90 INTEGER I,N
100 !
110 GOSUB Plot_area
120 GOSUB Label_area
130 GOSUB Load_data
140 GOSUB Convert_data
150 GOSUB Plot_data
160 GOTO 130
170 STOP
180 !
190 !
200 !SUBROUTINES
210 !
220 Load_data: !THIS LOADS RAW DATA FROM BOAT FILE :
230 !MASS STORAGE IS ":",700,0"
240 INPUT "ENTER A BOAT FILENAME:",File$ 
250 ASSIGN @Path TO File$ !CONNECTS TO FILE
260 ENTER @Path;Chan1(*) !LOAD CH1
270 'ENTER @Path;Chan3(*) !LOAD CH3
280 ASSIGN @Path TO * !CLOSE PATH
290 RETURN
300 !
310 Convert_data: !THIS CONVERTS THE RAW DATA TO DESIRED PLOT :
320 !
330 INPUT "ENTER UPPER LIMIT $:",N
340 FOR I=1 TO N
350 Resist(I)=(Chan1(I)*20) !VOLTS TO mOHMS
360 DISP I,Resist(I)
370 NEXT I
380 !
390 FOR I=1 TO N
400 Temp(I)=(Chan3(I)/.033)
410 DISP I,Temp(I)
420 NEXT I
430 !
440 RETURN
450 !
460 Plot_area: !THIS ROUTINE PROVIDES DESIRED PLOT AREA
470 !FOR LARGE AREA PLOT OF R VS T
480 !
490 OUTPUT @Hp7090;"IP1700,1700,9800,7000;"
500 OUTPUT @Hp7090;"IZ1700,1700,9800,7000;"
510 OUTPUT @Hp7090;"GL10,101"
520 OUTPUT @Hp7090;"SP1,D601"
530 !
540 !ABOVE PROVIDES 10 BY 10 GRIDS,
550 RETURN
560 !
570 !
580 Plot_data: !THIS ROUTINE RELOTS CONVERTED DATA
590 !

```

```

600
610      !
620      OUTPUT @Hp7090;"SC0,300,-1000,4000;"  

630      IX-AXIS IS 0 TO 300 KELVIN  

640      IY-AXIS IS -10 TO 40 MOHMS  

650      OUTPUT @Hp7090;"SP2,LT6;"  

660      !
670      FOR I=1 TO N  

680      IF I=1 THEN OUTPUT @Hp7090;"PUPA";Temp(I);Resist(I)*100  

690      OUTPUT @Hp7090;"PDPA";Temp(I);Resist(I)*100  

700      NEXT I  

710      OUTPUT @Hp7090;"SC;PU;"  

720      !
730 Label_area:    !LABEL THE AREA  

740      OUTPUT @Hp7090;"IP1700,1700,9800,7000;"  

750      OUTPUT @Hp7090;"IZ1700,1700,9800,7000;"  

760      OUTPUT @Hp7090;"GL10,6;"  

770      OUTPUT @Hp7090;"SC0,300,-100,400;"  

780      OUTPUT @Hp7090;"SP2,PUPA0,0;"  

790      OUTPUT @Hp7090;"L04,SI.2,.3;"  

800      FOR X=0 TO 300 STEP 30  

810      OUTPUT @Hp7090 USING "K";"PA";X;"-30;LB";X;CHR$(3)  

820      NEXT X  

830      !
840      OUTPUT @Hp7090;"PA150,-60;LBTEMPERATURE (K)";CHR$(3)  

850      OUTPUT @Hp7090;"PA0,0;L018;"  

860      !
870      FOR Y=-100 TO 400 STEP 50  

880      OUTPUT @Hp7090 USING "K";"PA-7,";Y;"LB";Y/10;CHR$(3)  

890      NEXT Y  

900      !
910      OUTPUT @Hp7090;"L04;PA-20,150;DI0,1,LBRESISTANCE (milliohms)";  

920      !
930      OUTPUT @Hp7090;"DI1,0,SC;L0;"  

940      !
950 END

```

```

10 !RATIO
20 ! THIS PROGRAM RETRIEVES SAVED BDAT FILES TO PLOT THE :
30 !RATIO OF POST-IRRADIATED OVER PRE-IRRADIATED RESISTANCES
40 !FOR A GIVEN SAMPLE.
50 !
60 ASSIGN @Hp7090 TO 705
70 OPTION BASE 1
80 REAL Chan(1:1000),Chan3(1:1000)
90 REAL Resist(1:1000),Temp(1:1000),Ratio(1:1000)
100 REAL Ratioa(1:1000),Ratioab(1:1000),Ratioac(1:1000)
110 REAL Resistp(1:1000),Resista(1:1000),Resistb(1:1000),Resistc(1:1000)
120 REAL Tempp(1:1000),Tempa(1:1000),Tempb(1:1000),Tempc(1:1000)
130 INTEGER I,J
140 !
150 GOSUB Plot_area
160 GOSUB Label_area
170 GOSUB Load_data
180 GOSUB Convert_data
190 GOSUB Plot_data
200 GOSUB Load_a
210 GOSUB Convert_a
220 GOSUB Plot_a
230 DISP "END OF PROGRAM"
240 STOP
250 !
260 !
270 !SUBROUTINES
280 !
290 Load_data: !THIS LOADS RAW DATA FROM BDAT FILE
300 !MASS STORAGE IS :,700,0"
310 LINPUT "ENTER A BDAT FILENAME:",File$
320 ASSIGN @Path TO File$ !CONNECTS TO FILE
330 ENTER @Path:Chan1(*) !LOAD CH1
340 ENTER @Path:Chan3(*) !LOAD CH3
350 ASSIGN @Path TO * !CLOSE PATH
360 RETURN
370 !
380 Convert_data: !THIS CONVERTS THE RAW DATA TO DESIRED PLOT
390 !
400 FOR I=1 TO 850
410 Resistp(I)=(Chan(I)*20) !VOLTS TO MOHMS
420 DISP Resistp(I)
430 Ratio(I)=Resistp(I)/Resistp(I)
440 NEXT I
450 !
460 FOR I=1 TO 850
470 Tempp(I)=Chan3(I)/.033
480 Temp(I)=DROUND(Tempp(I),3)
490 DISP Ratio(I),Temp(I)
500 NEXT I
510 !
520 RETURN
530 !
540 Plot_area: !THIS ROUTINE PROVIDES DESIRED PLOT AREA
550 !FOR LARGE AREA PLOT OF R VS T
560 !
570 OUTPUT @Hp7090;"IP1700,1700,9800,7000;"
580 OUTPUT @Hp7090;"IZ1700,1700,9800,7000;"
590 OUTPUT @Hp7090;"GL8,8;"
600 OUTPUT @Hp7090;"SP1,D60;"
610 !
620 !ABOVE PROVIDES 8 BY 8 GRIDS.
630 RETURN

```

```

640      !
650 Label_area:    !LABEL THE AREA
660      OUTPUT @Hp7090;"IP1700,1700,9800,7000;"*
670      OUTPUT @Hp7090;"IZ1700,1700,9800,7000;"*
680      OUTPUT @Hp7090;"SL8,B;"*
690      OUTPUT @Hp7090;"SC60,300,.80,120;"*
700      OUTPUT @Hp7090;"SP2,PUPA0,0;"*
710      OUTPUT @Hp7090;"L04,S1.2,.3;"*
720      FOR X=60 TO 300 STEP,30
730      OUTPUT @Hp7090 USING "K";"PA";X;"78;LB";X;CHR$(3)
740      NEXT X
750      OUTPUT @Hp7090;"PA180,.76;LBTEMPERATURE (K)";CHR$(3)
760      OUTPUT @Hp7090;"PA0,0;L018;"*
770      FOR Y=80 TO 120 STEP 5
780      OUTPUT @Hp7090 USING "K";"PA50,";Y;"LB";Y/100;CHR$(3)
790      NEXT Y
800      OUTPUT @Hp7090;"L04;PA30,100;DI0,1,LBRATIO: R(100MR) / R(
PRE);CHR$(3)
810      OUTPUT @Hp7090;"DI1,0,SC1,L01"
820      RETURN
830      !
840 Plot_data:    !THIS ROUTINE RELOTS CONVERTED DATA
850      *
860      !
870      OUTPUT @Hp7090;"SC60,300,.80,120;"*
880      !X-AXIS IS 60 TO 300 KELVIN
890      !Y-AXIS IS .80 TO 1.2 NORAMLIZED
900      OUTPUT @Hp7090;"SP2,LT;"*
910      !
920      FOR I=1 TO 850
930      IF I=1 THEN OUTPUT @Hp7090;"PUPA";Temp(I);Ratio(I)*100
940      OUTPUT @Hp7090;"PDPA";Temp(I);Ratio(I)*100
950      NEXT I
960      OUTPUT @Hp7090;"PU;"*
970      RETURN
980      !
990 Load_a:      !LOADS SECOND FILE
1000      !
1010      MASS STORAGE IS ":",700,0"
1020      LINPUT "ENTER A BDAT FILENAME:",File$*
1030      ASSIGN @Path TO File$*
1040      ENTER @Path;Chan1(*)
1050      ENTER @Path;Chan3(*)
1060      ASSIGN @Path TO *
1070      RETURN
1080      !
1090 Convert_a:   !FILE 2
1120      FOR I=1 TO 300
1130      Temp(I)=Chan3(I)/.033
1140      Temp(I)=DROUND(Temp(I),3)
1150      Resist(I)=(Chan1(I)*20)
1160      NEXT I
1170      !
1180      RETURN
1190      !

```

```
1200 Plot_a:      |
1210             OUTPUT @Hp7090;"SC60,300,0000,120001"
1220             OUTPUT @Hp7090;"SP2,LT2"
1230             FOR I=1 TO 850
1240             FOR J=1 TO 560
1250             IF Tempa(J)<>Tempa(I) THEN GOTO 1310
1260             Ratioa(J)=Resista(J)/Resistp(I)
1270             Ratioa(J)=ROUND(Ratioa(J),3)
1280             DISP Resista(J),Resistp(I),Ratioa(J),Tempa(I),Tempa(J)
1290             IF J=1 THEN OUTPUT @Hp7090;"PUPA";Tempa(J);Ratioa(J)*10000
1300             OUTPUT @Hp7090;"PDPA";Tempa(J);Ratioa(J)*10000
1310             NEXT J
1320             NEXT I
1330             RETURN
1340             |
1350 END
```

APPENDIX C. EQUIPMENT LAYOUT

Much of the equipment utilized in this experiment was borrowed from Lockheed Missiles and Space Company. The superconductor samples were manufactured by Dr. Chu at the University of Houston, and obtained through Lockheed. Figure C1 is a schematic of the experimental layout, including target area and control station/data collection center. Specific equipment models used were:

Gaseous helium - 217 cubic feet, industrial grade.

Liquid helium - 240 liters

Liquid helium flow controller - Air Products

Liquid Transfer Helitran - Model LT-3-110, Air Products

Digital Temperature Controller/Indicators (2) - Series 3700, Scientific Instruments, Inc.

4-Wire AC Resistance Bridge - Model LR-400, Linear Research Corp.

Thermoluminescent Dosimeters (TLD) - CaF₂, Victoreen Corp.

TLD Reader - Model 2800M, Victoreen Corp.

Superconductor Experimental Layout

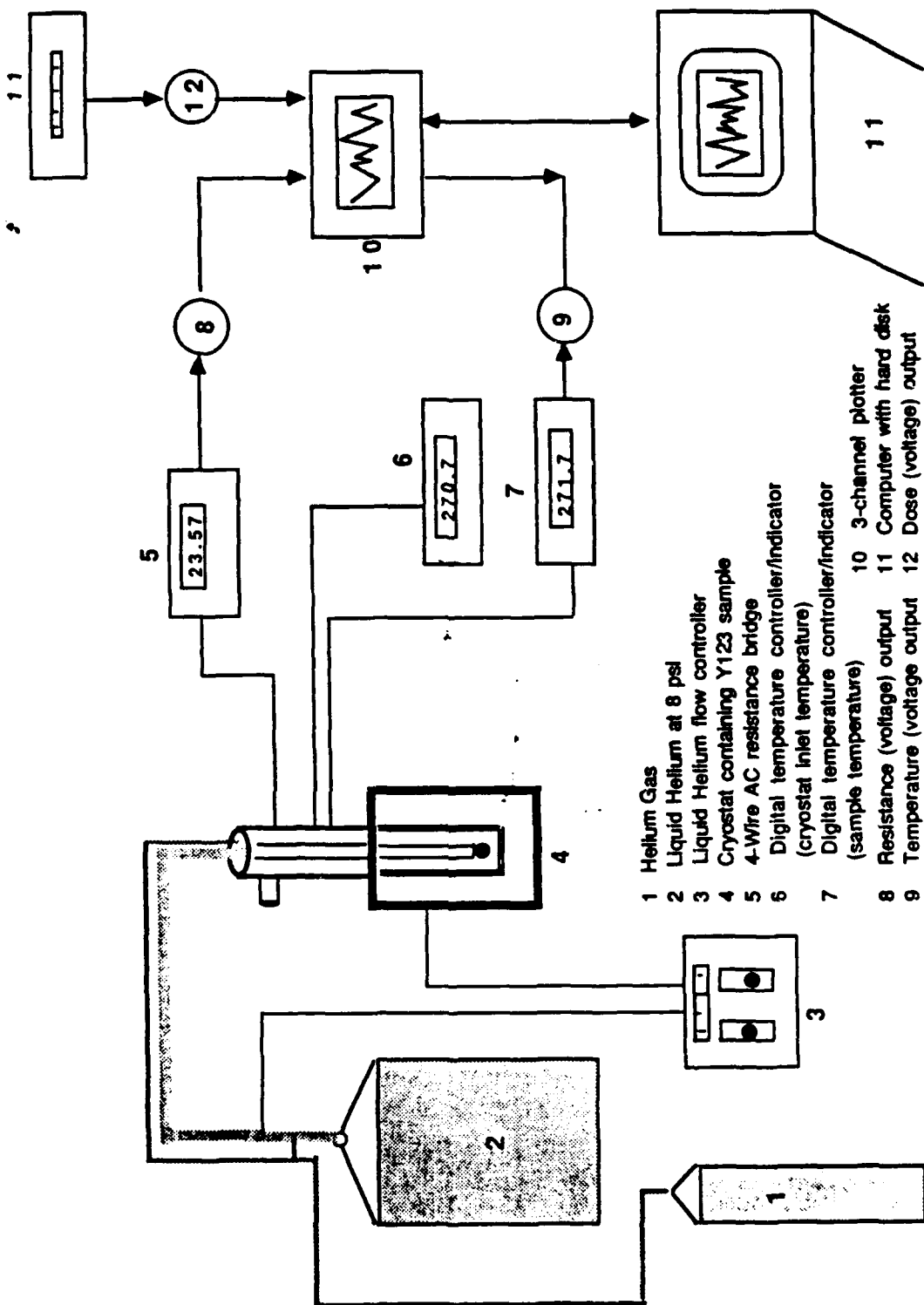


Figure C1: Experiment Equipment Layout

APPENDIX D. DOSIMETRY

Dosimetry, here referred to as the determination of actual dose from the electron beam produced by the LINAC, was accomplished using calcium-flouride (CaF_2) thermoluminescent dosimeters (TLD's) due to their linear response over a wide range of absorbed dose. Upon exposure to the beam, electrons in the TLD's are elevated from the conduction to valance band and, literally, trapped. After exposure, the TLD's are heated in a TLD reader (Victoreen Model 2800M in this experiment). The temperature is slowly raised whereupon the trapped electrons in the TLD's obtain enough energy to re-excite back to the conduction band. A radiated photon results, which is in the visible region. By use of a photomultiplier tube, the total number of emitted photons is related to the radiation exposure, hence dose. The saturation level for the TLD reader is approximately 8 kilorads. To establish very high doses, the linearity of the CaF_2 TLD is utilized to establish charge-dose conversion plots.

A secondary emissions monitor (SEM) was placed in the path of the electron beam, downstream of the target. The SEM utilizes a foil which emits secondary electrons due to impact of the primary electrons in the beam. The electrons charge a capacitor and create a voltage across it. The voltage is

determined by a voltage integrator connected to the capacitor and is proportional to the charge stored in the capacitor. This voltage signal, proportional to the charge, is also linearly proportional to the dose absorbed by the TLD [Ref 1].

A plot of dose versus voltage (or charge) is obtained by setting a particular capacitance and repeatedly exposing TLD's to various voltage settings such that values for dose as a function of voltage (or charge) are obtained below the saturation point of the TLD or TLD reader. From this data a linear fit is made, allowing scaling and determination of the necessary voltage (or charge) required to deliver a desired dose to a target, in this case the superconductor sample. This procedure was performed prior to every irradiation of the superconductor samples, and the conversions routines incorporated into the program designed to plot resistance and temperature versus dose. This was done to account for differing beam characteristics from various irradiations. The TLD's were placed inside a plastic baggie at the corner, and mounted within the cryostat's aluminum outer cover at the position of the sample location to account for potential shielding and/or enhancement due to bremsstrahlung. Figures D1, D2, and D3 show dose versus voltage for the electron beam prior to incremental irradiations to 6, 40, and 54 megarads (6, 46, 100 megarads cumulative doses) to the hot sample. The dates correspond to when data was obtained as shown in Tables

I and II. Figures D4, D5, and D6 similarly depict dose versus voltage for the cold sample. The total charge, rather than the voltage, is used to provide the necessary settings to the electron beam due to the ability to select various values of capacitance, allowing the time for exposure to a desired dose to be optimized. The applied voltage is monitored via a digital counter at the control station to control beam on/off times to arrive at a desired dose.

Dosimetry 4 August

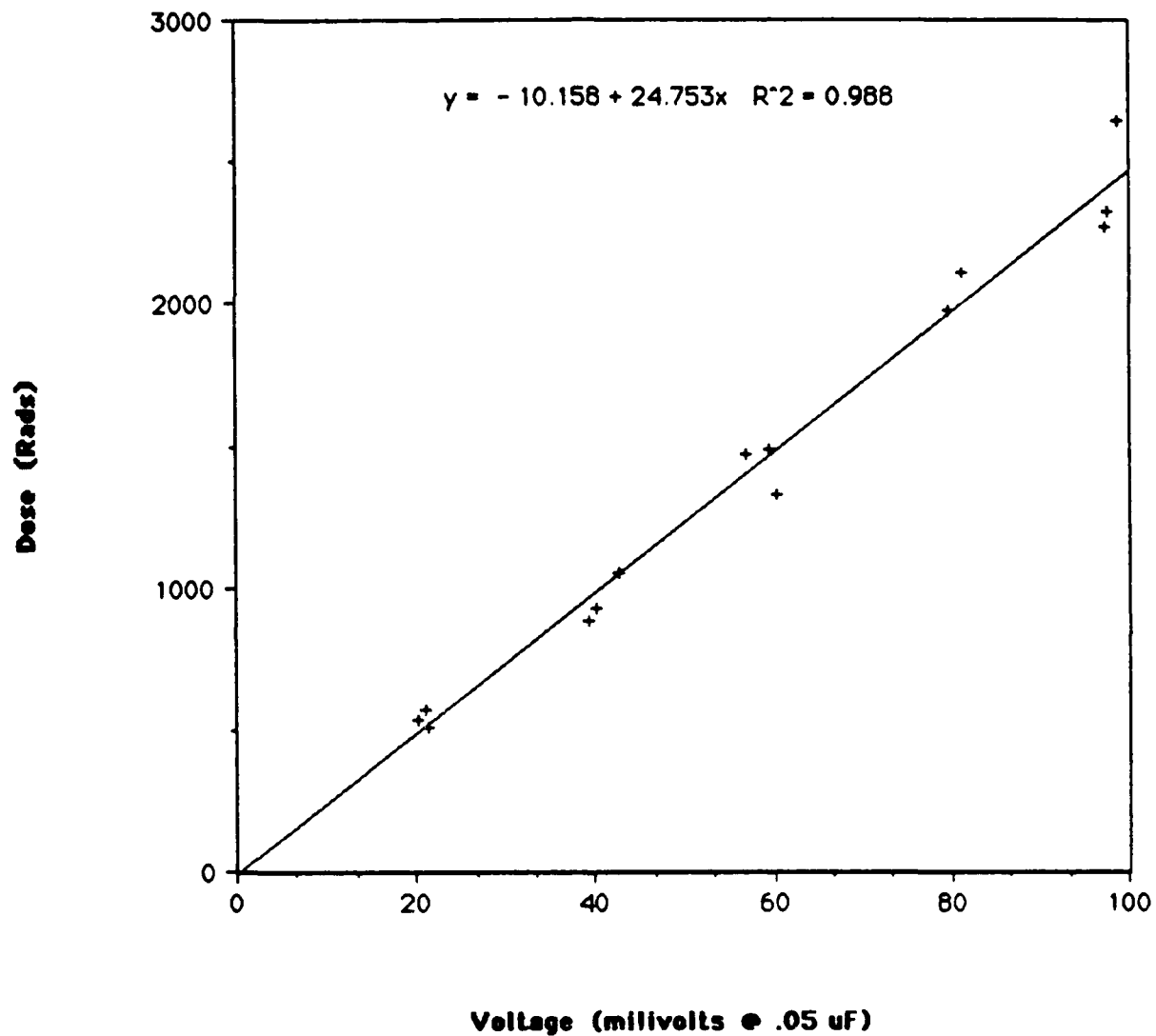


Figure D1: Dose versus SEM voltage on 4 August 1989.

Dosimetry 9 August

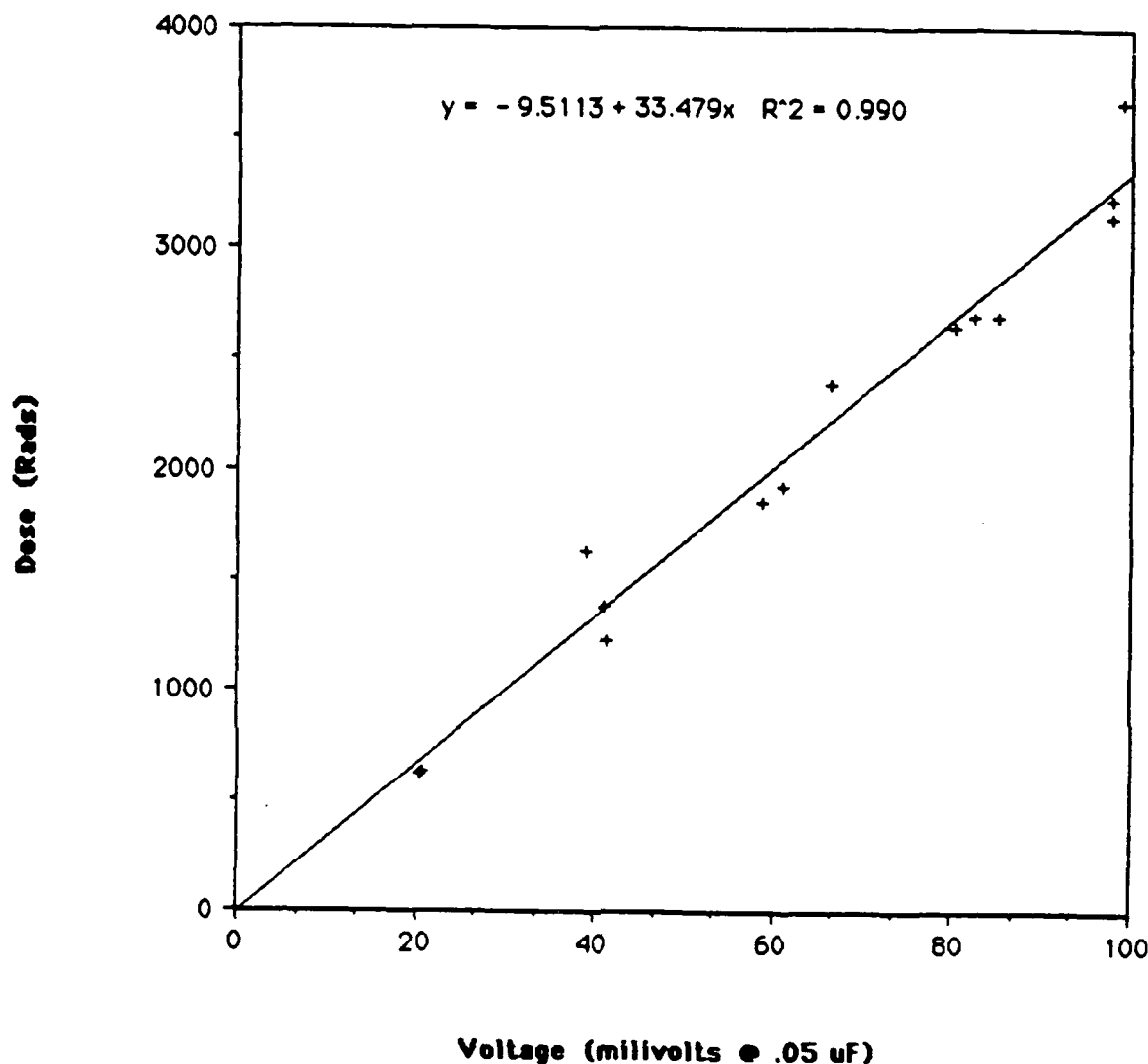


Figure D2: Dose versus SEM voltage on 9 August 1989.

Dosimetry 10 August

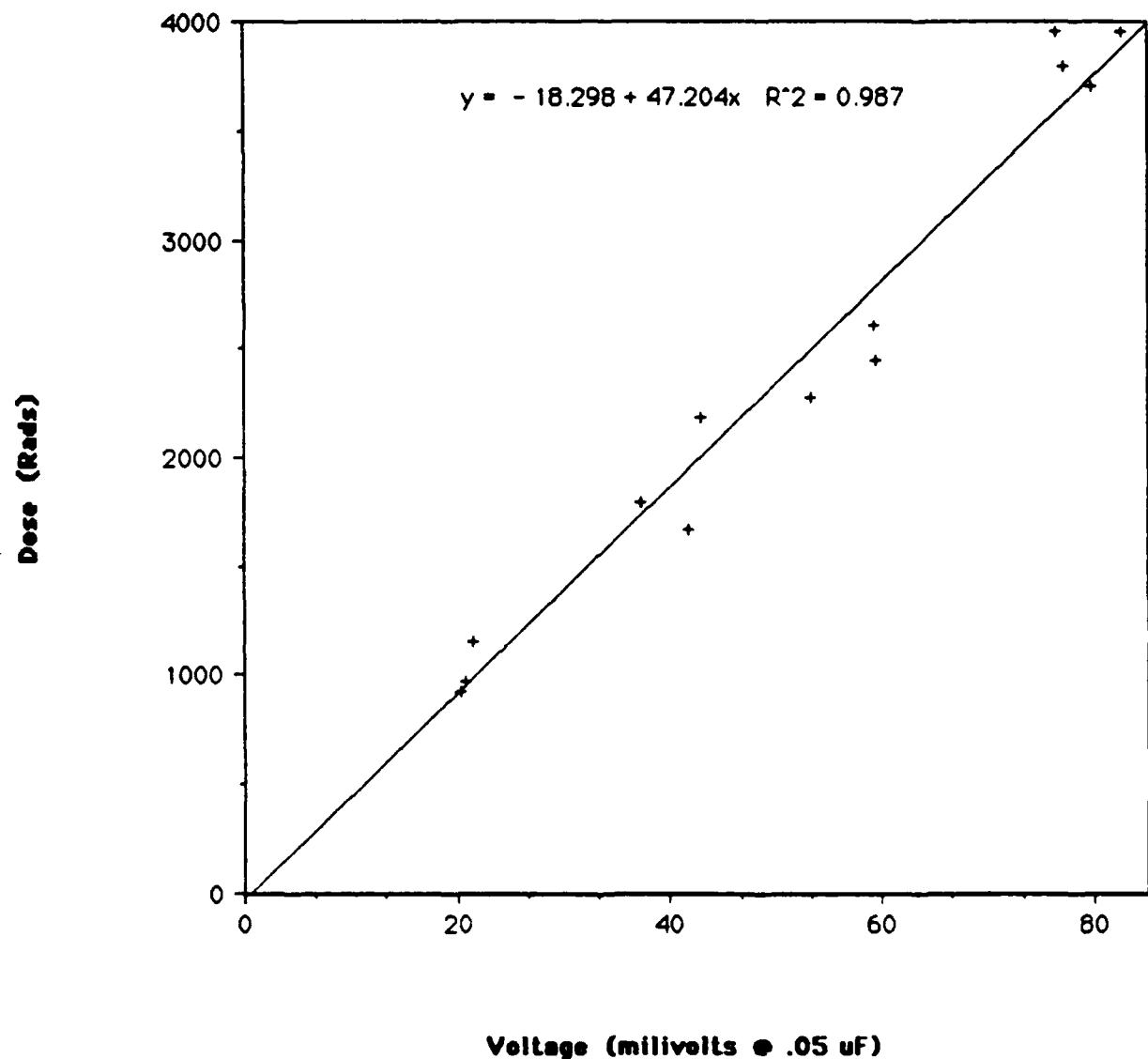


Figure D3: Dose versus SEM voltage on 10 August 1989.

Dosimetry 26 September

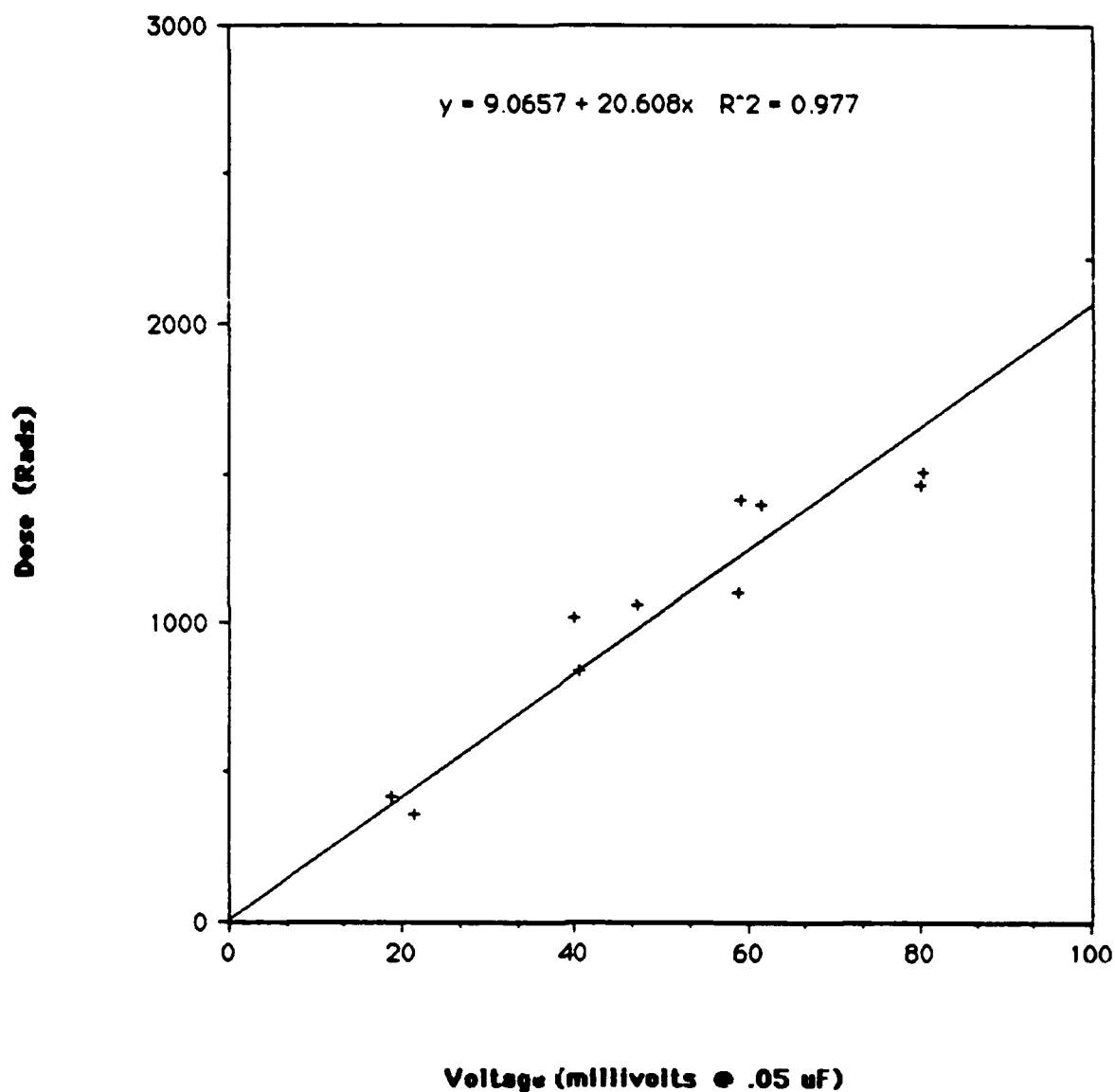


Figure D4: Dose versus SEM voltage on 26 September 1989.

Dosimetry 27 September

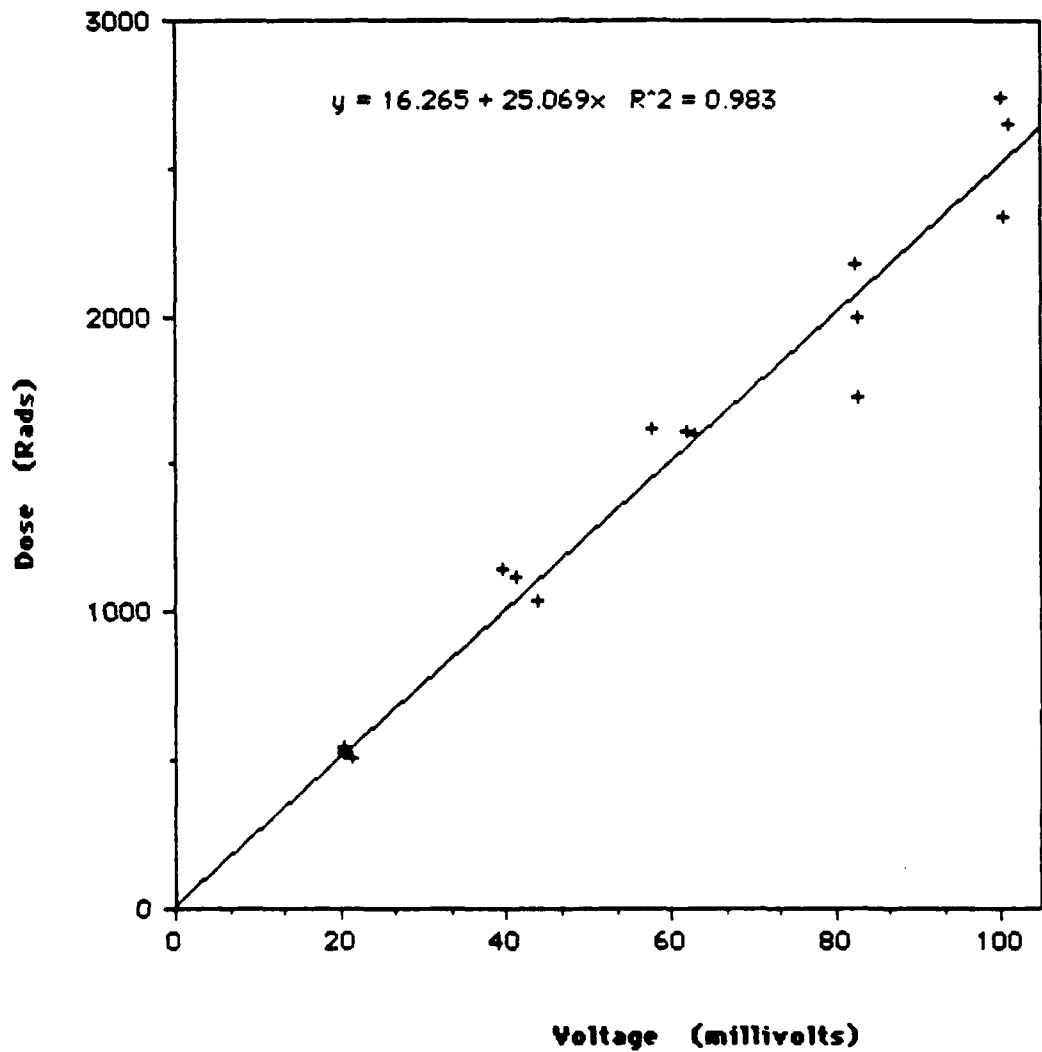


Figure D5: Dose versus SEM voltage on 27 September 1989.

Dosimetry 28 September

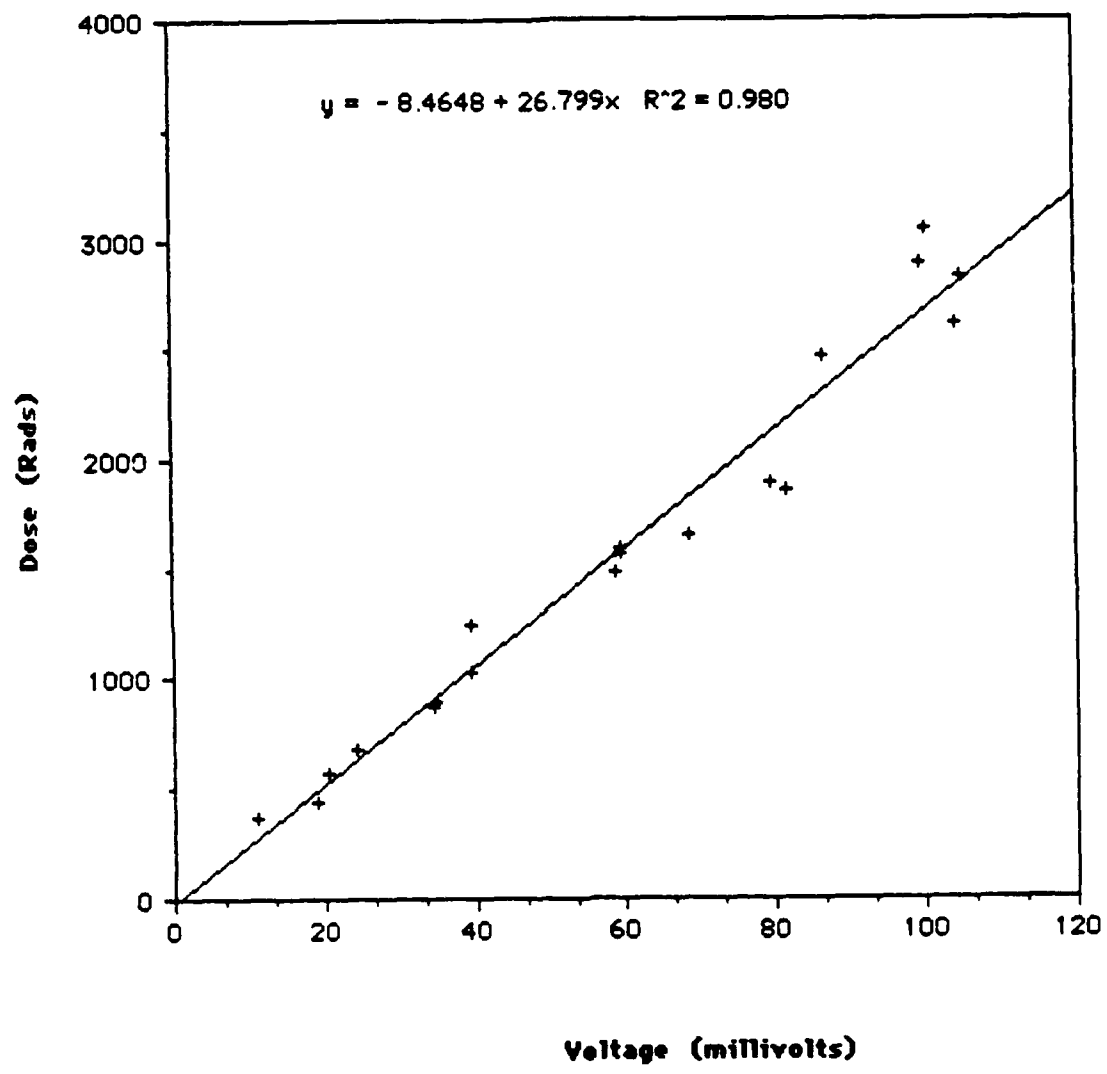


Figure D6: Dose versus SEM voltage on 28 September 1989.

APPENDIX E. SUPERCONDUCTOR THEORY

BCS theory (named for it's authors Bardeen, Cooper, and Schrieffer in 1957) explains the superconducting behavior in the following manner: As an electron moves past lattice ions, it changes their positions slightly by coulomb attraction, creating a locally increased positive charge density. As the electron moves past the displaced ion, the ion oscillates back and forth about it's original location, much like a harmonic oscillator. The ion vibrates with the velocity of sound in the medium. The quantum of vibration is known as a phonon. As each phonon propagates through the lattice it encounters other electrons, and acts as an attractive force, coupling the electrons which are known as Cooper pairs. This force is not enough to overcome the coulomb repulsion of the electron's, and the electrons experience a distant attraction. The average maximum distance of attraction is known as the coherence length. The electrons are of opposite spin and momentum. As the coupled electron pairs move through the lattice they change the effect of the phonon interaction, reducing the attraction of the electrons as they approach velocities near that of sound in the medium. This happens at the surface of the superconductor under the influence of a critical magnetic field. The attraction of the Cooper pairs lowers the energy

of the pair relative to the Fermi Energy of the unpaired electrons. The energy is lowered because of the work done to separate the electrons. The magnetic field affects all electron pairs, and it is impossible to differentiate any particular pair from another in terms of momentum. The phonons emitted by an electron pair interact with other electrons within the coherence length so that additional attraction exists between electrons of the pair, which is stronger than the individual phonon attraction. If no magnetic field is present, the momentum of all pairs is zero. If a magnetic field is present, all pairs have the same momentum. The additional strong attraction between electrons of a pair is the energy gap of the superconductor. For most superconductors, the energy gap is 10^3 - 10^4 larger than the energy of an isolated electron pair. As the temperature of the superconducting material is increased, the energy gap decreases. This occurs because the temperature of the lattice is based on the spectrum of phonons propagating continuously throughout the lattice and causing random movement of the lattice atoms. As temperature increases, the amplitude and frequency of the movement of lattice atoms increases, and these movements interfere with the propagation of the phonons between coupled electron pairs. This results in the pairs with a consequent decrease in the energy gap. Past the critical temperature of the materials, electrons have gained enough energy to overcome the phonon attraction,

and superconducting behavior breaks down. While electron density and strength of the electron-phonon interactions are greater in materials with high critical temperatures, BCS theory predicts an upper limit to the strength of this interaction, and therefore a maximum critical temperature of 30 to 40K. The classification of superconductors into two types is based upon their reaction to magnetic fields. Type I superconductors completely exclude magnetic flux while Type II superconductors have a more complicated reaction to magnetic fields. Type I superconductors are typically pure elements, while Type II superconductors are typically compounds.

The Y123 compound exhibits a critical temperature around 95K. Eleven other 123 superconductors can be created by substituting different rare earth elements for the yttrium. It is presently felt that something may be occurring in these metal oxide superconductors that requires an extension to or replacement of the BCS theory [Ref. 6]. Most recent theories center on the peculiar bonding between the copper and oxygen atoms. The copper atom should donate two electrons to fill the oxygen atoms outer shell, but in the Y123 material the copper donates between two and three electrons. In the 123 compounds, the oxygen content changes the copper's valance state, and corresponds strongly with the superconducting properties. A material with too many empty oxygen sites will not superconduct. It's been suggested that the phonon

mechanism of metal superconductors was not the major contributor to pairing in ceramics. Phonon frequencies vary with the mass of the atom. The use of different isotopes in BCS superconductors changes the critical temperatures in a predictable way, but use of different isotopes of oxygen, barium, and copper in the Y123 left the superconductor unchanged. Various explanations to this behavior are given. One is the excitonic model which states that the displaced electron-hole pairs (excitons) perform the same attractive function as phonons in metals. The other theory concerns a magnetic interaction as the instigator of the attractions. A resonating valance bond model states that antiferromagnetism exists in an insulating phase of the metal oxides. Remnants of the antiferromagnetism appear in the superconducting state, contributing to the phenomena. This leads to the conclusion that the ceramics conducted charge via charged bosons instead of electrons [Ref. 7].

APPENDIX F. ELECTRON INTERACTIONS WITH MATTER

There are four types of interactions between electrons and matter: elastic and inelastic collisions of electrons with nuclei or atomic electrons.

The primary mechanism by which electrons lose energy in matter is inelastic collisions. Such a collision would normally result in an excitation or emission of the bound electron of the atom. An inelastic collision with the nucleus deflects the incident electron causing a quantum of electromagnetic radiation to be emitted in the form of a gamma or x-ray. This process is known as bremsstrahlung (braking) radiation. The kinetic energy of the deflected electron will be reduced by the amount of energy in the photon that is produced in this process.

In elastic collisions, the incident electron is deflected, but does not radiate energy. The electron loses enough energy to conserve momentum when it collides with an atomic electron, energy and momentum are conserved, therefore not enough energy is transferred to cause ionization. In either case these forms of collisions do not result in lattice displacement defects.

Due to the size of the electron in comparison to the atoms in the Y123 material, the most probable encounter will be one that results in an inelastic collision. The most

probable energy loss per mass thickness (dE/dx) for these inelastic collisions is called collisional stopping power. Collisional stopping power is proportional to the bound electron density of the struck atom. Higher atomic number elements will have a greater chance of interaction with the incident electron. Collisional stopping power is also inversely proportional to the square of the incident electron velocity. So a higher energy electron, due to greater velocity, will have a lesser chance of interacting within a given thickness of a material.

For the Y123 material, the distribution of energy loss was found by Sweigard [Ref. 1] to be 62% due to bremsstrahlung and 38% due to collisional. The radiative stopping power is not of interest since damage to the lattice, which would show up as a change in the resistivity of the Y123 material, would result from permanent displacement defects from collisions with the bound electrons. Bremsstrahlung would result in an enhanced dose from either x-ray or gamma photons in the material, however the size of the Y123 sample will negate the effect of these since secondary electron production from the gammas or x-rays is a volume effect [Ref. 8].

It is expected that exposure to large fluences of electrons resulting in large doses of absorbed radiation by the Y123 should result in some perceptible permanent damage to the lattice that would result in a change in the normal state resistivity and transition temperature.

LIST OF REFERENCES

1. Sweigard, E.L., "Effects of 67.5 MeV Electron Irradiation on Y-Ba-Cu-O and Gd-Ba-Cu-O High-Temperature Superconductors", Master's Thesis, Naval Postgraduate School, Monterey, California, December 1987.
2. Wolf, S.A., and Krezin, V.Z., eds., Proceedings of the International Workshop on Novel Methods of Superconductivity, Plenum Press, pp.961-967, 1987.
3. Maisch, W.G., et al., "Radiation Effects in High Tc Superconductors for Space Applications", IEEE Transaction on Nuclear Science, Vol. NS-34, No. 6, December 1987.
4. Shiraishi, K. et al., "Electron Irradiation Effects on a Ba₂YC_u₃O₇ Superconductor", Japanese Journal Of Applied Physics, Vol. 27, No. 12, December 1988.
5. Bohandy, J., et al., "Gamma Radiation Resistance of the High Tc Superconductor YBa₂Cu₃O_{7-δ}", Applied Physics Letters, Vol. 51, No. 25, 21 December 1987.
6. Williams, J.E.C., Superconductivity and it's Applications, Pion Ltd., 1970.
7. Fitzgerald, Karen, "Superconductivity: Fact vs. Fancy", IEEE Spectrum, Vol. 25, No. 5, pp. 30-41, May 1988.
8. Rudie, N.J., Principles and Techniques of Radiation Hardening, Vol. I, Western Periodicals, 1976.

Bibliography

1. Burcham, W.E., Nuclear Physics: An Introduction, McGraw-Hill Book Company, Inc., 1963.
2. Eisberg, R. and Resnick, R., Quantum Physics of Atoms, Molecules, Solids, Nuclei, and Particles, Second Edition, John Wiley and Sons, Inc., 1985.
3. Kittel, C., Introduction to Solid State Physics, Sixth Edition, John Wiley and Sons, Inc., 1986.
4. Knoll, G. F., Radiation Detection and Measurement, John Wiley and Sons, Inc., 1979.
5. Krane, K.S., Introductory Nuclear Physics, John Wiley and Sons, Inc., 1987.
6. Mayo, J.L., Superconductivity - The Threshold of a New Technology, Tab Books, Inc., 1988.

INITIAL DISTRIBUTION LIST

	No. Copies
1. Defense Technical Information Center Cameron Station Alexandria, VA 22304-6145	2
2. Library, Code 0142 Naval Postgraduate School Monterey, CA 93943-5002	2
3. Professor X. K. Maruyama, Code 61Mx Department of Physics Naval Postgraduate School Monterey, CA 93943-5002	3
4. Professor F. R. Buskirk, Code 61Bs Department of Physics Naval Postgraduate School Monterey, CA 93943-5002	2
5. Dr. L. J. Dries, Code 9740/202 Research and Development Division Lockheed Missiles and Space Co. 3251 Hanover Street Palo Alto, CA 94394-1191	2
6. U.S. Army Tank-Automotive Command RDE Library Building 200 Warren, MI 48397-5000	1
7. Survivability Division (AMSTA-RS) U.S. Army Tank-Automotive Command Building 200C Warren, MI 48397-5000	1
8. Don Synder, Code 61Ds Department of Physics Naval Postgraduate School Monterey, CA 93943-5002	1
9. Harold Rietdyk, Code 61Hr Department of Physics Naval Postgraduate School Monterey, CA 93943-5002	1

- | | |
|--|---|
| 10. Dr. J. C. Ritter, Code 6611
Naval Research Laboratory
Washington, D.C. 20375 | 1 |
| 11. Dr. W. G. Maisch
Naval Research Laboratory
Washington, D.C. 20375 | 1 |
| 12. Dr. William Stapor
Naval Research Laboratory
Washington, D.C. 20375 | 1 |
| 13. Gregory J. Wolfe
11056 Canterbury Drive
Sterling Heights, MI 48077 | 3 |